Exploratory study of single and multi-step dissolution-precipitation syntheses of carbonate-containing hydrocalumite

UNIVERSITEIT VAN PRETORIA
UNIVERSITY OF PRETORIA
YUNIBESITHI YA PRETORIA

Ansuretha Wiid

Exploratory study of single and multi-step dissolution-precipitation syntheses of carbonate-containing hydrocalumite

Ansuretha Wiid

UNIVERSITEIT VAN PRETORIA
UNIVERSITY OF PRETORIA
YUNIBESITHI YA PRETORIA

Submitted in partial fulfilment of part of the requirements for the degree of Master of Engineering in the Faculty Engineering, the Built Environment and Information Technology, University of Pretoria, Pretoria

2015

Exploratory study of single and multi-step dissolution-precipitation syntheses of carbonate-containing hydrocalumite

Synopsis

Hydrocalumite is a calcium/aluminium-based layered double hydroxide. This material has a wide range of applications, such as polymer additives, basic catalysts and water treatment agents. There are a variety of synthesis methods available of which co-precipitation is most widely used. The negative aspects of using most of the developed methods are use of high cost metal salts as reagents. These materials are not only high in cost but are highly corrosive and result in damage of production equipment.

A salt containing effluent is produced in these processes that can be harmful to the environment, thus requires treatment before disposal. As the interest in the use of hydrocalumite has increased, there is a need for environmentally friendly and more cost effective synthesis procedures. The aim of this study was to explore different reagents, time and temperature reaction conditions for the dissolution-precipitation synthesis of carbonate-containing hydrocalumite. In this method metal oxides/hydroxides reagents are used which are less corrosive and do not lead to harsh effluent production.

This method has two distinct steps namely precursor formation followed by intercalation. In the precursor formation step, it was found that for the reaction between calcium oxide and aluminium hydroxide the conversion of both the

calcium and aluminium sources increase as reaction time and temperature increase. It was confirmed that the dissolution of aluminium hydroxide is the limiting step. An aluminium conversion of ~90 % is reached at 80 °C at 6 h reaction time. A further increase in temperature reduces the reaction time immensely, with ~90 % aluminium conversion reached within 30 min at 100 °C and 120 °C. Extending the reaction times beyond these points does not have a significant influence on the conversion of aluminium as it remains constant at ~90 %.

Of the various carbonate sources tested for intercalation, sodium carbonate showed the most crystalline hydrocalumite samples. Using sodium bicarbonate as a carbonate source renders similar conversion results to sodium carbonate. When reacting these carbonate sources with the precursor, the conversion to hydrocalumite increased with increasing reaction time and temperature. There is a significant spike in the intensity of the primary hydrocalumite diffraction peak of the sodium carbonate samples at 60 °C and 70 °C for 10 h reaction time; resulting in the highest yield of hydrocalumite. Use of air, CO_2 (g), calcite and dry ice CO_2 (s) as carbonate sources resulted in poor formation of hydrocalumite.

Considering the results of the precursor formation and intercalation, the most promising synthesis conditions is to react calcium oxide and aluminium hydroxide at a temperature of 100 °C for 30 min, where after sodium carbonate should be added to the mixture and reacted for a further 10 h between 60 °C and 70 °C.

Keywords: hydrocalumite, synthesis, layered double hydroxides, green chemistry.

Acknowledgements

I would like to thank:

- Family and friends for all the emotional and financial support.
- Dr. F.J.W.J. Labuschagné for his supervision, time, knowledge and overall support.
- Miss. M.J. Schmidt for her contribution to this research and support throughout.
- Leibniz-Institut für Polymerforschung (IPF) Dresden e.V. for the great opportunity, experience and financial support. With special thanks to Dr. A. Leuteritz for his supervision and support.
- Mrs. W. Grote for all the XRD analysis done and the interpretation thereof at the University of Pretoria.
- Mr. G. Puts at the University of Pretoria and Mrs. L. Häussler at IPF Dresden for TGA analysis done and interpretation.
- The NRF, Thrip, Engelbrecht and Mentz and UP study abroad program for financial support.
- Colleges and friends in the UP department of Chemical Engineering for their support.

Contents

Synopsys i

Acknowledgements iii

List of Figures vii

List of Tables x

1. Introduction 1

2. Literature 3

2.1 Layered double hydroxides 3

2.1.1 Hydrotalcite 4

2.1.2 Hydrocalumite 5

2.1.3 Interlayer water and anions 6

2.1.4 Applications 7

2.2 Analysis and characterisation 9

2.2.1 X-ray diffraction (XRD) 9

2.2.1.1 Qualitative XRD 9

2.2.1.2 Quantitative XRD analysis 14

2.2.2 Thermogravimetric analysis (TGA) 14

2.2.3 Scanning electron microscopy (SEM) 16

2.3 Synthesis of LDHs 17

2.3.1 Co-precipitation 18

2.3.1.1 Constant pH titration 18

2.3.1.2 Buffer precipitation (Varying pH) 19

2.3.2 Urea hydrolysis 20

2.3.3 Sol gel 20

2.3.4 Post synthesis treatment 20

2.3.5 Synthesis from oxides/hydroxide 21

2.3.6 Industrial scale production 24

3. Experimental 26

3.1 Precursor: katoite synthesis 27

3.1.1 Apparatus 27

3.1.2 Planning 28

3.2.2 Method 31

3.3 Carbonate intercalation 32

3.3.1 Planning 32

3.3.2 Apparatus 34

3.3.3 Method 36

3.4 Use of calcite as combined calcium and carbonate source 37

3.5 Materials 38

3.6 Analysis and sample preparation 38

4 Results and Discussion 40

4.1 Precursor: katoite synthesis 40

4.1.1 Katoite formation with calcium oxide as calcium source 40

4.2 Carbonate intercalation 57

4.2.1 Sodium bicarbonate as carbonate source 57

4.2.2 Sodium carbonate as carbonate source 59

4.2.3 Air as carbonate source 64

4.2.4 CO_2 (g) as carbonate source 66

4.2.5 Dry ice as carbonate source 69

4.2.6 Use of calcite as carbonate and calcium source 70

4.3 Overall synthesis 72

5 Conclusions and recommendations 74

5.1 Precursor: katoite synthesis 74

5.2 Carbonate intercalation 75

5.3 The use of calcite as combined calcium and carbonate source 67

6 References 78

Appendix A: Rietveld refinement 84

Appendix B: FE-SEM micrographs 86

List of Figures

Figure 1: Illustration of layered double hydroxide structure and general formula (Forano *et al.*, 2006: 1022).....4

Figure 2: General hydrocalumite structure with M representing the interlayer anion (Wen *et al.*, 2015).....6

Figure 3: LDH applications (Cavani *et al.*, 1991). 8

Figure 4: Environmental applications of LDH (Forano *et al.*, 2006: 1064)...9

Figure 5: Typical X-ray pattern for LDHs (Goh, Lim & Dong, 2008). 10

Figure 6: XRD patterns for crystalline solid, amorphous solid/liquid and monatomic gas comparison (Cullity, 1956: 101). 11

Figure 7: X-ray diffraction Bragg's law geometrical illustration(Pecharsky & Zavalij, 2009: 143).....12

Figure 8: Unit cell axis with h,k,l indices indicated (Scintag, 1999).....13

Figure 9: LDH structure indicating basal spacing and unit cell illustration (Goh, Lim & Dong, 2008). 13

Figure 10: TGA results for hyrdocalumite, top: hydrothermal method (HC-SM), bottom: co-precipitation method (HC-COP) (Sánchez-Cantú *et al.*, 2013).....15

Figure 11: Scanning electron microscopic (SEM) image of general hexagonal platelet morphology of hydrotalcite (Kuang *et al.*, 2010). 17

Figure 12: SEM micrographs of hydrocalumite. Left: co-precipitation product, right: green synthesis method (Sánchez-Cantú *et al.*, 2013).....17

Figure 13: Cu_4Al_2-CO_3-LDH titration curve (Wiid, 2013). 19

Figure 14: Block diagram of effluent free hydrotalcite production (Labuschagne *et al.*, 2015).....24

Figure 15: Experimental setup of Büchiglasuster, Versoclave pressure reactor with controllers and Huber Petite Fleur Tango heater. .28

Figure 16: Katoite synthesis.....29

Figure 17: Temperature stability of katoite solubility and XRD results (Matschei, Lothenbach & Glasser, 2007). 30

Figure 18: Carbonate intercalation.....32

Figure 19: Temperature stability of hydrocalumite, solubility and XRD results (Matschei, Lothenbach & Glasser, 2007).....33

Figure 20: Experimental setup for intercalation with sodium and CO_2 gas sources. Left setup used for sodium bicarbonate, sodium carbonate and air. Right setup used for carbonation with CO_2 (g).....35

Figure 21: Dry ice experimental setup.....35

Figure 22: Katoite synthesis for various time intervals at 60 ºC. 40

Figure 23: Calcium and aluminium conversion to katoite at 60 ºC. 42

Figure 24: Katoite formation for various reaction times at 80 ºC. 43

Figure 25: Calcium and aluminium conversion to katoite at 80 ºC. 45

Figure 26: Katoite formation for various time intervals at 100 ºC. 46

Figure 27: Calcium and aluminium conversion to katoite at 100 ºC. 47

Figure 28: Katoite formation for various time intervals at 120 ºC. 48

Figure 29: Calcium and aluminium conversion to katoite at 120 ºC. 50

Figure 30: Aluminium hydroxide conversion. 51

Figure 31: Ca:Al ratio of katoite synthesis reactions. 52

Figure 32: SEM images showing deltoidal icositetrahedral morphology of katoite. a) 24-sided polyhedron bounded by (Fogg *et al.*, 2002b) faces. b) Basic solution grown katoite (Fogg *et al.*, 2002b). c) Dissolution-precipitation grown katoite.....53

Figure 33: SEM micrographs showing precursor formation morphology. 54

Figure 34: Katoite synthesis for at high and low time and temperature intervals. 56

Figure 35: Hydrocalumite synthesis for 2 h and 6 h reaction times. 58

Figure 36: Hydrocalumite synthesis for 10 h and 24 h reaction times. 58

Figure 37: Hydrocalumite synthesis for 2 h and 6 h reaction times. 60

Figure 38: Hydrocalumite synthesis for 10 h and 24 h reaction times. 61

Figure 39: Hydrocalumite synthesis at 60 ºC and 70 ºC. 61

Figure 40: TG and DTG analysis. 63

Figure 41: TGA data of $CaCO_3$ (Oniyama & Wahlbeck, 1995).....64

Figure 42: Katoite conversion for air experiments.....66

Figure 43: Hydrocalumite synthesis with CO_2 (g) as carbonate source. 67

Figure 44: Dry ice intercalation. 69

Figure 45: Hydrocalumite synthesis at varying time with calcite as carbonate source (van Graan, 2012).....71

Figure 46: Hydrocalumite synthesis with calcite as calcium and carbonate source. 71

Figure 47: Hydrocalumite produciton flow sheet. 73

Figure 48: FE-SEM micrographs of katoite formation at 60 ºC for 24 h reaction time.....86

Figure 49: FE-SEM micrographs for intercalation samples with sodium bicarbonate as carbonate source.....87

Figure 50: FE-SEM micrographs for intercalation samples with sodium carbonate as carbonate source. 88

List of Tables

Table 1: Precursor reaction conditions (van Graan, 2012). 30

Table 2: Precursor formation reaction conditions. 31

Table 3: Hydrocalumite reaction conditions (van Graan, 2012).....34

Table 4: Time and temperature reaction conditions for intercalation. 37

Table 5: Rietveld analysis of samples formed at 60 ºC.....41

Table 6: Rietveld analysis of the samples formed at 80 ºC. 44

Table 7: Rietveld analysis of the samples formed at 100 ºC. 47

Table 8: Rietveld analysis of the samples formed at 120 ºC. 49

Table 9: Rietveld refinement of samples derived from calcium hydroxide.57

Table 10: Quantitative results of carbonate intercalation from air.....65

Table 11: Quantitative results of carbonate intercalation from CO_2 (g). …68

Table 12: Quantitative results of carbonate intercalation from dry ice. ….70

Table 13: Quantitative results of sodium bicarbonate carbonate source....84

Table 14: Quantitative results of sodium carbonate intercalant source. 85

1. Introduction

Layered double hydroxides (LDHs) have attracted a large amount of attention in recent years as a result of its wide range of possible applications. This is mainly due to the ability to be tailored to a specific application due to their anion exchange capabilities. LDHs have unique properties such as anion capture (as a result of weak interlayer bonding), large surface area and thermal stability. (Cavani, Trifirò & Vaccari, 1991)

The main synthesis method used for LDHs production is the co-precipitation method. Metal salts are used as reagents which lead to several problems. These reagents are highly corrosive and lead to damage of processing equipment. On an industrial scale, large amounts of salt containing effluent is produced with this method. This effluent requires costly treatment before disposal and treatment is usually omitted. This is damaging to the environment (Duan *et al.*, 2008). There is a need to develop methods that are more environmentally friendly.

Methods in which metal oxides/hydroxides are used have been developed as greener alternatives to the co-precipitation method. One such a method is the dissolution precipitation method suggested by van der Westhuizen (2011) and van Graan (2012). This method is specifically aimed at the synthesis of hydrocalumite. There are two distinct steps to this method namely the precursor formation and intercalation.

The aim of this study was to investigate each step of the dissolution-precipitation method for the synthesis of carbonate-containing hydrocalumite. Synthesis parameters considered were reaction time, temperature and carbonate source with the goal of determining a set of conditions most promising to implement on a large scale commercial production facility. Short reaction times, low

temperatures, waste reduction and ease of synthesis were the focus points of the overall production. Lab scale experiments were conducted with use of a bench top reactor and simple hotplate setups. Temperatures were kept below 120 ^{o}C.

2. Literature

2.1 Layered double hydroxides

Layered double hydroxides (LDHs) are a group of natural and synthetic anionic clay materials. These materials have the general formula and layered structure illustrated in Figure 1. They consist of a metal hydroxide layer (brucite like in structure) that creates a net positive charge which is balanced with intercalated anions. These materials also contain various amounts of water which are hydrogen bonded to both interlayer anions and the hydroxide layers. Electrostatic interactions along with hydrogen bonds between layers and interlayer anions hold the layers together and form the 3D structure shown in Figure 1. (Auerbach, Carrado & Dutta, 2004: 373, Forano *et al.*, 2006: 1022).

It is possible to exchange interlayer anions and incorporate different metals into the layered structure by selecting the appropriate synthesis parameters. This property significantly increases the application possibilities of these materials. Applications include use as waste water treatment agents, polymer additives and basic catalysts. (Forano *et al.*, 2006: 1022).

Figure 1 indicates the various metals and interlayer anions that are theoretically possible and have been incorporated into LDHs. It is possible to synthesise LDHs with multiple cations in the layers expanding application possibilities even further (Jirátová *et al.*, 2002). The *x* in the general formula represents the molar fraction of M^{III} ions per total mole of metal ions which is suggested to be kept in a range of 0,2 to 0,4. The X represents the interlayer anion with charge q and n is the number of water molecules in the interlayer (Braterman, Xu & Yarberry, 2004: 391).

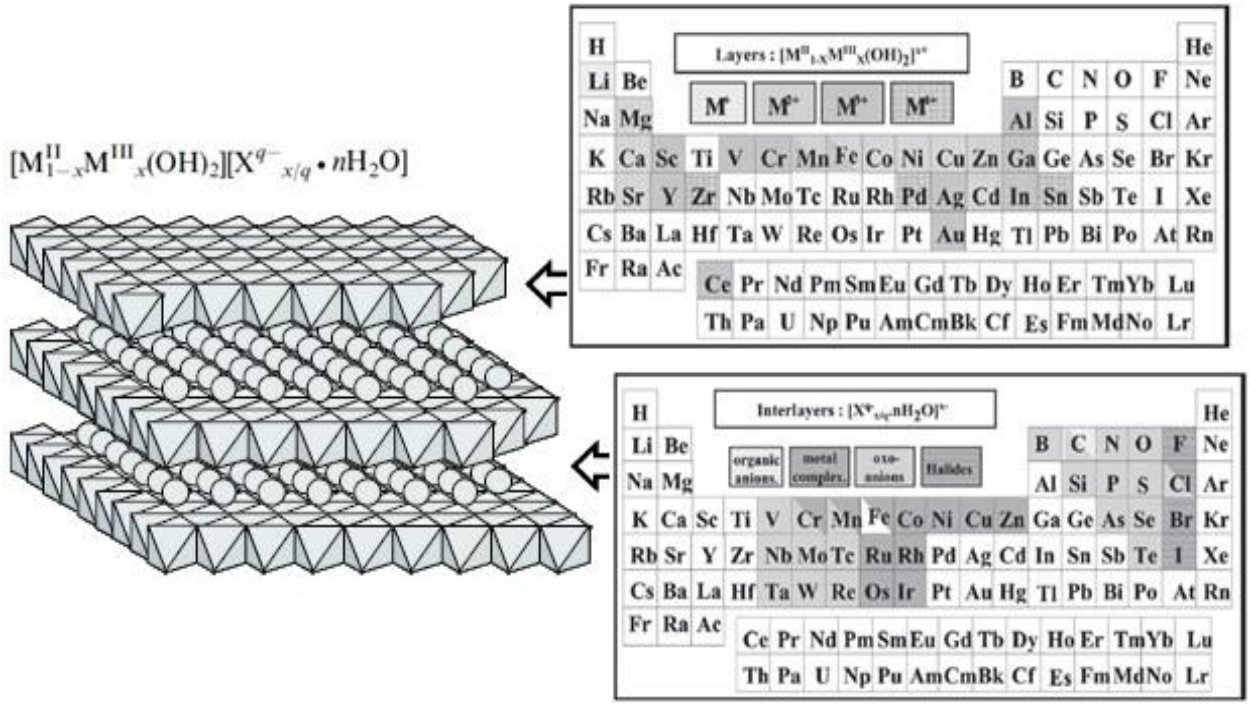

Figure 1: Illustration of layered double hydroxide structure and general formula (Forano *et al.*, 2006: 1022).

2.1.1 Hydrotalcite

Hydrotalcite is the most representative materials of the LDHs group. It occurs naturally as white, hydrous powder with a general formula of $Mg_6Al_2(OH)_{16}CO_3{\cdot}4H_2O$. Most of the synthetic LDHs resemble the natural occurring hydrotalcite and are widely referred to as hydrotalcite-like materials (HTlc) (Rousselot *et al.*, 2002).

The octahedra of the magnesium ions share edges to form infinite sheets which are stacked and held together by hydrogen bonds. These layers are a random arrangement of the divalent magnesium ions and trivalent aluminium with a net positive charge. The anion and water molecules are randomly located and free to move around the interlayer region by breaking and reforming bonds. It has many

applications and is widely used as a basic catalyst and additive material in polymers.

2.1.2 Hydrocalumite

Hydrocalumite share some common characteristics to hydrotalcite. In recent years interest in hydrocalumites has increased as a result of the benefits such as low cost, low toxicity and environmentally friendly preparation (Razvan *et al.*, 1993). Hydrocalumite consists of octahedra of calcium and aluminium hydroxides that share edges to form layers which are bi-dimensional with general formula of $[Ca_2M^{3+}(OH)_6]^+[A^{n-}_{1/n} \cdot mH_2O]^-$ (Rousselot *et al.*, 2002; López-Salinas *et al.*, 1996).

The structure (Figure 2), is similar to that of hydrotalcite, except that the laminar calcium and aluminium octahedra are not randomly arranged but orderly accommodated in the layers (Allmann, 1970). The brucite-like, or rather portlandite-like ($Ca(OH)_2$), layers are an ordered arrangement of Ca^{2+}, seven coordinated, and M^{3+} ions, six coordinated. The 7^{th} apex or the Ca-polyhedron is an interlayer water molecule. It is assumed that the ordered arrangement of hydrocalumite like materials are due to the size difference between Ca^{2+} and typical M^{3+} ions in a fixed ratio of 2:1. (Rousselot *et al.*, 2002; Tatematsu *et al.*, 1995).

Hydrocalumites have attracted much less attention in literature compared to hydrotalcite as a result of the relative difficulty in synthesising pure forms as well as less efficient calcination and rehydration behaviour (Rosenberg & Armstrong, 2005). Earlier investigations into calcium aluminates has been done mainly by the cement industry as a result of its importance in development and control of cement's chemical resistance and strength (Rosenberg & Armstrong, 2005).

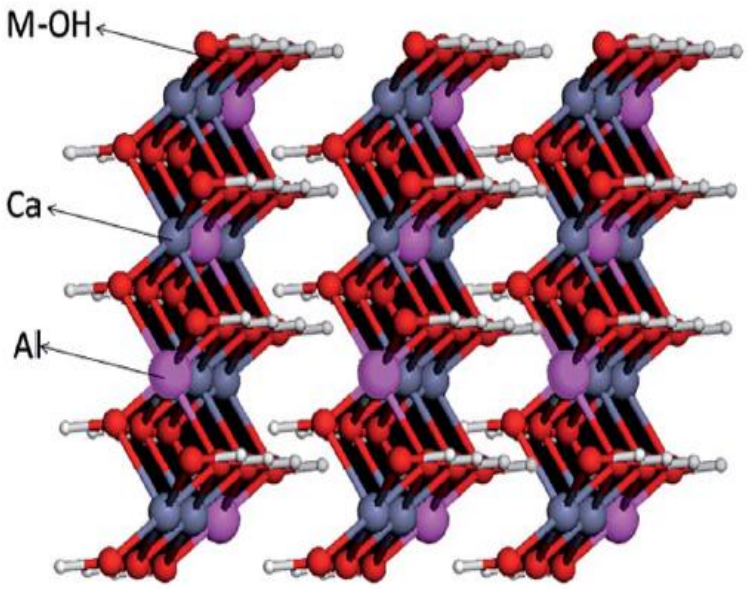

Figure 2: General hydrocalumite structure with M representing the interlayer anion (Wen *et al.*, 2015).

In the production process of alumina, hydrocalumite is formed as an unstable intermediate compound in Bayer liquors during the causticisation step (Rosenberg, Wilson & Roworth, 2013). Hydrocalumite with carbonate anion is also referred to as monocarboaluminate in studies regarding portlandite cement (Matschei, Lothenbach & Glasser, 2007).

2.1.3 Interlayer water and anions

Anions generally incorporated into the layered structure of hydrocalumite include for example Cl^-, NO_3^-, NO_2^-, OH^-, CO_3^{2-}, CO_4^{2-}. The carbonate ion is one of the most stable intercalants especially in high pH solutions. Its preferential intercalation can result in problems for cases where it is not the desired anion. In these cases synthesis is commonly conducted in a nitrogen environment. (Braterman, Xu & Yarberry, 2004: 380).

The localisation of water molecules to Ca-sites result in a well ordered structure of the interlayer and yields a better defined anion structure environment with sharper structural phase transitions than for hydrotalcite (Kirkpatrick *et al.*, 1999). The amount of water molecules in hydorcalumite is generally 15 or less and can range up to 20 depending on their production method (Tatematsu *et al.*, 1995).

2.1.4 Applications

LDHs have many potential applications in a wide range of areas such as photochemistry, electrochemistry, catalysis, biomedical etc. Some of these applications are summarised in Figure 3 below. These compounds can be used as synthesised but are frequently calcined to fit the application. Calcination of LDHs result in valuable properties such as high surface area, basicity, thermal stability and allows for exploitation of the memory effect (Forano *et al.*, 2006: 1029).

LDHs also have a wide range of environmental applications which is discussed in detail in the *Handbook of Clay Science* (Forano *et al.*, 2006: 1063-1065). Some of these applications are summarised in Figure 4. The hydrocalumite structure is very close to that of AFm (alumina, ferric oxide, monosulfate) phase which occur in hydrated cement and has been proposed to be a potential concrete hardening accelerator.

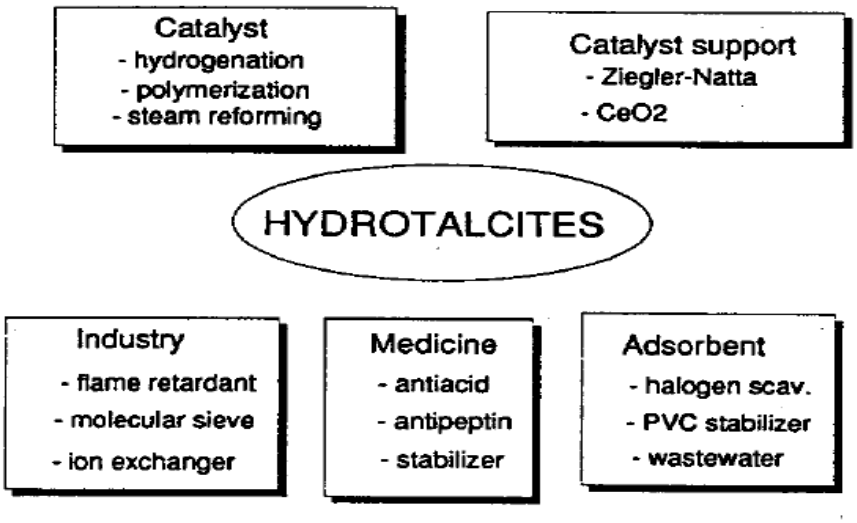

Figure 3: LDH applications (Cavani *et al.*, 1991).

Pure hydrocalumite, with no $CaCO_3$ contaminant, containing cements proved to have enhanced performance with regard to early compressive and flexural strength when compared to pristine concrete samples. Based on these results Wongaiyakawee *et al.*(2012) prepared hydrocalumite/polymer nanocomposites to improve physical properties in the matrix, to determine if the same effects would apply.

LDHs are also being explored as second generation flame retardants in polymers due to its capability of high smoke suppression and low/non toxicity. This makes it preferable compared to the halogen-based counterparts (Kuang *et al.*, 2010). Hydrocalumite has also been proven to be a precursor for calcium aluminium mixed oxide used as a catalyst in biodiesel production (Kocík, Hájek & Troppová, 2015).

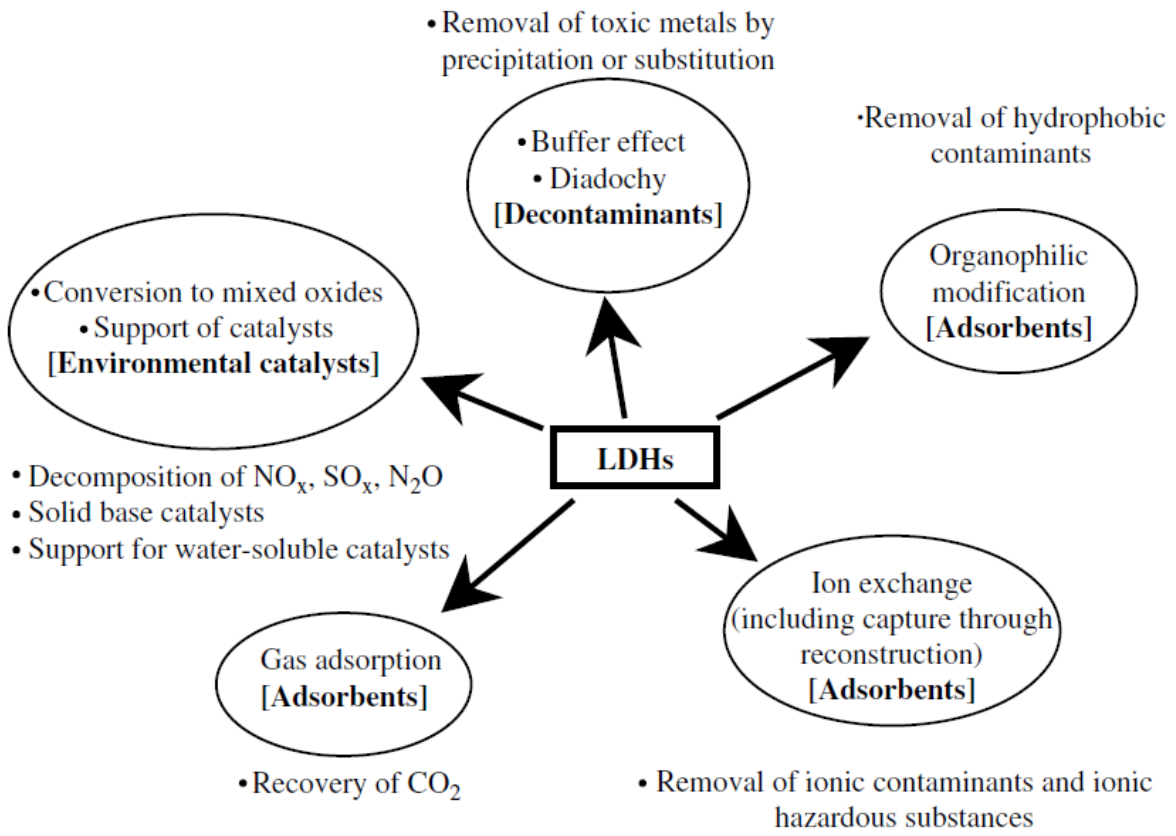

Figure 4: Environmental applications of LDH (Forano *et al.*, 2006: 1064).

2.2 Analysis and characterisation

2.2.1 X-ray diffraction (XRD)

2.2.1.1 Qualitative XRD

X-rays can interact with a crystalline phase and produce a diffraction pattern. Each crystalline phase has its own unique pattern and in a mixture each phase will produce its own pattern independent form others. X-ray diffraction patterns serve as a fingerprint and is ideal for characterisation of phases present in a crystalline sample. (Cullity, 1956) XRD is the main tool for identification of LDH structures. The general XRD patterns of LDHs are a strong series of basal reflections conventionally indexed which correspond to the successive orders of the interlayer spacing (Auerbach, Carrado & Dutta, 2004: 400).

XRD patterns for LDHs are usually generated from randomly orientated powder samples. A typical LDH XRD pattern is shown in Figure 5 below. Here one can see the characteristic XDR pattern for LDH materials. At low 2**θ** values it has sharp or broad reflections which become less intense at higher 2**θ** values. (Goh, Lim & Dong, 2008).

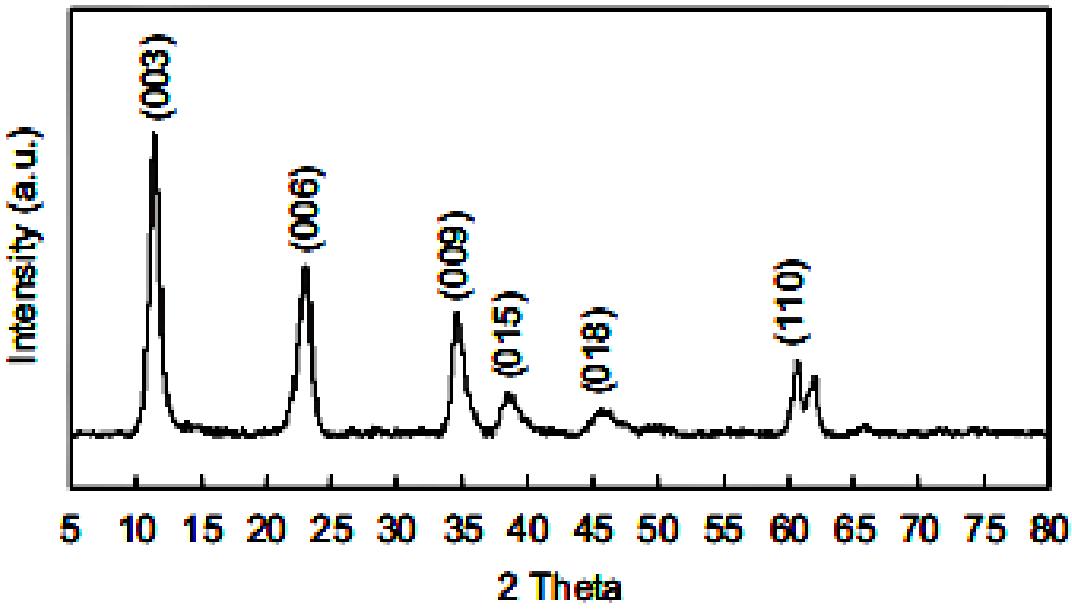

Figure 5: Typical X-ray pattern for LDHs (Goh, Lim & Dong, 2008).

Phases are identified by comparing the spectra to standards. Relative estimation of proportions of different phases in multiphase systems are calculated by comparing peak intensities of the identified phases. The intensity of the peaks are an indication of the total scattering from each plane in the crystal structure. This is directly dependent on distribution of a specific atom in the structure. (Connolly, 2012) Difficulties in X-ray data interpretation are a result of poor crystallinity and disordered stacking of the layers causing the diffraction lines to be broad and asymmetric (Cavani, Trifirò & Vaccari, 1991).

Figure 6 illustrates XRD patterns of crystalline, amorphous materials and monatomic gases. Monatomic gases are not relevant to this study. XRD patterns for LDH materials of low crystallinity are a combination of the crystalline and amorphous spectra.

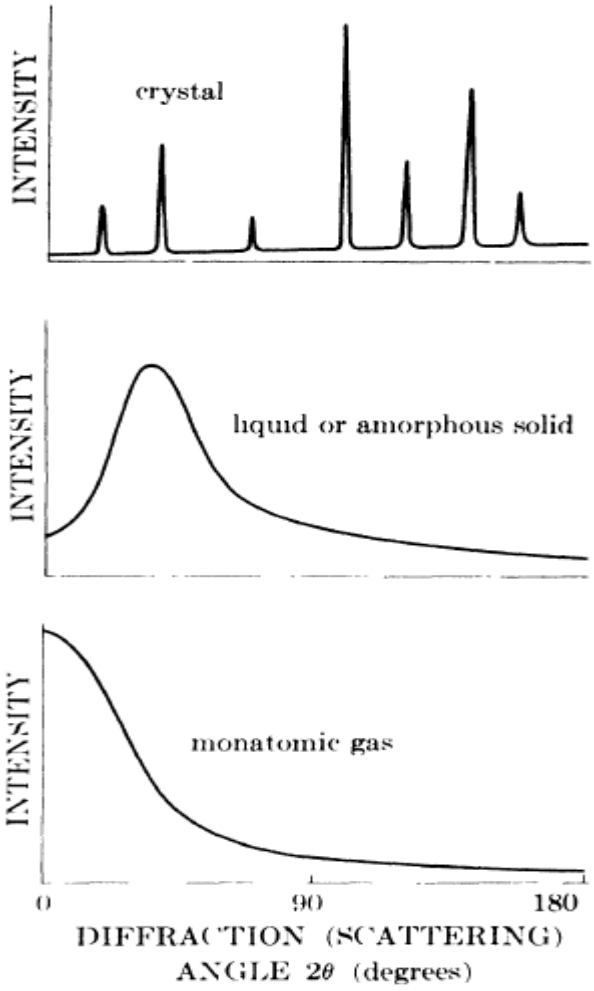

Figure 6: XRD patterns for crystalline solid, amorphous solid/liquid and monatomic gas comparison (Cullity, 1956: 101).

Bragg's law (Equation 1) can be used to calculate the inter layer spacing of LDH layers. Bragg's law is geometrically illustrated in Figure 7. The distance between atomic layers in the crystal is represented by the **d** variable, lambda (**λ**) is the wave length of the incident X-ray beam and **n** is an integer.

When an X-ray beam incident on a pair of parallel planes, separated by an interplanar **d** spacing, the two beams make an angle **θ** with the planes.

Bragg's law: $$\mathbf{n}\,\lambda = 2\,\mathbf{d}\,\sin(\boldsymbol{\theta}) \quad (1)$$

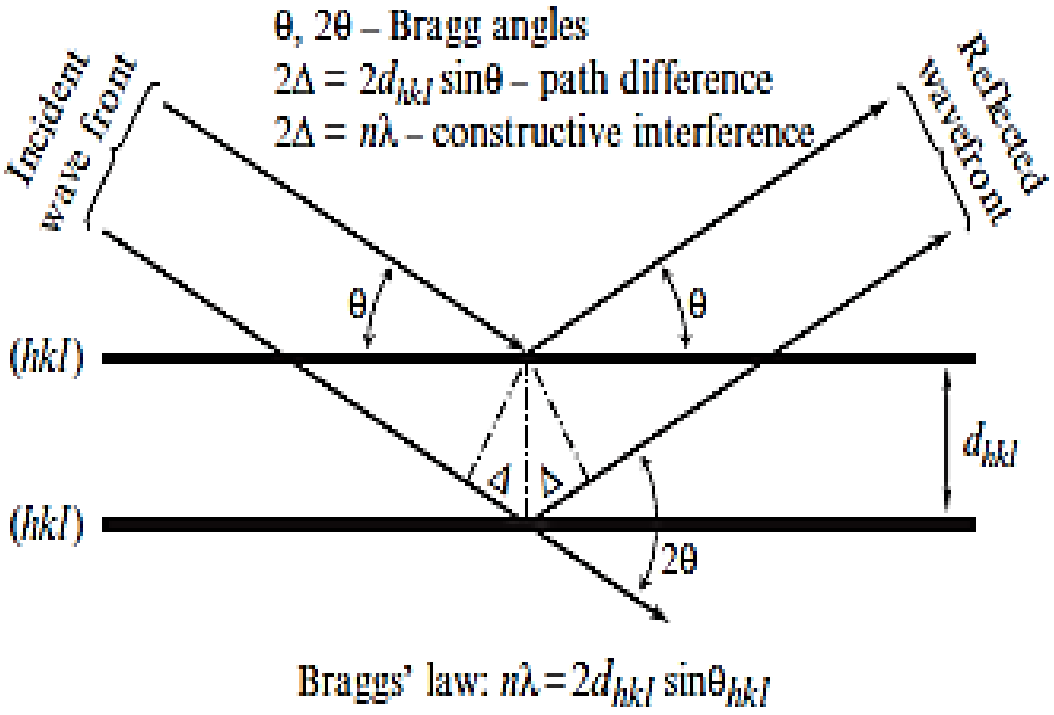

Figure 7: X-ray diffraction Bragg's law geometrical illustration (Pecharsky & Zavalij, 2009: 143).

The brucite like sheets of LDH can stack in three different orientations, either rombohedral, monoclinical or hexagonal. Hydrocalumite generally has a rombohedral space group with R-3 symmetry. The parameters of the unit cell and layer spacing, shown in Figure 8 and Figure 9, are **a** and **c** = 3**c**', and **c**' corresponds to the thickness of the layer and one interlayer, it is dependent on the anion size and orientation. The M^{2+}/M^{3+} ratio can be derived from the **a** parameter which is calculated with $\mathbf{a} = 2\,\mathbf{d}_{110}$. The $\mathbf{d}_{110}$ required to calculate **a**, corresponds

to the d spacing of the 110 reflection. The approximate chemical formula can be calculated form these parameters along with elemental analysis.

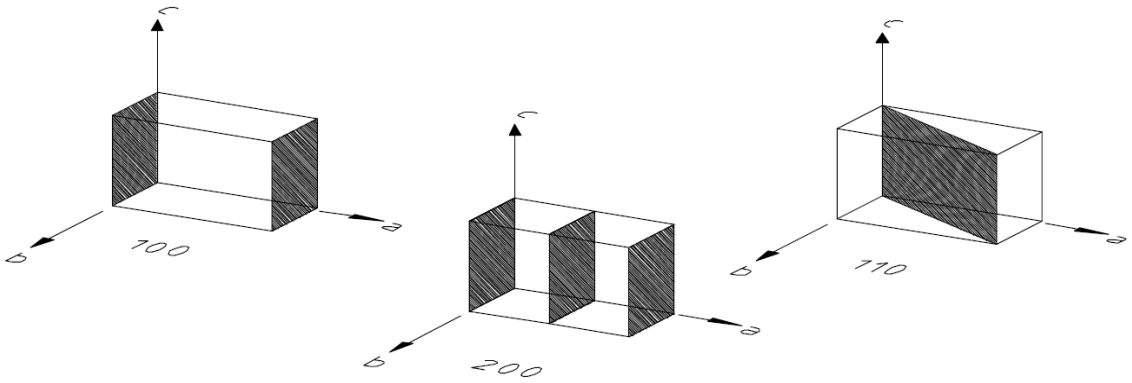

Figure 8: Unit cell axis with h,k,l indices indicated (Scintag, 1999).

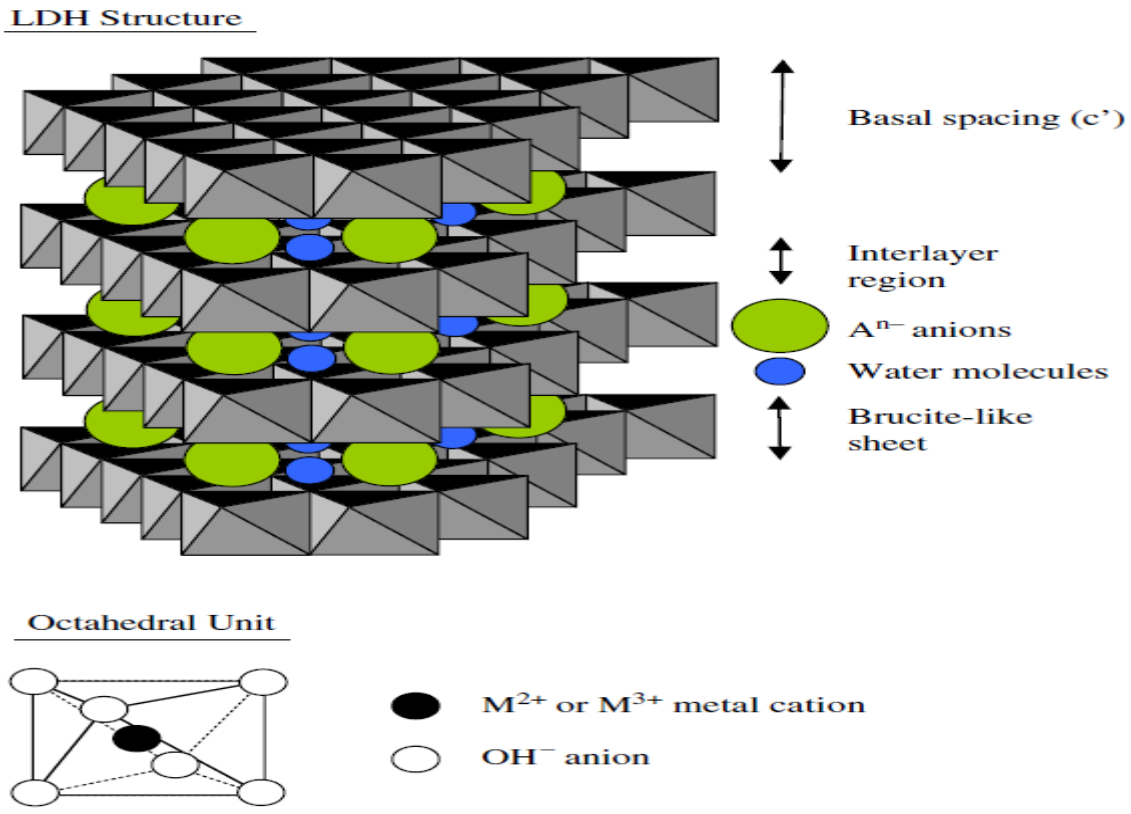

Figure 9: LDH structure indicating basal spacing and unit cell illustration (Goh, Lim & Dong, 2008).

2.2.1.2 Quantitative XRD analysis

Quantitative phase analysis is a powerful method with which the quantities of multicomponent crystalline materials can be determined. A successful quantitative analysis requires precise and accurate identification of the positions and intensities for a given diffraction pattern. There are a few variations of methods available to conduct a quantitative analysis based on peak intensity ratios. (Connolly, 2012).

The most successful of these methods result from addition of an internal standard where the area ratios of standard and present phases are then calculated. The full pattern analysis or Rietveld refinement method determines quantities not only form the intensities but the entire diffraction pattern, thus it is capable of much greater accuracy and precision. This method requires information regarding the crystal structure of all phases present in the sample. (Connolly, 2012).

2.2.2 Thermogravimetric analysis (TGA)

Thermogravimetric analysis entails heating a sample at a constant rate and recording the mass as it changes. Different types of water and hydroxyl groups and other volatile complexes in the clay matrix are liberated with increase in temperature. TGA can be used to qualitatively estimate the binding energies of the various waters and hydroxyls to characterise the mineral. (Auerbach, Carrado & Dutta, 2004).

The thermal behaviour of LDHs are characterised by two main endothermic transitions. At low temperatures the reversible loss of interlayer water without the collapse of the structure along with loss of hydroxyl groups from the layer. This is followed by a loss of anions at higher temperatures. These transitions depend on many factors such as the ratio of divalent and trivalent ions in the layer, anion type, hydration, drying and other heat treatments. LDHs containing

aluminium have the first transition in the range of 97 °C to 297 °C and the second 347 °C to 477 °C (Cavani, Trifirò & Vaccari, 1991).

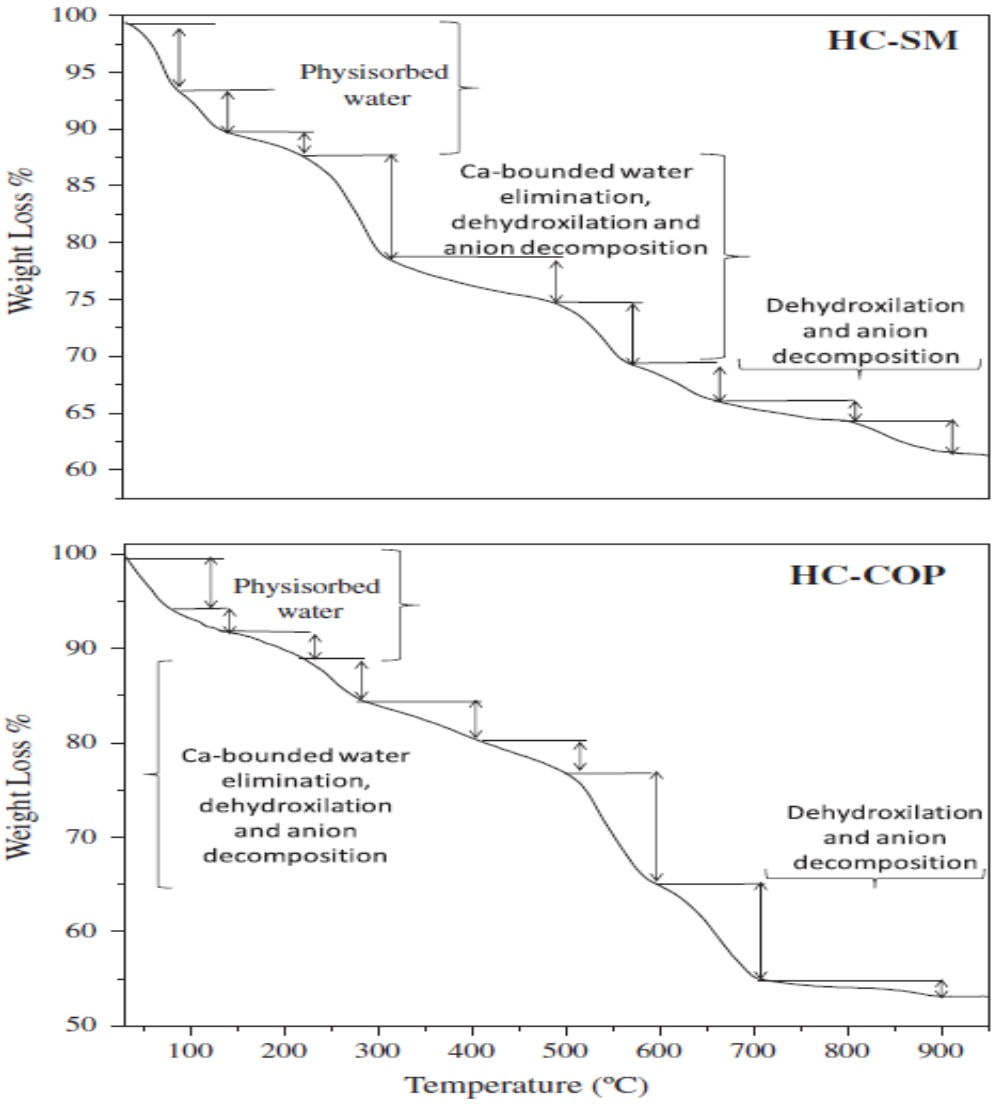

Figure 10: TGA results for hyrdocalumite, top: hydrothermal method (HC-SM), bottom: co-precipitation method (HC-COP) (Sánchez-Cantú *et al.*, 2013).

Two TGA graphs are shown in Figure 10 for hydrocalumite produced with an environmentally friendly method, discussed in section 2.3.5, and the conventional co-precipitation method. There are three main regions of significant mass loss

for both of the samples. These regions are indicated and it is clear that there is not a significant change in mass loss of each region when the two synthesis methods are compared except that the transitions of the hydrothermal sample are more defined. (Sánchez-Cantú *et al.*, 2013).

2.2.3 Scanning electron microscopy (SEM)

SEM allows one to observe the shape of LDH crystallites and the manner in which they aggregate. Crystalline growth for inorganically intercalated LDHs, is along the **a** and **b** axes, perpendicular to stacking direction. This maximises the exposure of hydroxyl groups to the aqueous phase since the hydroxides of the metal hydroxide layer are found in the **ab** plane. In general LDHs containing inorganic anions have hexagonal platelet shape and those containing carbonates have a diameter of about 1 µm. (Auerbach, Carrado & Dutta, 2004: 418).

Figure 11 shows the general hexagonal platelet morphology which is expected form LDHs that are hydrothermally produced. Figure 12 shows the morphology of hydrocalumite produced by two methods. The co-precipitation product shows low crystallinity compared to the product of the green synthesis method as discussed in section 2.3.5.

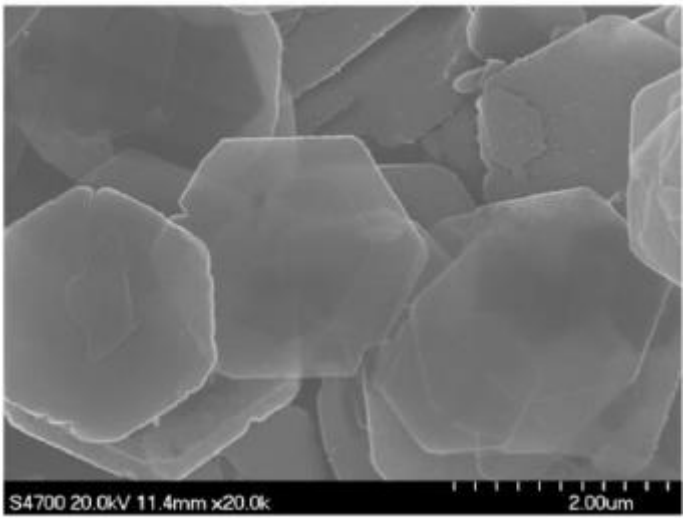

Figure 11: Scanning electron microscopic (SEM) image of general hexagonal platelet morphology of hydrotalcite (Kuang *et al.*, 2010).

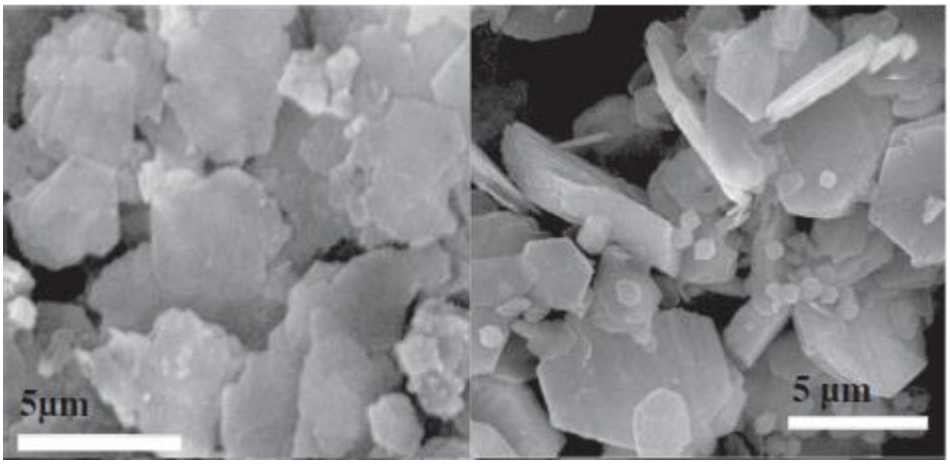

Figure 12: SEM micrographs of hydrocalumite. Left: co-precipitation product, right: green synthesis method (Sánchez-Cantú *et al.*, 2013).

2.3 Synthesis of LDHs

Production of LDHs is affected by many variables such as type of reagents, reaction time, temperature, pH, stirring speed and solution concentration. Altering any of these parameters can significantly change the physical and chemical properties of the product. Parameters need to be tailored to the specific application and characteristics required.

Most methods are based on the concept of mixing together soluble metal salts in a basic environment and incorporation of the selected anion which then results in precipitation of the desired phase. Main LDH synthesis methods include co-precipitation, urea hydrolysis and sol-gel synthesis. Co-precipitation is most widely implemented for the synthesis of hydrotalcite and hydrocalumite type LDHs. (Messersmith & Stupp, 1992).

2.3.1 Co-precipitation

There are two main co-precipitation methods that are used to prepare LDHs namely the constant pH titration and buffer precipitation. These methods involves mixing the relevant metal salts in a base solution, in the presence of the desired anion (Auerbach *et al*, 2004:376). Supersaturation of the precipitating agent is rapidly reached and maintained which leads to continuous nucleation and simultaneous growth of the particles. This results in a wide particle size distribution (Forano *et al*, 2006). It has been proven to be one of the most reliable and reproducible methods of synthesis (Cavani *et al*, 1991).

2.3.1.1 Constant pH titration

This method as described by Miyata (1980) entails the simultaneous and gradual addition of metal cation solution and base solution to a flask under vigorous stirring. The titration tempo of the solutions is adjusted to keep the mixed solution at a relatively constant pH typically around 10. The synthesis pH selected should be higher than the pH at which the desired LDH precipitates. The LDH phase is preferentially precipitated as the metal cations and anion disperse into the basic medium. The precipitation occurs close to the region of the metal salt inlet. In this area the pH is not constant and the formation of the least soluble metal hydroxide is rapid. (Auerbach *et al*, 2004:376).

2.3.1.2 Buffer Precipitation (Varying pH)

This method entails slow titration of a base solution, typically NaOH, into a solution containing metal salts and anion (it is fully described by Boclair & Braterman (1999)). This method gives insight into the influence of pH on LDH systems. The resultant titration curve which is generally observed for LDH has two distinct plateaus as seen in Figure 13 with sharp transitions in between. Each transiton represents conversion form one stable phase to another.

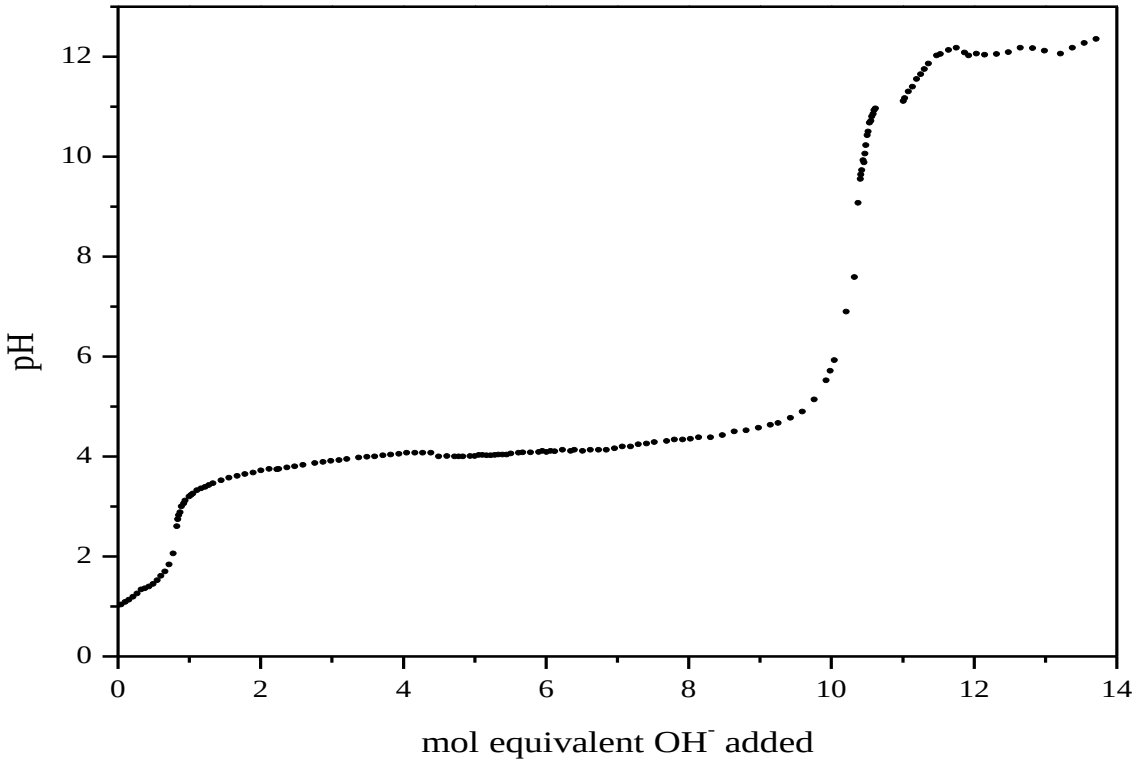

Figure 13: Cu_4Al_2-CO_3-LDH titration curve (Wiid, 2013).

The first plateau corresponding to the formation of the metal hydroxide with the lowest solubility and the second one represents the formation of LDH. For aluminium containing systems the first plateau is the formation of aluminium hydroxide ($Al(OH)_3$) approximately at a pH of 4. The divalent metal and additional hydroxide ions cling to the precipitated $Al(OH)_3$. This is followed by rearrangement, hetero nucleation of LDH and dissolution of the $Al(OH)_3$

precipitate between the first and second plateau regions. (Auerbach *et al*, 2004:376).

2.3.2 Urea hydrolysis

Urea is a weak Brønsted base which is highly soluble in water and has a number of properties that makes it a good agent for precipitating from a homogeneous solution. The use of a base retardant separates the nucleation from the growth steps and aging is prevented from the start. Urea hydrolysis occurs in two steps. The first step is the rate determining step which is the formation of ammonium cyanate. The second step is the hydrolysis of cyanate into ammonium carbonate which can be controlled by temperature. (Forano *et al.*, 2006: 1028-1029).

These two reactions, depending on the temperature, gives a pH of around 9 which is suitable for precipitating a large range of metal hydroxides. The LDHs formed with this method have large well crystallised hexagonal platelets with a narrow particle size distribution. Particle size is controlled by the reaction temperature and concentration of reagents. (Costantino *et al.*, 1998).

2.3.3 Sol gel

This process involves formation of a mobile colloidal suspension by dissolving metal alkoxides in an organic solvent under reflux. Water is slowly added causing internal cross linking to form a gel. The resultant product has good homogeneity, stoichiometry control, high surface area and porosity. (Auerbach, Carrado & Dutta, 2004: 376).

2.3.4 Post synthesis treatment

LDHs synthesised with conventional methods tend to have poor crystallinity and the metal hydroxide layers are disordered. Post synthesis or in situ treatments are generally used to improve these characteristics. Post synthesis methods include

aging through Ostwald ripening where smaller particles dissolve, reform and grow to larger more perfect particles. Hydrothermal, microwave and ultrasonic treatments are also used to increase crystallinity and particle size. (Auerbach *et al*, 2004:386).

After the desired LDHs has been prepared with the traditional methods discussed above the products are generally filtered to remove excess anions that could lead to possible further reaction. This washing process results in an effluent stream typically containing sodium salt that needs to be treated before disposal as it is harmful to the environment. Due to high energy cost of evaporation the salt containing mother liquor is generally discharged directly which leads to environmental pollution. (Duan *et al*, 2008).

2.3.5 Synthesis from oxides/hydroxide

LDHs can be synthesised by hydration of metal oxides and/or hydroxides in the presence of an anion source, where LDHs form through a dissolution-precipitation process (Auerbach, Carrado & Dutta, 2004: 382-383). The main distinguishing factor of hydrothermal synthesis is that one does not start with pre-dissolved metal cations as in other methods. The metal oxides and hydroxides have low solubility in water at ambient conditions. To allow for dissolution of the reagents higher temperatures, longer reaction times and possible pre-treatment of reagents are required for successful synthesis (Duan *et al.*, 2008).

Another approach as explained by Goh, Lim & Dong (2008), is the reconstruction method which exploits the memory characteristic of LDHs. The calcination of a LDH with a thermally liable anion in the interlayer results in an amorphous oxide mixture. The calcined material is then rehydrated in the presence of the anion to be intercalated.

This method is limited to the use of a starting materials that contain a thermally liable anion and limiting the calcination temperature to below the point where spinel formation occurs which are resistant to rehydration. (Auerbach, Carrado & Dutta, 2004: 376).

A number of methods have been developed for the production of hydrocalumite from oxides and hydroxides. One of the earliest methods was developed by Carlson and Berman (1960) where calcium aluminate, calcium hydroxide and alumina reagents were mixed in solution along with sodium carbonate and allowed to react for two months. The hydrocalumite product formed contained small amounts of calcite, gibbsite and tricalcium aluminate hexahydrate (katoite). Great care was taken to pre-treat the oxide/hydroxide reagents by heating calcite to form calcium oxide. The anhydrous aluminate used was prepared by heating calcite along with alumina at 1250 ^{o}C for several hours. This is a high energy consumption process.

Duan *et al.* (2008) patented an environmentally friendly method in which metal hydroxides are mixed with water in a reactor with addition of CO_2 in the form of gas or dry ice. The filtration and washing stage of synthesis is omitted and samples dried at 70 ^{o}C. In the patent examples, hydrocalumite was synthesised with this method within 12 h at 250 ^{o}C.

Sánchez-Cantú *et al.* (2013) used an environmentally friendly method for synthesis of nitrate containing hydrocalumite. Calcium hydroxide and boehmite (AlO(OH)), a more reactive aluminium hydroxide species, are used to synthesise hydrocalumite. The boehmite is dissolved in an acid solution of HNO_3 and reagent mixtures pH was adjusted with ammonium hydroxide. This method is claimed to be green in the sense that the final slurry does not require washing to eliminate the unreacted ions as in the conventional co-precipitation method.

Water use is also reduced to a minimum. This material showed similar catalyst activity to the co-precipitation product and can be considered as a viable method of production.

Both van der Westhuizen (2011) and van Graan (2012) proposed a two-step dissolution-precipitation synthesis route. The main differences between this method and those already established is that the synthesis occurs in two distinct steps and requires no pre-treatment of reagents. The first step is the dissolution of calcium oxide and aluminium hydroxide, in the absence of a carbonate source, with subsequent precipitation of a mixed metal hydroxide precursor (katoite ($Ca_3Al_2(OH)_{12}$) and portlandite ($Ca(OH)_2$)). The second step entails dissolution of the precursor in the presence of the anion source followed by precipitation of the desired LDH material. It was concluded that the dissolution of aluminium hydroxide is the limiting step in the synthesis and high conversions where reached after 2 days at 70 ^oC with similar results within 1 hour at 180 ^oC.

Similar work was done by Wen *et al*. (2015), who synthesised hydrocalumite form A.R. grade calcium hydroxide, aluminium hydroxide and sodium carbonate in a two-step process. The first step is the reaction step between calcium- and aluminium hydroxide and the second step is the addition of the carbonate source which they called the crystallisation step. They investigated the reaction time of each step and found for both 4 hours was required to produce hydrocalumite. The product compounded with PVC increased the thermal stability significantly. No indication was given about the temperature at which the two steps were conducted. They stated that the reaction products were aged for 20 hours at 60 ^oC.

2.3.6 Industrial scale production

It is clear that a wide range of applications are possible and the popularity of hydrocalumite is constantly increasing as a result of their versatility and environmentally friendly characteristics. With this increase of interest it is of value to investigate environmentally friendly synthesis methods which can be implemented on an industrial scale. With regards to the synthesis of hydrotalcite the environmentally friendly synthesis procedure suggested by Labuschagne *et al*. (2015) is illustrated in Figure 14. This process entails use of run of the mine materials as reagents with no pre-treatment required.

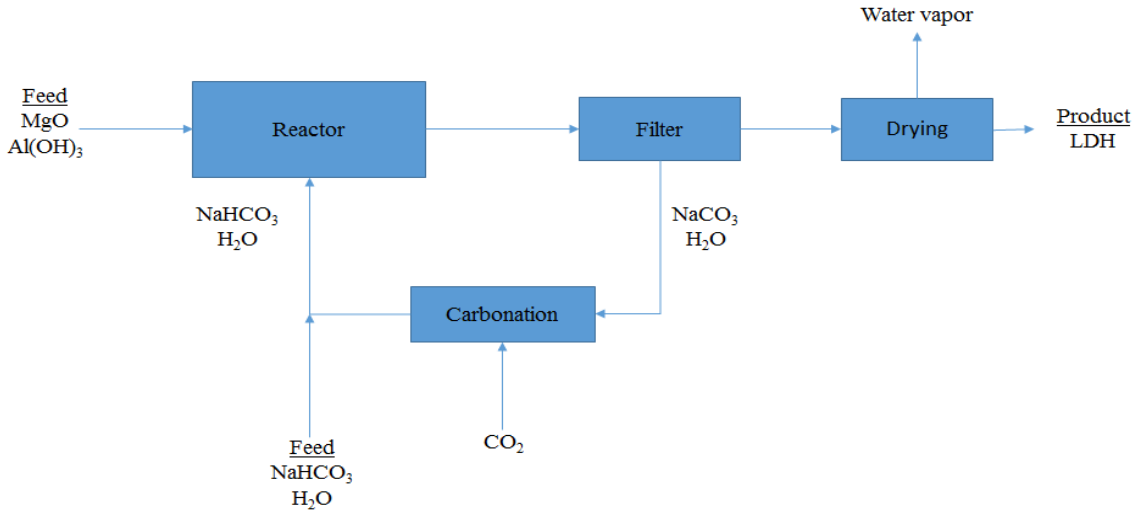

Figure 14: Block diagram of effluent free hydrotalcite production (Labuschagne *et al.*, 2015).

All process water is recycled and the carbonate source is reused in the system. In doing so it reduces the amount of raw materials required and overall water demand. The energy requirement is significantly reduced compared to that brought upon by high temperature pre-treatment of reagents required in many other hydrothermal hydrotalcite productions. (Mitchell *et al.*, 2007; Xu & Lu, 2005; Roy & Osborn, 1953).

A similar process was suggested by Wen *et al.* (2015) for the production of hydrocalumite for use as a thermal stabiliser in PVC (see Section 2.3.5 above). The resultant effluent stream of NaOH is suggested to be directly used in the production of aluminium hydroxide stripping allowing for a zero discharge process. Kuwahara & Yamashita (2015) developed a method of using blast furnace slag to produce hydrocalumite and in so providing a sink for the otherwise underutilised by product of iron production.

3. Experimental

Finding optimal reaction conditions for the synthesis of a desired LDH is very complex as many factors need to be considered. Temperature and pH should be in such a range that the metal oxides dissolve and re-precipitates as the desired LDH. Reaction time should be sufficiently long to allow for dissolution of reagents, re-precipitation and growth of the LDH crystals. Considering the discussion in Section 2.3.5 it is evident that the interest in the use of hydrocalumite-like materials is increasing and there is a movement towards more environmentally friendly production methods.

The methods discussed in Section 2.3.5 show that a variety of starting materials, reaction times and temperatures have been explored. All of them are however not completely based on green chemistry principles. It is the aim of this study to determine the effects of reagents, time and temperature on the synthesis of carbonate-containing hydrocalumite based on the two step dissolution-precipitation method described by van der Westhuizen (2011) and van Graan (2012).

Environmental considerations and green chemistry synthesis principles are also of great importance. Experimental setups were designed to generate as much data, as quickly as possible to identify reaction paths and conditions that are most viable for further optimisation and implementation in a large scale industrial production facility. Important factors for industrial synthesis include fast reaction rates at reduced temperature conditions whilst ensuring ease of synthesis and high product yields.

Experiments were based on the results obtained by van der Westhuizen (2011) and van Graan (2012) who found that:

- Hydrocalumite can be synthesised through two distinct dissolution-precipitation steps with metal oxide/hydroxide reagents.
- Elimination of carbonate source in the first step allows for the formation of katoite, a precursor material.
- Dissolution of the precursor in the presence of a carbonate source result in yield of the LDH product. (An additional calcium source is needed for complete conversion to LDH.)
- Aluminium dissolution was confirmed to be the limiting or rate determining step in the synthesis.

The two steps of the dissolution-precipitation method entail the precursor formation step followed by intercalation of the selected anion. Each step was investigated separately with regards to time and temperature conditions. Carbonate was the only anion incorporated and various sources were tested. An additional experiment with the use of calcite as additional calcium and carbonate source was conducted. Experimental conditions of these synthesis steps are discussed blow.

3.1 Precursor: katoite synthesis

3.1.1 Apparatus

The first part of the synthesis, the precursor synthesis, was conducted in a Büchiglasuster Versoclave pressure reactor fitted with a 1 L vessel, magnetic drive and top mount mixing shaft and impeller. It was fitted with a sampling tube that reaches a quarter-length from the bottom of the reactor which allowed for insitu sampling. Two manual dosing pods were fitted on top of the vessel. The reactor was connected to a Huber Petite Fleur Tango 1,5 kW heater and 0,48 kW cooler. This unit used silicone oil for indirect heating and Refrigerant-R290 for indirect cooling to control the sample temperature and was fitted with a circulation pump. Figure 15 shows the set up and operating specifications. All

the precursor synthesis experiments were conducted at the Leibniz-Institut für Polymerforschung Dresden e. V. under a collaboration agreement.

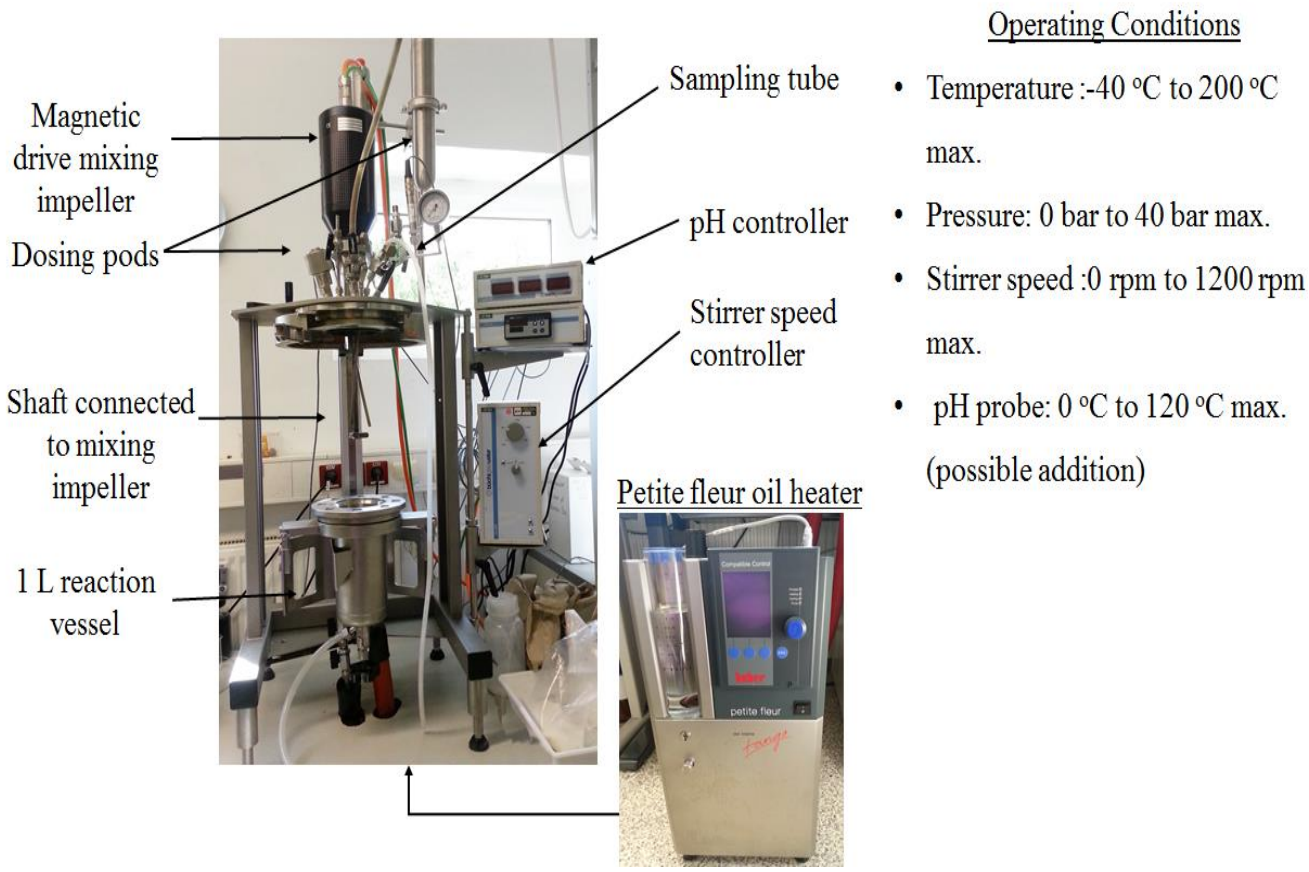

Figure 15: Experimental setup of Büchiglasuster, Versoclave pressure reactor with controllers and Huber Petite Fleur Tango heater.

3.1.2 Planning

Two calcium sources were tested (Figure 16). A temperature and time analysis was conducted for calcium oxide. Calcium hydroxide was tested at high and low temperature points based on initial experimental results obtained from calcium oxide.

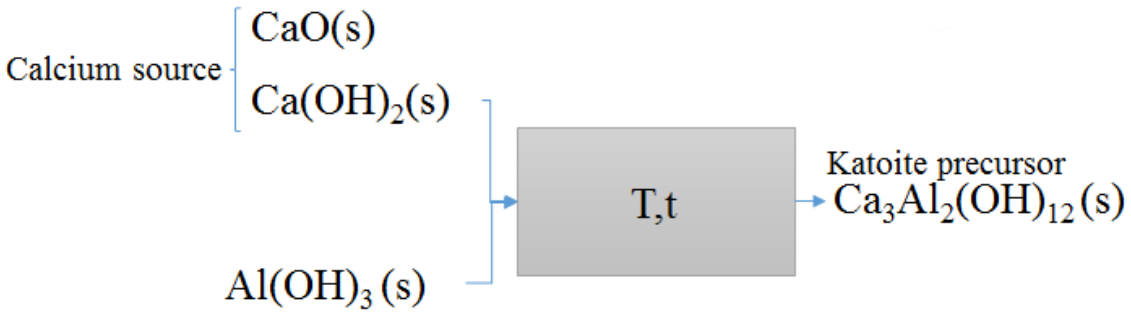

Figure 16: Katoite synthesis.

A full thermodynamic study on the components of portlandite cement was conducted by Matchei, Lothenbach & Glasser (2007). The temperature stability results for katoite (also known as hydrogarnet or C_3AH_6) are shown in Figure 17. The markers in the solubility figures below indicate experimental values and lines indicate calculated results of the thermodynamic models. Katoite is thermally stable over the range of temperature shown, 5 °C to 105 °C, considering that the solubility and crystallinity does not change significantly. At low temperatures, ~5 °C, some hydrocalumite, (also known as monocarboaluminate (Mc)) is present in the sample due to contamination form carbonate exposure.

Wen *et al*. (2015) investigated the time effect of both the precursor and intercalation steps and found 4 hours for each to be sufficient. A reaction time of 2 hours resulted in unreacted katoite and larger amounts of calcite formation. It was not stated at which temperature each step was performed but it was indicated that the products were aged at 60 °C for 20 hours.

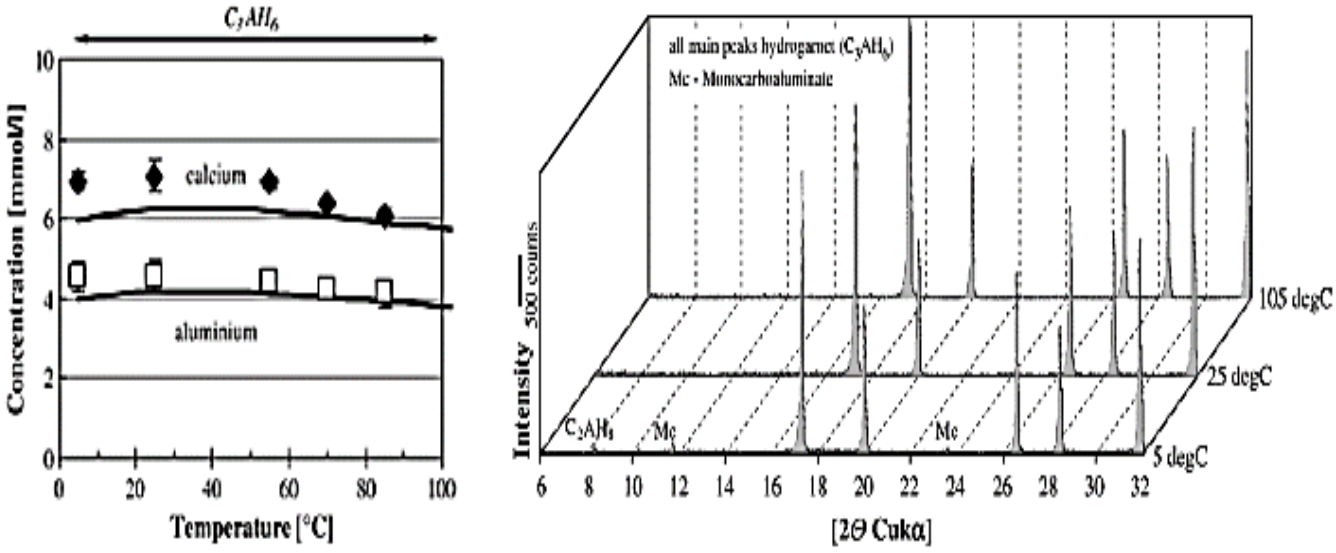

Figure 17: Temperature stability of katoite solubility and XRD results (Matschei, Lothenbach & Glasser, 2007).

The combined effect of time and temperature of each step has not yet been investigated thoroughly. Initial experiments were conducted by van Graan (2012) at conditions shown in Table 1. An increase in time and temperature resulted in an increase in conversion of reagents to katoite. Similar results were achieved at 120 ºC and 180 ºC. Considering these results a range of 60 ºC to 120 ºC for 5 min to 24 h was selected for precursor formation based on the thermal stability behaviour of katoite.

Table 1: Precursor reaction conditions (van Graan, 2012).

Temperature (ºC)	Time
70	2 h, 2 d
120	5 h
180	1 h

3.1.3 Method

Aluminium hydroxide and calcium source powder reagents were added in stoichiometric amounts, according to Equations 2 and 3, to water. This slurry was mixed for 5 min on a magnetic stirrer in a 2 L glass beaker, before adding the slurry to the reactor. A solids concentration, based on the expected product yield, of between 20 % and 30 % was suggested by van der Westhuizen (2011). An initial test resulted in insufficient mixing at 30 %. As a result, 20 % was selected and kept constant throughout. This slurry was mixed for 5 min on a magnetic stirrer plate in 2 L glass beaker, before adding the slurry to the reactor. Stirrer speed of 450 rpm was selected. This was the maximum speed at which the reactor could run for the precursor synthesis.

The rapid exothermal reaction of calcium oxide with water to form calcium hydroxide, Equation 4, raised the slurry temperature to approximately 95 °C. The reactor was preheated to 60 °C before the slurry was added. Reaction conditions are summarised in Table 2. No pH adjustments were made since the naturally high pH of calcium oxide and calcium hydroxide is sufficient for the dissolution of the aluminium phase (van Graan, 2012).

$$CaO + H_2O \rightarrow Ca(OH)_2 \quad (2)$$

$$3Ca(OH)_2 + 2Al(OH)_3 \rightarrow Ca_3Al_2(OH)_{12} \quad (3)$$

Table 2: Precursor formation reaction conditions.

Calcium source	Time	Temperature (°C)
CaO	10 min, 30 min, 1 h, 2 h, 4 h, 6 h, 8 h, 10 h, 24 h	60, 80, 100, 120
$Ca(OH)_2$	2 h, 24 h	60, 120

3.2 Carbonate intercalation

The ability to intercalate anions is one of the most important properties of LDHs. Some anions are more likely to be intercalated than others and carbonate is the most preferential (Forano *et al.*, 2006: 1033).

3.2.1 Planning

A bulk batch of katoite/calcium hydroxide was synthesised as discussed in section 3.1.2 at 120 ºC and 3 h. This was based on preliminary results which showed high conversion of reagents to katoite at these conditions. Where possible carbonate intercalation experiments were conducted in duplicate. Different carbonate sources as intercalants were tested in this step (Figure 18). A time and temperature analysis was done for sodium bicarbonate, sodium carbonate and carbonation from air. High and low temperature experiments were conducted for calcium carbonate and flow rate experiments were conducted with CO_2 gas. In the case of carbonation with dry ice (CO_2 (s)) test runs were conducted with varying loadings. Air and CO_2 (g) experiments were contributed to the study by Schmidt (2015).

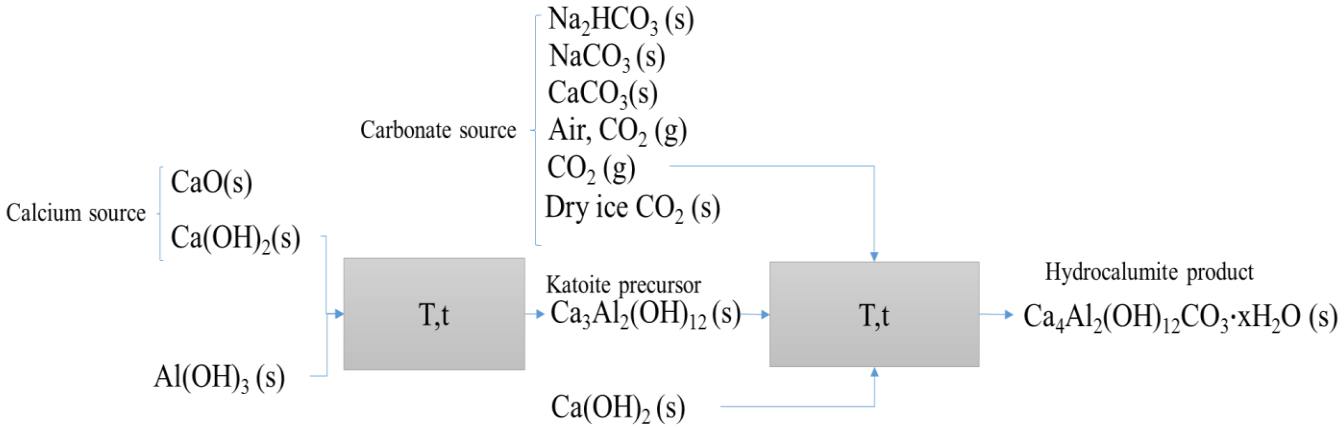

Figure 18: Carbonate intercalation.

The stability results of hydrocalumite, over a temperature range of 5 °C to 110 °C are illustrated in Figure 19. Hydrocalumite is relatively stable for temperatures below 70 °C, at temperatures of > ~85 °C it breaks down into katoite and calcite phases. It was found that as the temperature increases, the pH of the solution drops and the LDH starts to decompose. It should be noted that the reaction time for these results was 42 days. The effect of time is not illustrated in these results. The carbonate concentration could not be detected since the concentration was below detection limits and carbonate solubility was computed assuming a saturation of the supernatant with regards to calcite. (Matschei, Lothenbach & Glasser, 2007)

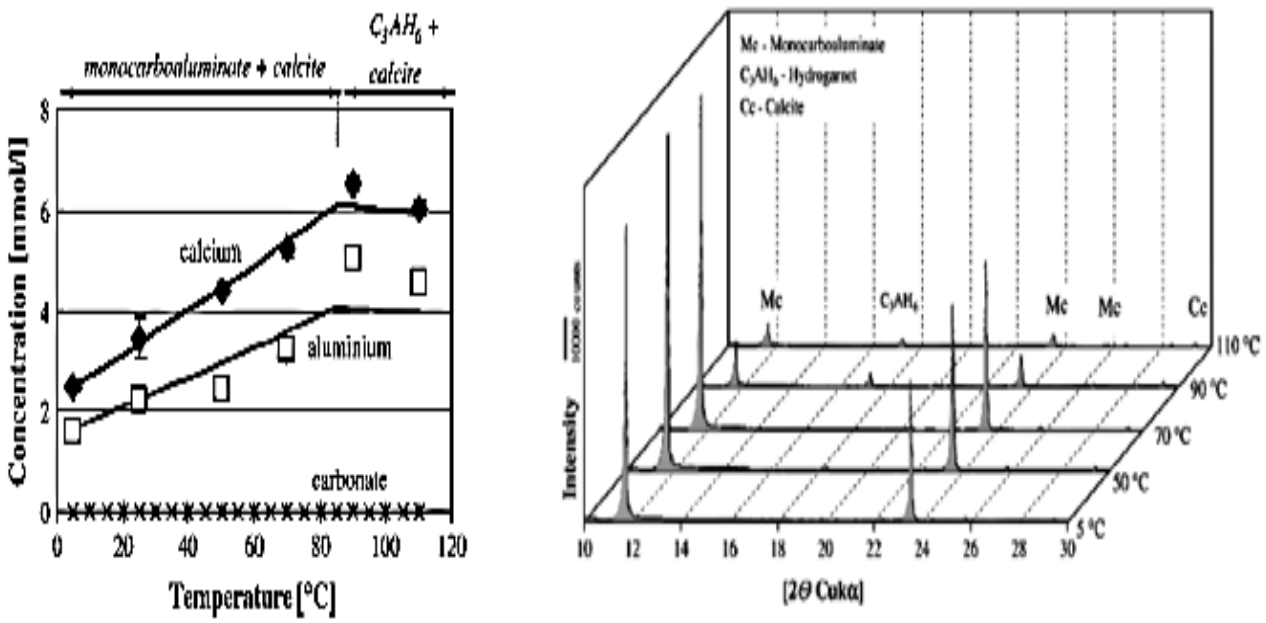

Figure 19: Temperature stability of hydrocalumite, solubility and XRD results (Matschei, Lothenbach & Glasser, 2007).

Initial experiments were conducted by van Graan (2012) at conditions in Table 3. The intercalation reactions conducted at ambient conditions and 70 °C for 1 hour showed low conversion where the 70 °C for 1 day reaction time resulted in a 73 %

katoite conversion to hydrocalumite. A range of ambient temperature to 70 ^{o}C for 2 hours to 24 hours was selected. This was done to ensure that the reaction temperature remained below the decomposition temperature of hydrocalumite within reaction times that are short enough for commercial viability.

Table 3: Hydrocalumite reaction conditions (van Graan, 2012).

Temperature (^{o}C)	**Time**
Amb	2 d
70	1 h, 1 d

3.2.2 Apparatus

A basic setup of a hotplate magnetic stirrer and glass beaker was used for the carbonate intercalation with air, CO_2 (g), $NaHCO_3$ and $NaCO_3$. Experimental setup for these runs are shown in Figure 20. The hotplate on the left is a WiseStir model MSH-20D with temperature control form Wisd laboratory instruments, the hotplate on the right is a Agimatic model N with temperature control from Selecta fitted with a Sensoterm electronic thermometer. Teflon coted magnetic stirrer bars were used in all setups.

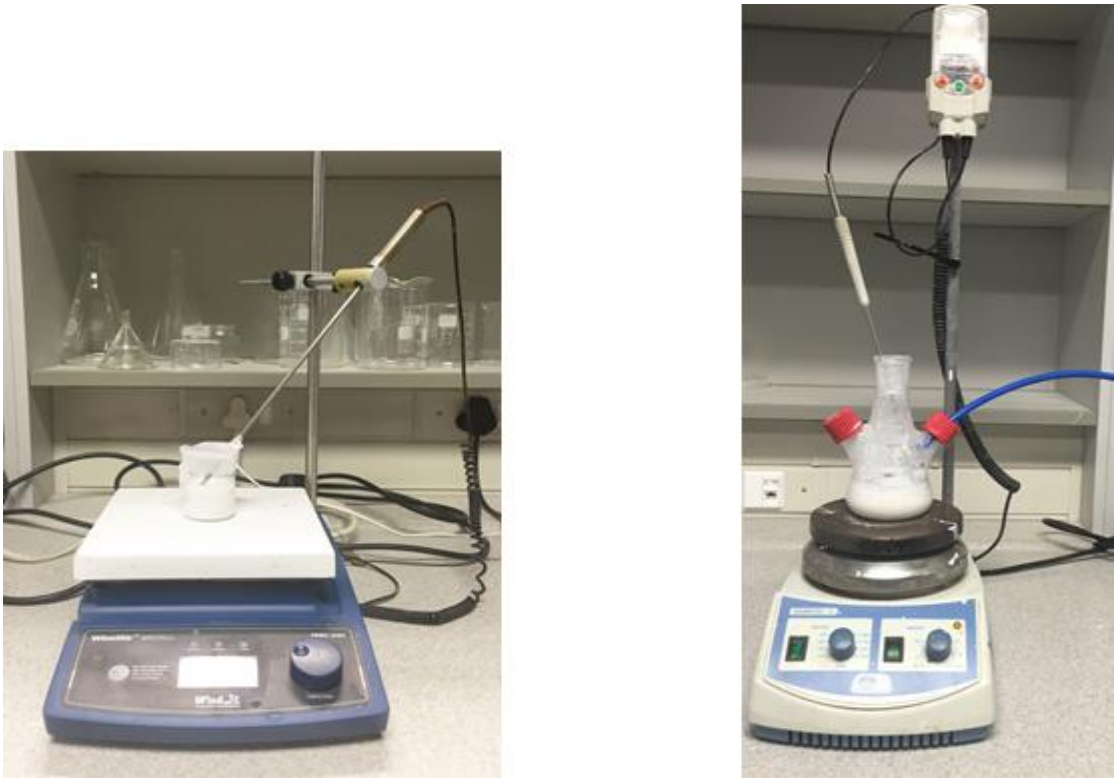

Figure 20: Experimental setup for intercalation with sodium and CO_2 gas sources. Left setup used for sodium bicarbonate, sodium carbonate and air. Right setup used for carbonation with CO_2 (g).

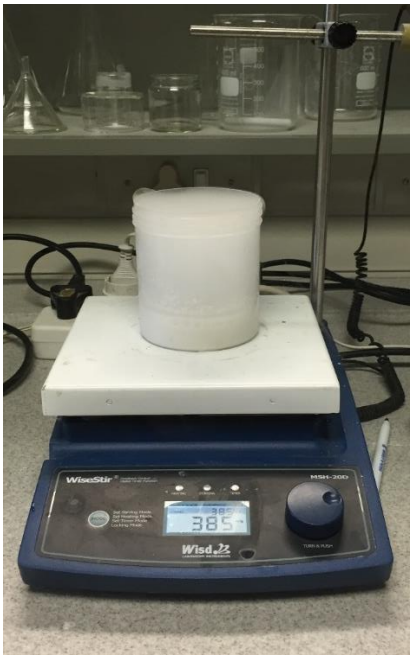

Figure 21: Dry ice experimental setup.

3.2.3 Method

Water was heated on a magnetic hotplate stirrer to the desired temperature in a beaker. The precursor was added to the water and allowed to stir for 5 min where after the carbonate source was added in stoichiometric ratio according to Equations 4 to 7. Stirrer speed of 400 rpm was used. The speed for the intercalation experiments were selected as it was the highest speed at which the slurry seemed fully mixed and did not stir out of control.

The beaker was closed off with transparent film, for $NaHCO_3$ and $NaCO_3$ experiments, to prevent carbonation from air and evaporation of water. In the case of intercalation by air the beaker was left open to the atmosphere, temperature was controlled and water added to make up for evaporated water. CO_2 (g) was bubbled through the slurry solution as shown in the Figure 20. Table 4 below shows the intercalation experimental conditions.

$$Ca_3Al_2(OH)_{12} + Ca(OH)_2 + NaHCO_3 + 4H_2O \rightarrow Ca_4Al_2(OH)_{12}CO_3{\cdot}3H_2O + NaOH \quad (4)$$

$$Ca_3Al_2(OH)_{12} + Ca(OH)_2 + Na_2CO_3 + 4H_2O \rightarrow Ca_4Al_2(OH)_{12}CO_3{\cdot}5H_2O + 2NaOH \quad (5)$$

$$Ca_3Al_2(OH)_{12} + Ca(OH)_2 + CO_{2\,(g\ or\ s)} + 4H_2O \rightarrow Ca_4Al_2(OH)_{12}CO_3{\cdot}5H_2O \quad (6)$$

$$Ca_3Al_2(OH)_{12} + Ca(OH)_2 + CaCO_3 + 4H_2O \rightarrow Ca_4Al_2(OH)_{12}CO_3{\cdot}5H_2O \quad (7)$$

The use of sodium bicarbonate and sodium carbonate (Equations 4 and 5) result in formation of sodium hydroxide according to Equations 8 and 9. This reaction is highly unstable as a result of the reversible nature of bicarbonate. It is highly pH dependent (IBT, 2003).

$$NaHCO_3 + H_2O \leftrightarrow NaOH + H_2CO_3 \quad (8)$$

$$Na_2CO_3 + H_2O \leftrightarrow 2NaOH + CO_2 \quad (9)$$

Dry ice experiments were conducted at different loadings (Table 4) and allowed to sublimate to completion. The stoichiometric amount of dry ice needed in the experiments were 1 g. All samples were filtered with a vacuum filter and dried overnight in Memmert 100 Universal bench top lab oven at 140 ^oC for precursor samples and 60 ^oC for intercalation samples. Dried samples were ground using a mortar and pestle before being sent for analysis.

Table 4: Time and temperature reaction conditions for intercalation.

Carbonate Source	**Time (h)**	**Temperature (^oC)**
$NaHCO_3$ (s), $NaCO_3$ (s)	2, 6, 10, 24	~25 (ambient), 40, 50, 60, 70
$CaCO_3$ (s)	0,25, 0,5, 1, 18	~25 (ambient), 70
Air, CO_2 (g)	2, 6, 12, 24	~25 (ambient), 40, 50, 60,70, 80
CO_2 (g) @ 27 mL/min	2, 24	~25 (ambient), 60
CO_2 (g) @ 47 mL/min	2, 24	~25 (ambient), 60
	Loading (g)	
Dry ice, CO_2 (s)	1, 2, 3, 10	~25 (ambient)

3.3 Use of calcite as combined calcium and carbonate source

An additional experiment was conducted in which calcite was use, in a one-step synthesis, as both calcium and carbonate source. This was done with the same experimental apparatus and method as discussed in Sections 3.1.1 and 3.1.2. The reaction is shown in Equation 10. These experiments were conducted at the same time and temperature conditions as the calcium hydroxide (Table 2).

$$4CaCO_3 + 2Al(OH)_3 + (3+x)H_2O \rightarrow Ca_4Al_2(OH)_{12}CO_3 \cdot xH_2O \quad (10)$$

3.4 Materials

All powdered chemicals used were chemically pure (CP) reagents grade. Calcium oxide ≥ 99 % (CAS no: 1305-78-8) and aluminium hydroxide ≥ 99 % (CAS no: 21645-51-2). Calcium hydroxide ≥ 95 % (CAS no: 1305-62-0) and calcium carbonate ≥ 99 % (CAS no: 471-34-1) form Sigma Aldrich. Sodium bicarbonate (CAS no: 144-55-8) and sodium carbonate (CAS no: 497-19-8) from Merck Millipore. CO_2 (g) ≥ 99 % supplied by Afrox and CO_2 (s) 16 mm pellets supplied by Dry Ice International.

3.5 Analysis and sample preparation

X-ray powder diffraction patterns were recorded on an X'pert-Pro Diffractometer system from PANalytical with continuous scanning using a step size of 0,001° between the ranges 5,00418° and 89,996178 ° 2θ. Co-Kα radiation was generated with a wavelength of 0,1789 nm at 50 mA current and 35 kV voltage by a diffractometer. The irradiated length was kept at 15 mm with a specimen length of 10 mm. The distance Focus-diverge slit was kept at 100 mm and the measuring time was kept Δt = 14,52 s for each point.

Thermogravimetric analysis was conducted on a Hitatchi simultaneous thermogravimetric analyser TA7 000 Series equipment and TA7000 thermal analysis software. Samples were loaded into alumina pans and run in a nitrogen environment at 10 °C increase per minute form ~30 °C up until ~1 000 °C.

Some samples were characterised by scanning electron microscope (SEM) to determine particle size and morphology. Samples for microscopic analysis were prepared by loading the samples onto a transparent adhesive surface and applying it to an aluminium platelet with double sided carbon tape. Excess sample was

blown down by high pressure air, with care taken not to cross contaminate samples. Samples were coated in an Emitech K950X carbon vacuum evaporator with 8 layers of carbon to ensure conductivity. The samples were investigated with ZEISS, SIGMA FE-SEM (field emission SEM). Micrographs were taken at magnifications of 4 000, 10 000, 25 000 and at 40 000 in some cases and an accelerating voltage of 1 kV was used for observation.

4 Results and Discussion

Qualitative XRD analysis was used as the main analysis technique in this study and was conducted for all samples. Primary and secondary peaks of detected phases are indicated by markers on the qualitative patterns. Quantitative XRD or Rietveld refinement and TGA analysis were conducted on selected samples to support quantitative XRD results and are discussed where relevant. The molar compositions of samples were calculated form the Rietveld results.

4.1 Precursor: katoite synthesis

4.1.1 Katoite formation with calcium oxide as calcium source

The XRD results of katoite samples reacted for different time intervals at 60 ºC are compiled Figure 22 and Table 5. The main phases present in these samples are unreacted calcium hydroxide and aluminium hydroxide. Calcium carbonate is formed as an unwanted by product in this reaction. Negligible amounts of calcium carbonate are present in the samples (less than 0,5 mol %). This indicates that the formation of calcite is not a dominant reaction in this step.

The primary aluminium hydroxide peak at a 2 θ value of 21,3º is narrow and of high intensity (Figure 22). This indicates that the aluminium hydroxide is of a highly crysalline nature (showing large narrow peaks in the XRD patterns). This will hamper dissolution of the aluminium source. At a reaction time of 4 h the characteristic peaks of katoite (2 θ of 20,01º and 45,91º) become visible and increase slightly in intensity as the reaction time increases. The quantitative analysis, Table 5, shows that significant amounts (39,91 mol %) of katoite only start to form at the extended reaction time of 24 h.

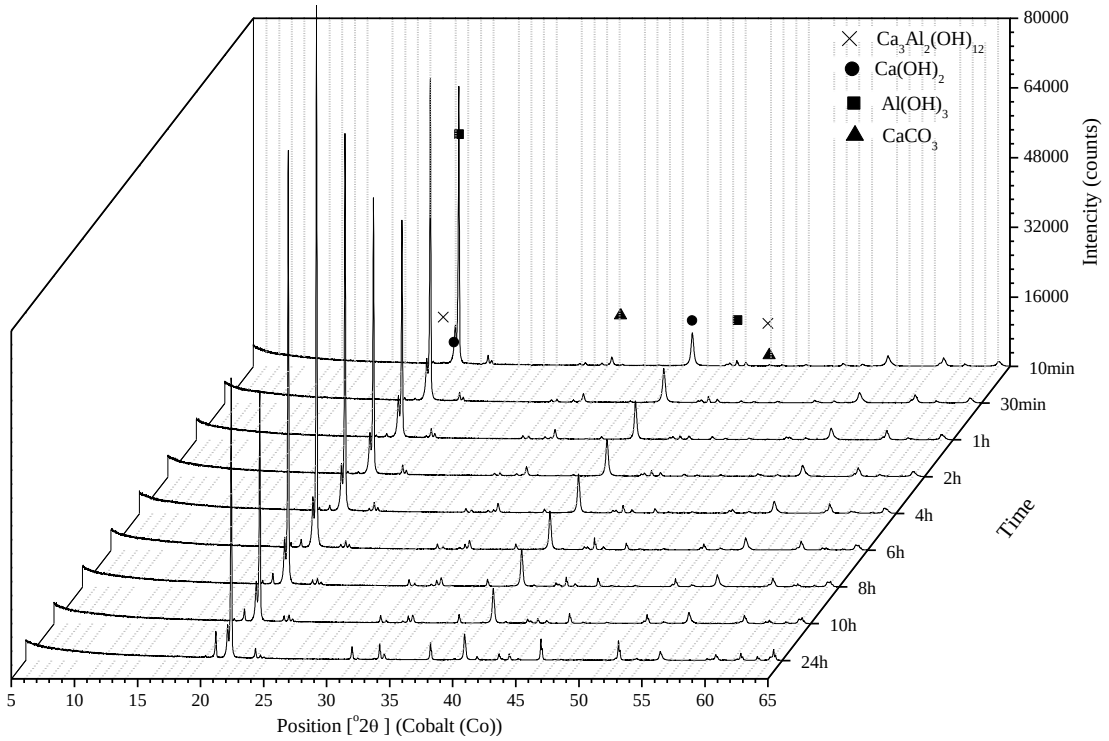

Figure 22: Katoite synthesis for various time intervals at 60 °C.

Table 5: Rietveld analysis of samples formed at 60 °C.

Time	Chemical Species (mol %)			
	$Ca_3Al_2(OH)_{12}$	$Ca(OH)_2$	$Al(OH)_3$	$CaCO_3$
5 min	0,00	51,14	48,35	0,50
30 min	0,00	50,14	49,51	0,34
1 h	1,56	51,46	46,75	0,23
2 h	0,00	50,36	49,18	0,46
4 h	2,06	46,30	51,46	0,18
6 h	2,89	41,78	55,21	0,12
8 h	4,06	43,37	52,40	0,18
10 h	6,92	51,45	41,55	0,09
24 h	39,91	54,98	4,87	0,23

Figure 23 shows the conversion of the calcium and aluminium to the desired katoite phase, calculated from the quantitative analysis results. The trend shows that as time increases, both calcium and aluminium conversions increase. The conversion of aluminium stays below that of calcium by approximately 10 % up until 10 h reaction time. This confirms the conclusion made by van Graan (2012) that aluminium dissolution is the limiting or rate determining step in the synthesis. At 24 h, the calcium conversion falls below that of aluminium. It is possible that some of the aluminium has dissolved and is present in the amorphous phase. The amorphous aluminium would not be taken into account by the XRD analysis. Considering these results, it is clear that reaction at 60 °C is insufficient for the dissolution of the aluminium phase which prevents reaction with calcium and the subsequent precipitation of katoite.

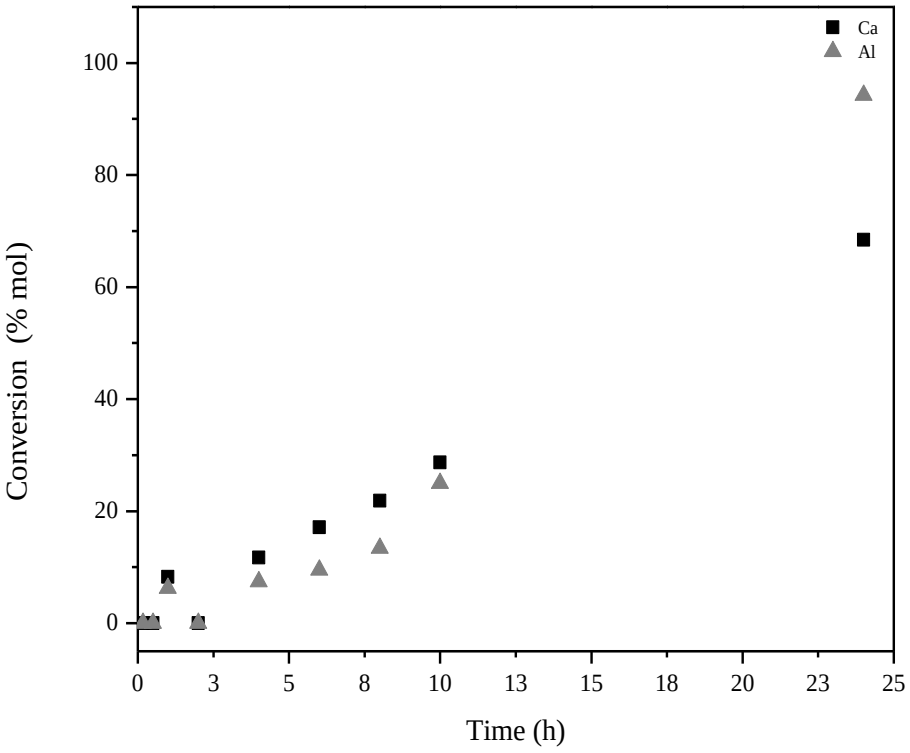

Figure 23: Calcium and aluminium conversion to katoite at 60 °C.

Figure 24 and Table 6 shows the formation of reaction products at 80 °C. Here, the characteristic peaks of katoite become more visible (2 θ of 20,01° and 45,91°). The peak intensity of aluminium hydroxide relative to katoite is significantly decreased compared to that of the 60 °C samples. This indicates an increase in dissolution of aluminium hydroxide into boehmite (Al(O)OH) and subsequent precipitation as katoite. The intensity of the aluminium hydroxide peak decreases steadily with increasing reaction time. A sharp drop is observed between 4 h and 6 h followed by continuous decline thereafter. The primary katoite peak (20,01°) shows a steady increase as the time is increased.

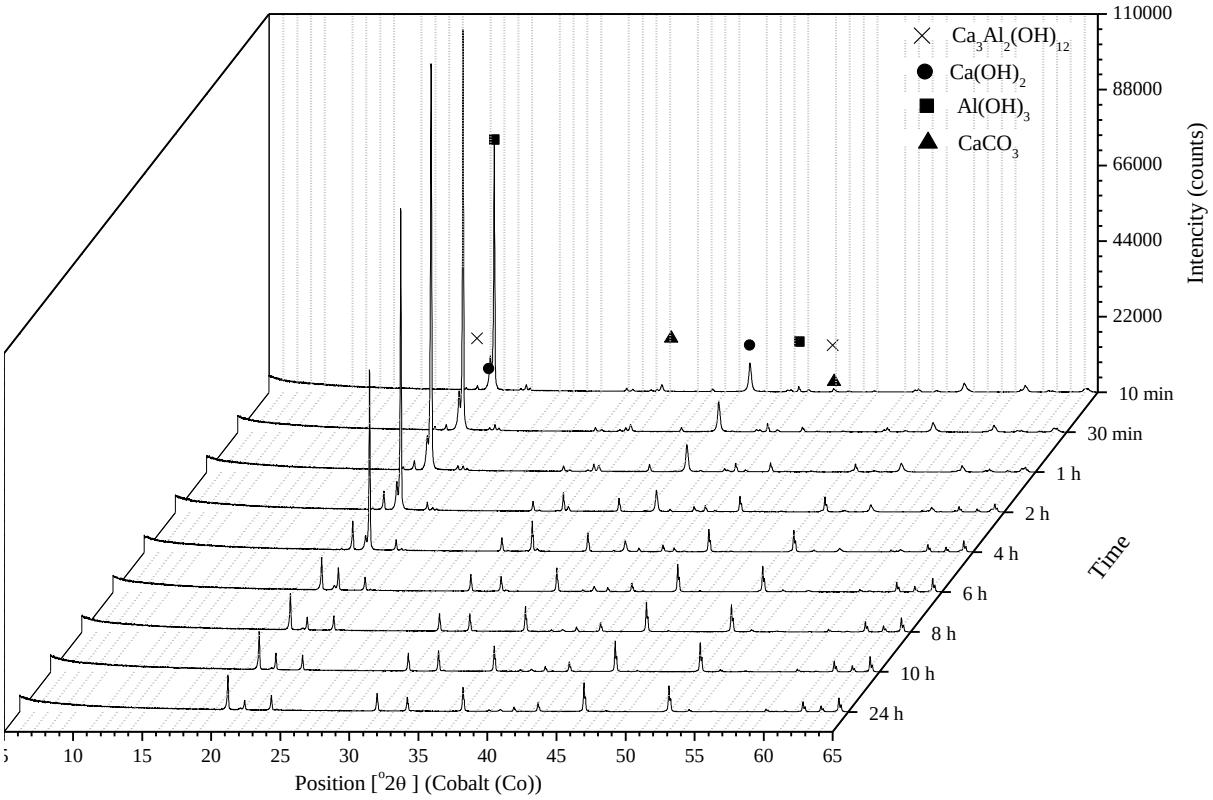

Figure 24: Katoite formation for various reaction times at 80 °C.

In Table 6 it can be seen that at 2 h reaction time a significant amount (55,49 mol%) katoite is already formed. This is a significant increase from the reactions at 60 °C as the highest amount of katoite formed was 39,91 mol% when reacted for 24 h at 60 °C. With a small increase in temperature, the reaction time

can be significantly reduced. Calcite formation is still below 0,4 % for all samples. There is a decrease in the katoite formation at 10 h and 24 h. This could indicate that there is an optimum around 8.

Table 6: Rietveld analysis of the samples formed at 80 °C.

Time	Chemical Species (mol %)			
	$Ca_3Al_2(OH)_{12}$	$Ca(OH)_2$	$Al(OH)_3$	$CaCO_3$
5 min	2,04	48,51	49,27	0,18
30 min	2,66	43,18	54,02	0,13
1 h	5,41	42,16	52,40	0,03
2 h	55,49	39,72	4,64	0,15
4 h	56.74	23.08	19.64	0.03
6 h	61,76	17,28	20,62	0,34
8 h	79,32	6,61	13,97	0,09
10 h	76,18	5,89	17,77	0,15
24 h	65,82	8,56	28,94	0,19

Figure 25 shows the conversion of the calcium and aluminium for the samples at 80 °C. The same trend is visible as in the 60 °C experiments, with conversion of both species increasing with an increasing in time. Higher conversions are reached more rapidly compared to the 60 °C samples. The two data points at 2 h and 4 h seem to be out of place as they don't follow the same trend. The aluminium conversion is higher than that of calcium, which is not the case for the other samples in this set. This may be due to experimental error. The conversion of both calcium and aluminium increase rapidly and then plateau off above 2 h reaction time, where it stays around 90 % for both species.

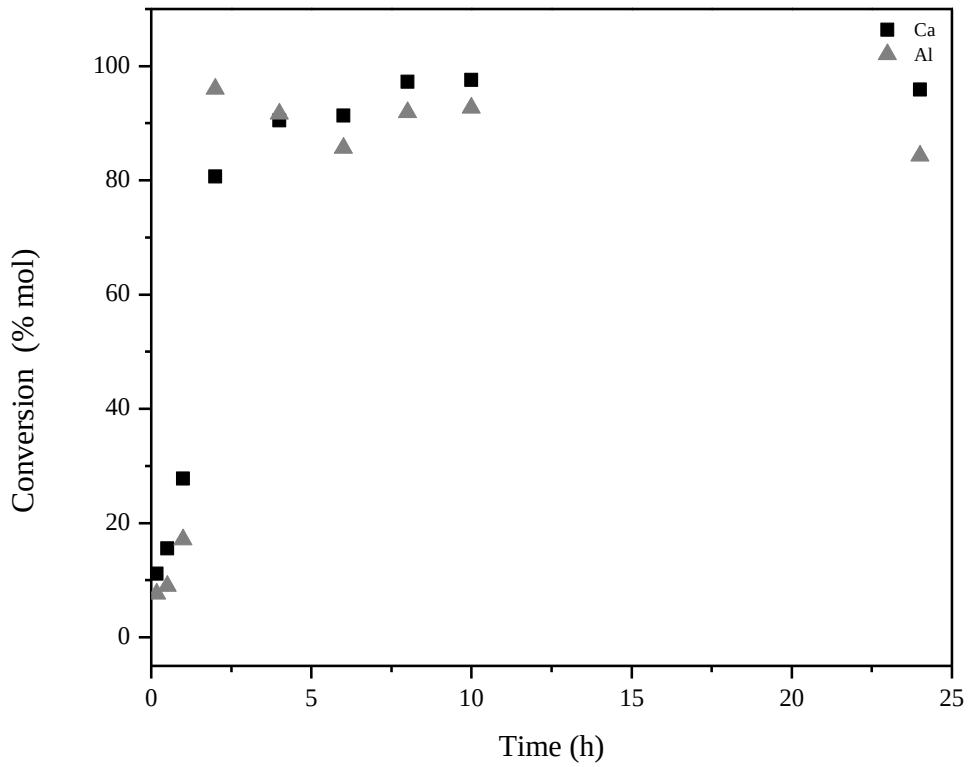

Figure 25: Calcium and aluminium conversion to katoite at 80 ºC.

Figure 26 and Table 7 shows the XRD and Rietveld refinement results of the samples reacted at 100 ºC. Unreacted calcium hydroxide and aluminium hydroxide phases are still present in all the samples. Peak intensities of these phases decrease with an increase in reaction time, as observed for samples reacted at 80 ºC. It should be noted that there is an increase in the formation of calcite. At 60 ºC and 80 ºC, the calcite formation remained under 0,5 mol%, as shown in Table 5 and Table 6. The calcite content goes above 1 % for the reactions at 100 ºC (Table 7).

Within only 5 min, 47,98 mol% katoite has formed, and any a further increase in reaction time does not seem to have a strong effect on the formation of katoite. After 30 min, the katoite formation goes up to 61,44 mol% then remains between 60 mol% and 66 mol% up to 24 h reaction time. This indicates that, at this

temperature, an increase in time does not have a significant effect on the increase of katoite formation. .

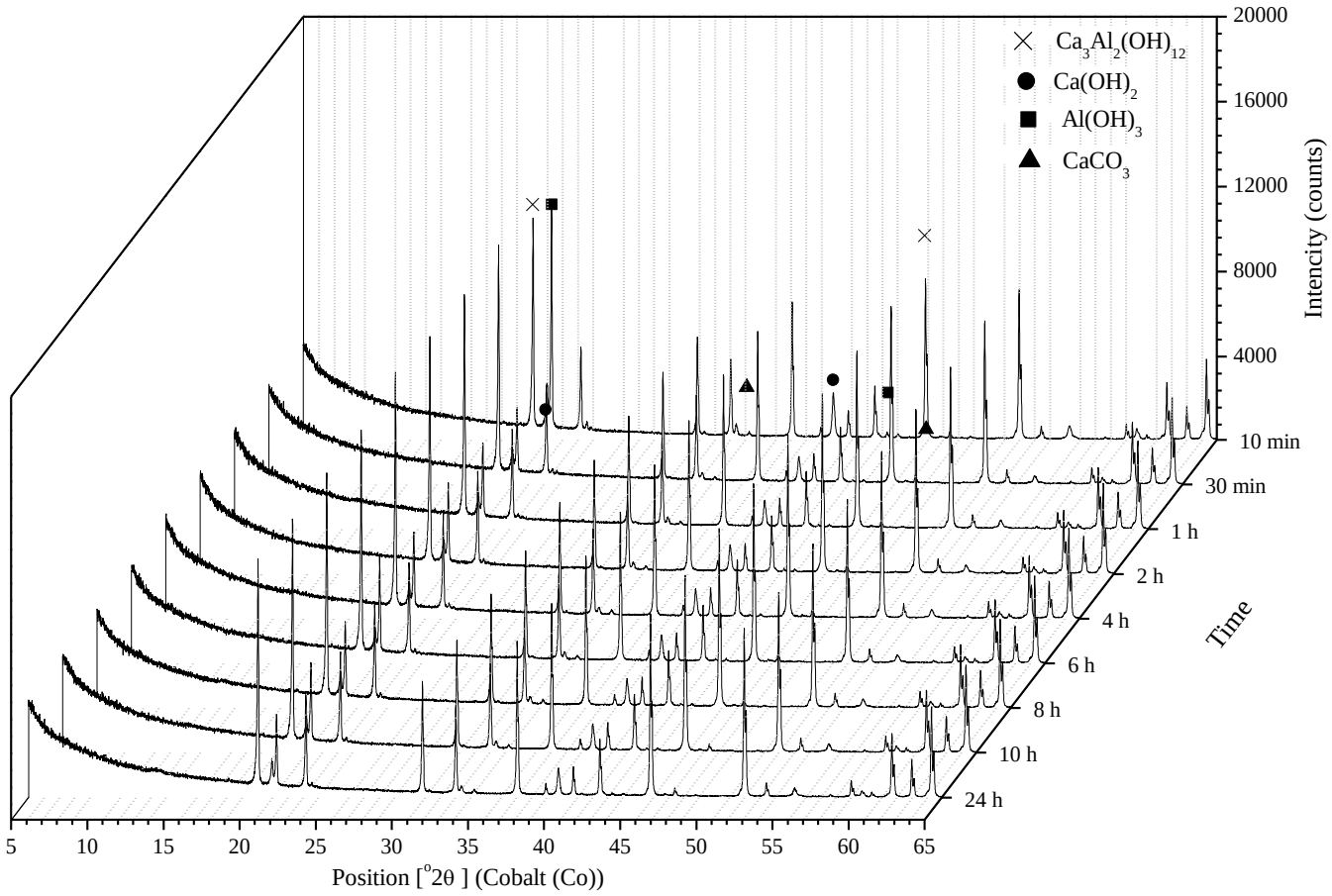

Figure 26: Katoite formation for various time intervals at 100 ºC.

Figure 27 shows the conversion of the aluminium and calcium to katoite reacted at 100 °C. Again the conversion of the aluminium specie is always slightly lower that of calcium. The difference in conversion is much smaller than that the reactions at lower temperatures, form ~10 % at 60 ºC to ~2 % at 100 ºC. It is clear that the conversion stays relatively constant over the entire time range. The conversion of both species is much more consistent together at 100 °C than 60 °C or 80 °C.

Table 7: Rietveld analysis of the samples formed at 100 °C.

Time	Chemical Species (mol %)			
	$Ca_3Al_2(OH)_{12}$	$Ca(OH)_2$	$Al(OH)_3$	$CaCO_3$
5 min	47,98	30,42	20,52	1,08
30 min	61,44	18,64	18,58	1,34
1 h	61,22	20,08	17,19	1,51
2 h	61,22	19,06	18,23	1,49
4 h	60,75	18,75	18,61	1,90
6 h	63,10	19,29	15,92	1,68
8 h	62,26	18,79	17,13	1,82
10 h	65,50	15,92	17,34	1,23
24 h	61,71	21,01	15,60	1,68

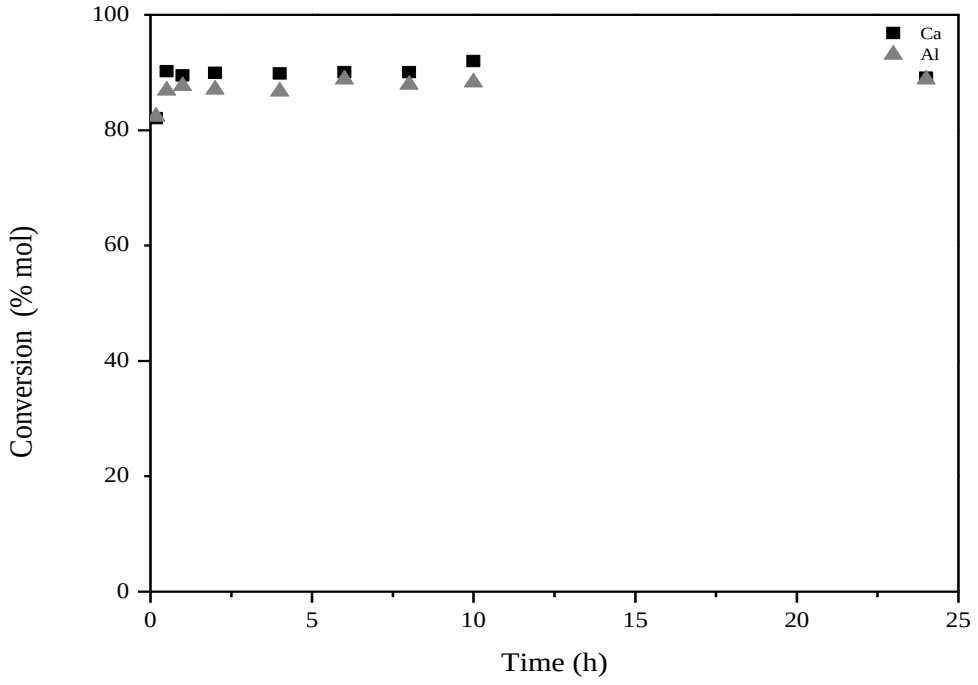

Figure 27: Calcium and aluminium conversion to katoite at 100 °C.

The results for reactions at 120 ºC are very similar to those at 100 ºC. Katoite peaks are present at each time interval (Figure 28). The aluminium hydroxide and calcium hydroxide peaks are still present; however, they decrease in intensity, relative to katoite, as the time increases.

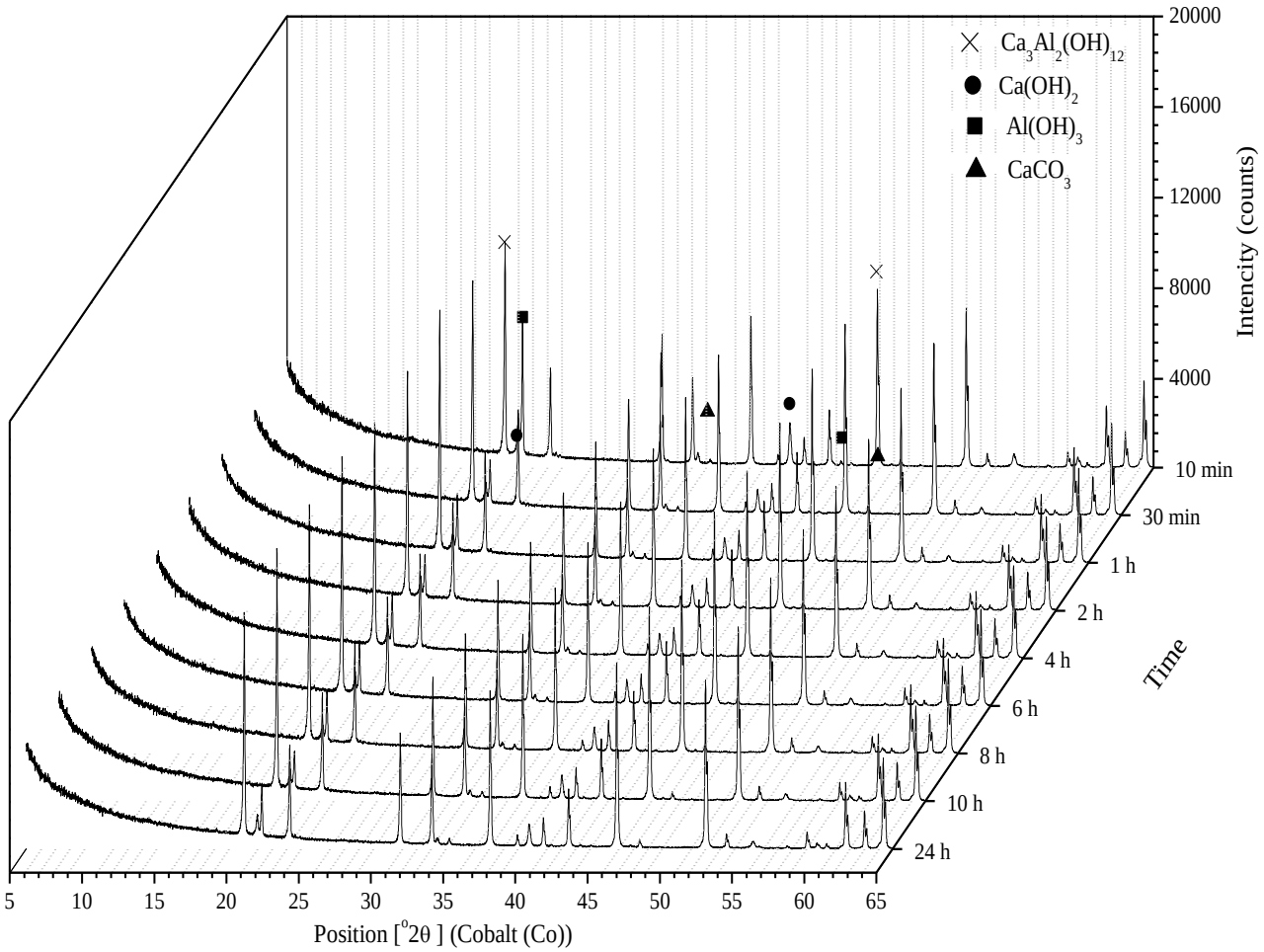

Figure 28: Katoite formation for various time intervals at 120 ºC.

An increase in calcite content is noted from the quantitative results in Table 8. It increases to above 2 mol%. Therefore, it can be concluded that calcite formation increases as temperature increases, but not to such an extent that it significantly inhibits the formation of katoite. There is still unreacted calcium hydroxide present in all the samples, which would have to dissolve and react with the aluminium to form katoite. This is of larger concern than the small amount of

calcite formation. After just 5 min of reaction time, a large amount (56,85 mol%) of katoite had already formed. The amount of katoite increases and stays relatively constant around 69 mol% for the rest of the temperature intervals. This shows that for a higher reaction temperature, katoite formation is rapid and as time increased conversion is more constant. Therefore, running reactions at elevated temperatures could cut down production time significantly.

Table 8: Rietveld analysis of the samples formed at 120 °C.

Time	Chemical Species (mol %)			
	$Ca_3Al_2(OH)_{12}$	$Ca(OH)_2$	$Al(OH)_3$	$CaCO_3$
5 min	56,85	26,60	15,38	1,16
30 min	68,71	16,53	13,00	1,76
1 h	67,48	12,29	18,59	1,64
2 h	67,67	12,66	18,27	1,40
4 h	68,70	11,82	17,88	0,79
6 h	63,91	12,78	20,16	2,12
8 h	66,28	17,75	13,73	2,24
10 h	68,90	17,18	11,61	2,30
24 h	68,15	16,44	12,75	2,65

Figure 29 shows the conversion of calcium and aluminium at 120 °C. It is clear that there is no longer a difference between the conversion of calcium and aluminium, and the conversion of both stay constant at around 92 %, after 30 min reaction time.

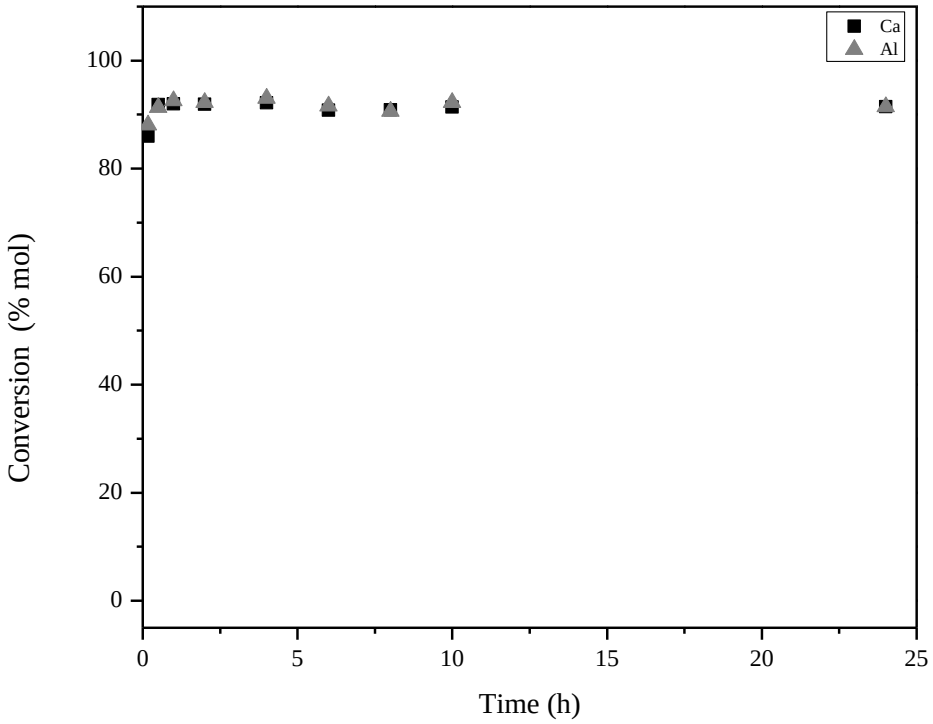

Figure 29: Calcium and aluminium conversion to katoite at 120 ºC.

The conversion results in Figure 23, Figure 25, Figure 27 and Figure 29 indicate that the dissolution of aluminium hydroxide is the limiting step in reaction. The conversion of aluminium hydroxide for all the samples discussed above are summarised as a contour plot in Figure 30. It is clear that 60 ºC is insufficient for the complete dissolution of aluminium hydroxide, and a long reaction time is required to get significant conversions. A temperature of 80 ºC and reaction time of at least 2 hours is required to reach conversions above 80 %. When the temperature is increased to 100 ºC, high conversions are reached almost instantly.

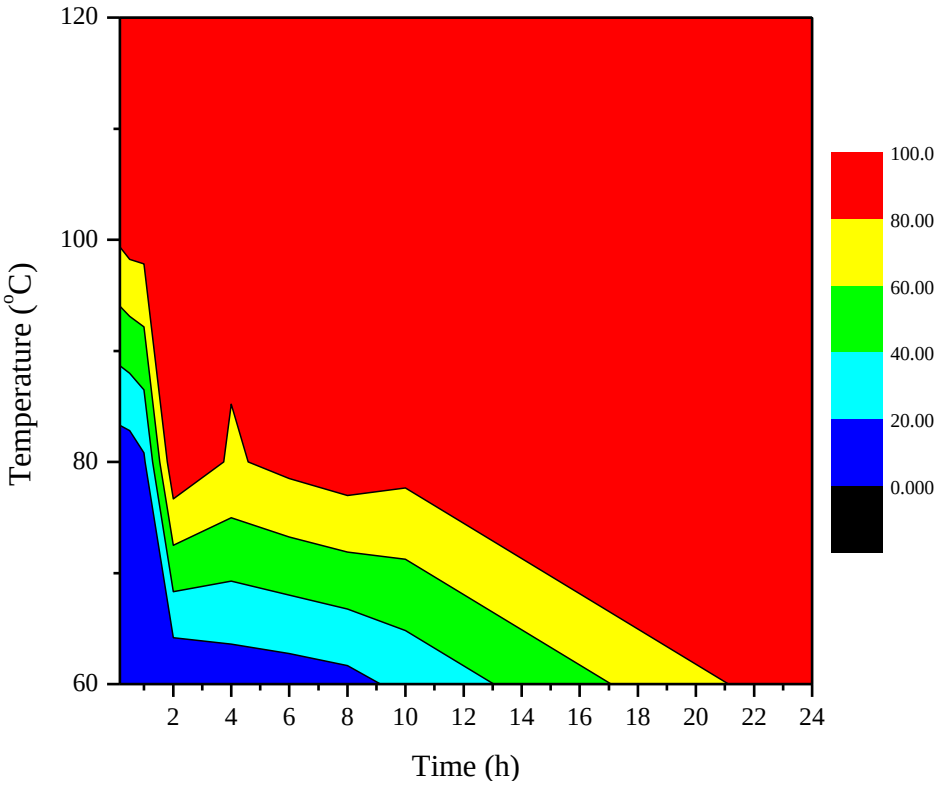

Figure 30: Aluminium hydroxide conversion.

The calcium/aluminium ratios for all product samples discussed above are summarised in Figure 31. The ratio of Ca:Al for successful katoite formation should be 1,5. The ratio fluctuates between 1 and 0,8 for the 60 °C samples. A temperature of 60 °C is not favourable for katoite formation, as the aluminium does not dissolve enough to react with calcium and precipitate as katoite, rather it seems to settle down in the mixture. Samples are taken from the bottom of the reaction vessel as discussed in Section 3.1.1.

The aluminium content could be higher than desired as a result of poor dissolution in the mixture and resulting in a low Ca:Al ratio. It is interesting to note that the outlier points (60 °C at 24 h; 80 °C at 2 h and 120 °C at 15 min) have ratios above 1,5, resulting in a much higher conversions of aluminium. The ratio seems to stabilise at 80 °C and 4 h, which corresponds to the conversion in Figure 30.

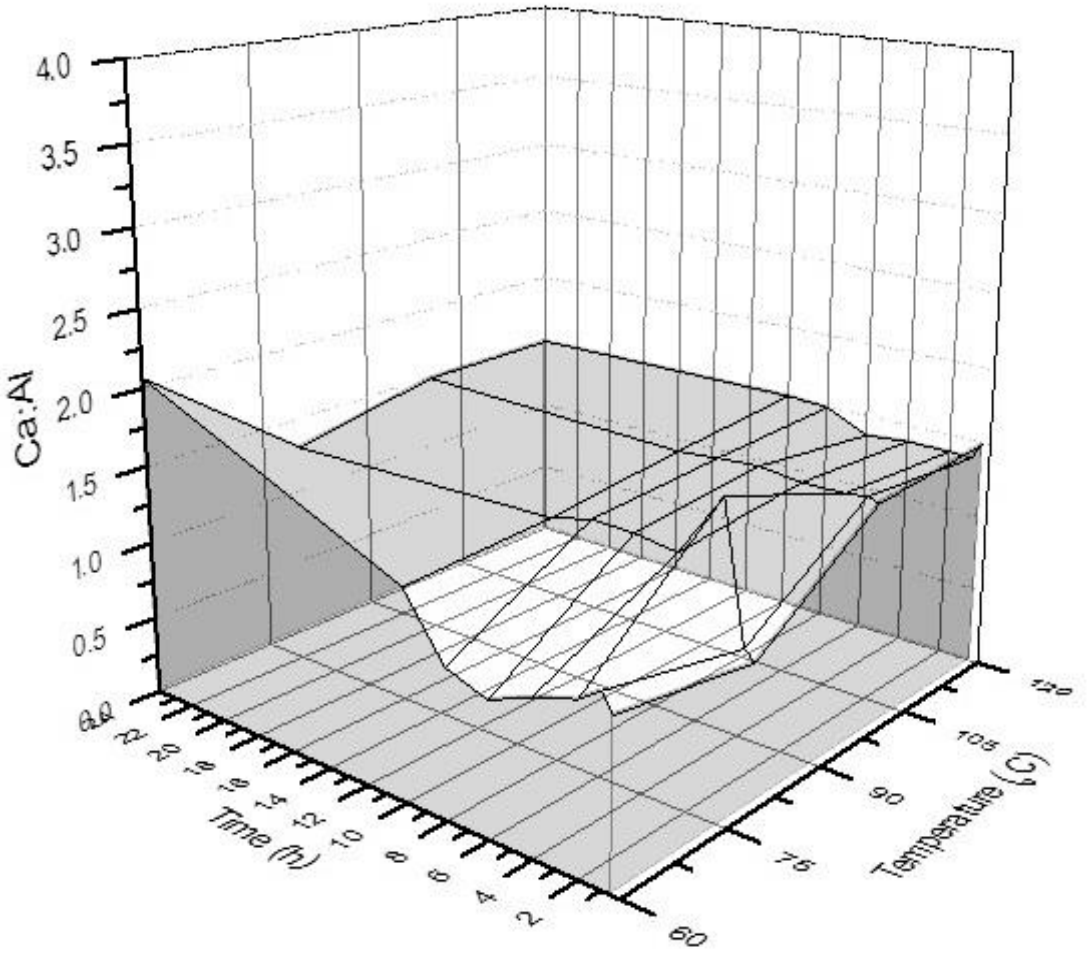

Figure 31: Ca:Al ratio of katoite synthesis reactions.

The general morphologies of katoite grown from a basic solution are 24-sided deltoidal icositetrahedral, rhombic dodecahedral, octahedral and tetrakis hexahedral. The resultant morphology is influenced by the presence of growth modifiers in the reaction solution (Fogg *et al.*, 2002a; Fogg *et al.*, 2002b). The morphologies of selected samples are shown in Figure 33 below. In Figure 32 the ideal deltoidal icositetrahedral morphology (Figure 32 (a)) is shown alongside actual SEM micrographs of basic solution grown katoite (in NaOH solution for 24 h at 95 ^{o}C) (Figure 32(b)) and the dissolution-precipitation sample reacted for 24 h at 120 ^{o}C (Figure 32(c)). The 60 ^{o}C samples are not included in Figure 33, but can be viewed in Appendix B, since the XRD results showed poor katoite

formation. It can be seen, in Figure 33 moving down the columns, that as the temperature increases, the morphology becomes more defined. In the first image, at 80 °C and 15 min, the bulk of the sample morphology is ill-defined agglomerates. At 24 h and 80 °C, the morphology starts to become visible but is still unevenly formed (Whittington, Fallows & Willing, 1997). As the temperature increases, the size of the particles decreases and become more defined and more uniform. The morphology of the 120 °C samples do not differ significantly with time, showing the formation of highly crystalline katoite product within 15 min reaction time.

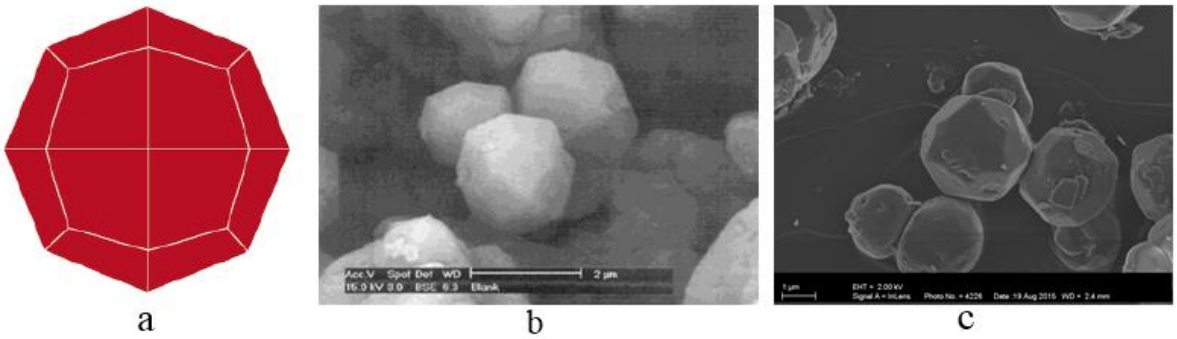

Figure 32: SEM images showing deltoidal icositetrahedral morphology of katoite. a) 24-sided polyhedron bounded by (Fogg *et al.*, 2002b) faces. b) Basic solution grown katoite (Fogg *et al.*, 2002b). c) Dissolution-precipitation grown katoite.

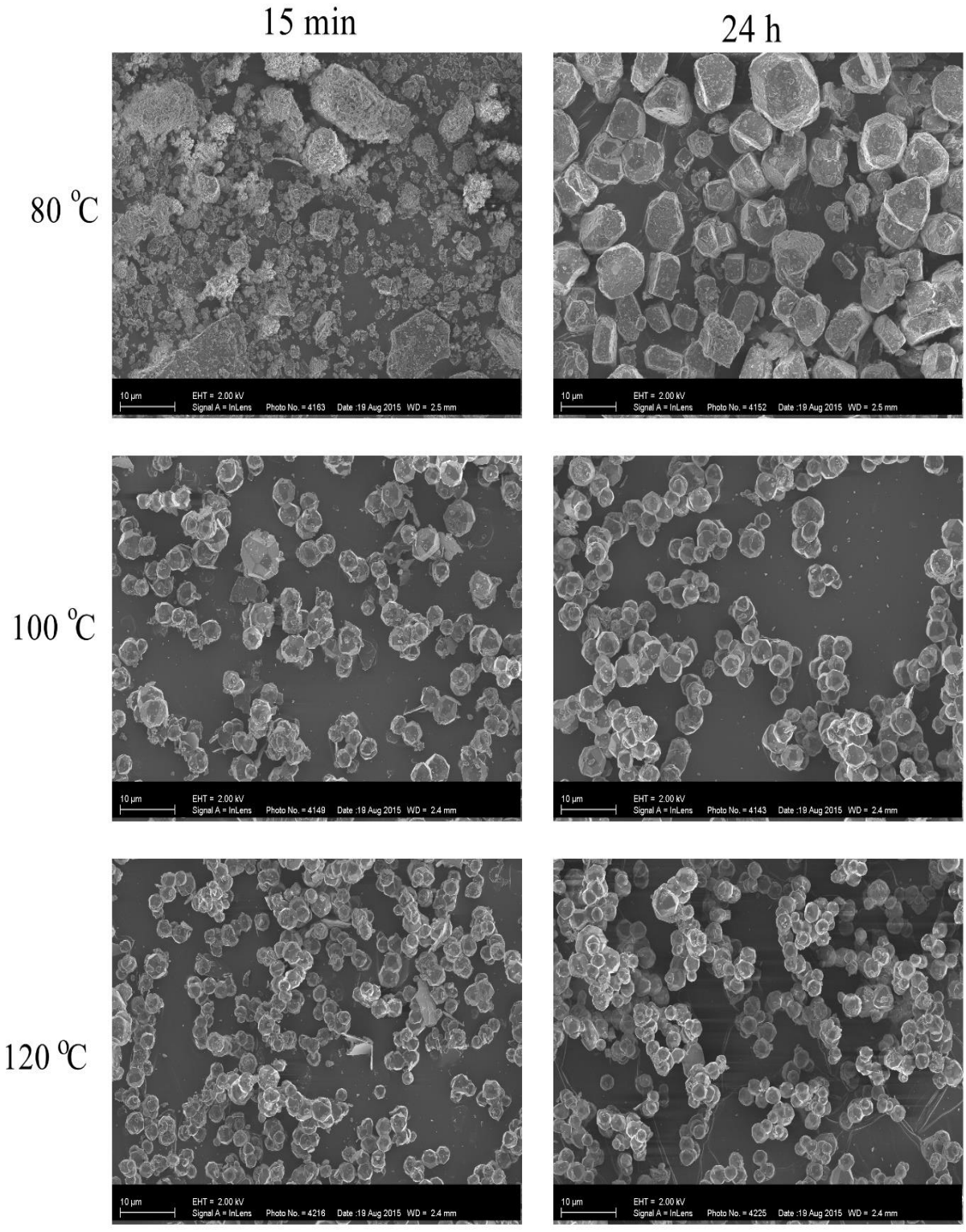

Figure 33: SEM micrographs showing precursor formation morphology.

4.1.2 Katoite formation from calcium hydroxide

Four runs were done at high and low temperatures and time intervals to compare the results to calcium oxide derived samples. The XRD results of these samples are shown in Figure 34 and Table 9. It was hypothesised that the results would prove to be similar to those of calcium oxide. The XRD results of the 120 ^{o}C are similar to that obtained for calcium oxide. The katoite peaks are prominent and in the same intensity range. The katoite primary peak intensity of calcium oxide derived samples, ~10 000 counts, are higher than that of the calcium hydroxide derived samples, ~7 000 counts. This indicates a more crystalline product was formed during the calcium oxide reactions. The katoite molar contents of these samples are also comparable.

The results of the 60 ^{o}C products are not in line with what was expected. The reaction mixture was not exposed to any carbonate source during synthesis. The only possible exposure to CO_2 in air was during post-synthesis treatment in the filtration and drying steps, in the same way as all other precursor formation experiments were conducted. The results indicate significant formation of hydrocalumite, as indicated in Table 9, which was not observed for any of the other samples. This indicates that there must have been carbonate exposure, which was not detected during the experimental run.

No calcite or unreacted calcium hydroxide was detected either. Another possibility is that hydroxide anions could have intercalated to form an LDH phase. This needs to be further investigated. The high katoite yields compared to calcium hydroxide, especially at 60 ^{o}C, makes this a very attractive option for synthesis. Calcium oxide showed extremely low conversion at 60 ^{o}C, thus the use of calcium hydroxide could significantly reduce the reaction temperature required.

Another observation is that there was no detection of aluminium hydroxide in any of these samples. It is possible that the aluminium could be in the amorphous phase, therefore, remained undetected. In calcium oxide samples, unreacted calcium hydroxide, aluminium hydroxide and small amounts of calcite were detected in all samples.

This could indicate that the use of calcium hydroxide is more favourable for the dissolution of aluminium hydroxide. It is recommended that these experiments be repeated, and a comprehensive time and temperature study be conducted with calcium hydroxide. It is also worth determining the effect of the calcium oxide vs calcium hydroxide slurry pH to determine if this could have an influence.

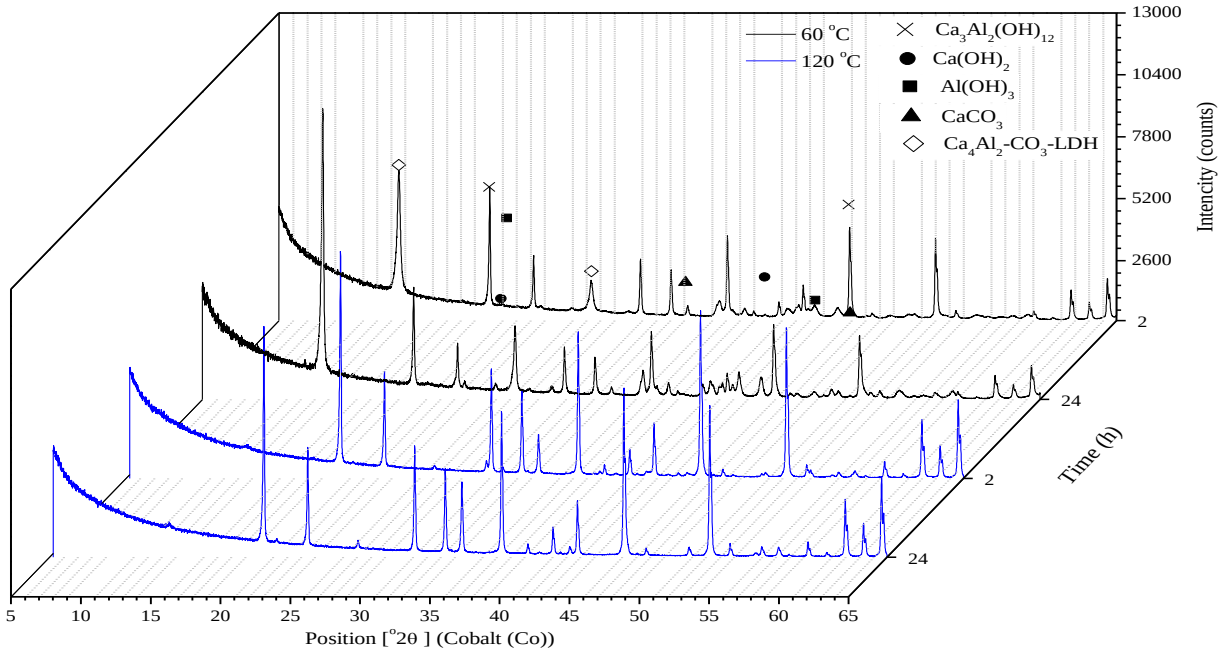

Figure 34: Katoite synthesis for at high and low time and temperature intervals.

Table 9: Rietveld refinement of samples derived from calcium hydroxide.

Temperature (°C)	Time (h)	Chemical Species (mol %)				
		$Ca_3Al_2(OH)_{12}$	$Ca(OH)_2$	$Al(OH)_3$	$CaCO_3$	Ca_4Al_2-CO_3-LDH
60	2	76.03	-	-	-	23.97
	24	55.01	-	-	-	44.99
120	2	78.86	19.80	-	1.34	-
	24	67.52	31.43	-	1.05	-

4.2 Carbonate intercalation

4.2.1 Sodium bicarbonate as carbonate source

The XRD results for samples where sodium bicarbonate was used as carbonate source are compared in Figure 35 and Figure 36. The general trend is that the intensity of the hydrocalumite peaks increases as the temperature and time were increased. The diffraction peaks become sharper and narrower, indicating formation of more crystalline products. Aluminium hydroxide detected in the samples is unreacted aluminium hydroxide from the precursor material. The aluminium hydroxide peaks stay relatively constant up to 6 h where after they decrease from 10 h and 50 °C.

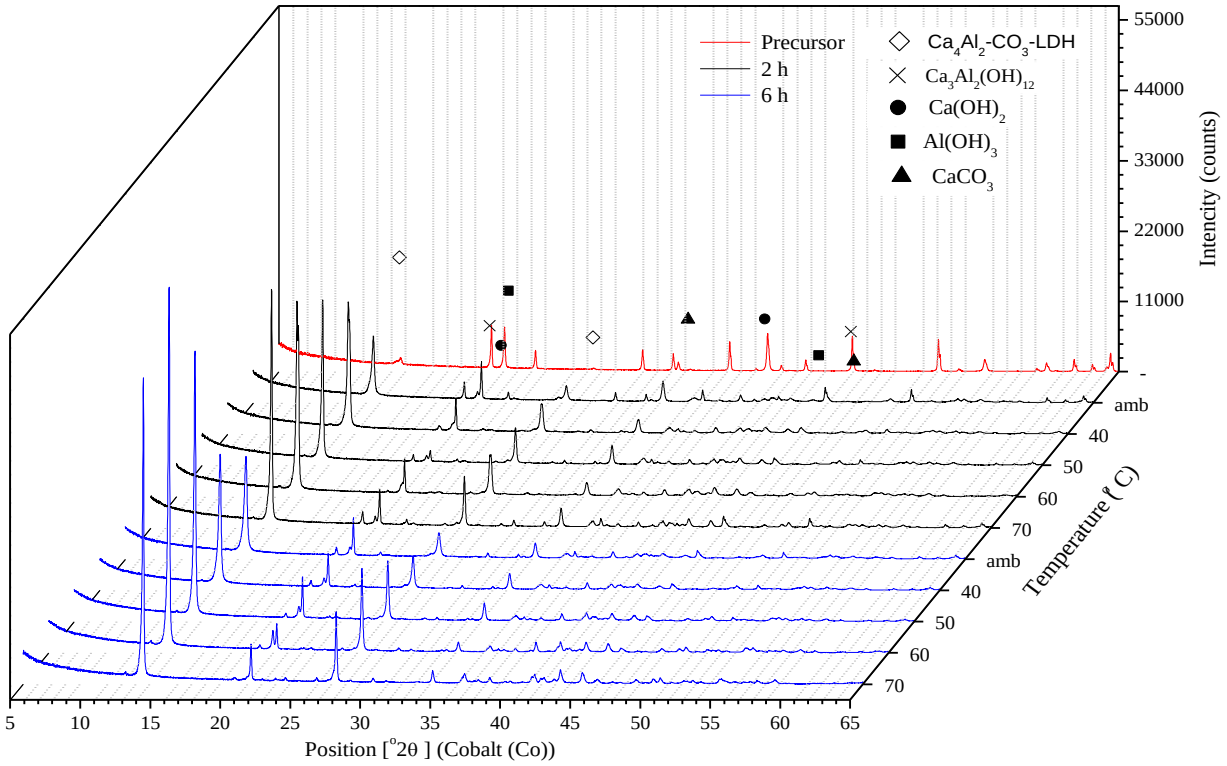

Figure 35: Hydrocalumite synthesis for 2 h and 6 h reaction times.

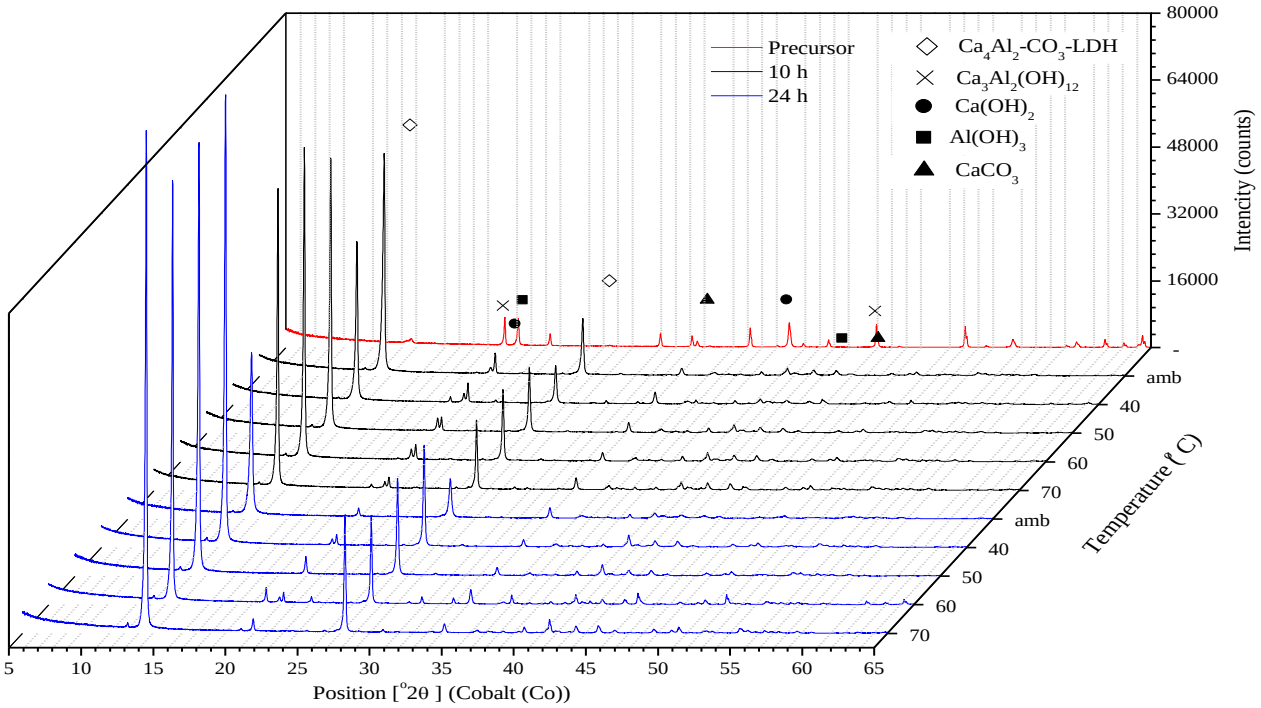

Figure 36: Hydrocalumite synthesis for 10 h and 24 h reaction times.

This could indicate possible dissolution of aluminium and may allow for further reaction with calcium hydroxide present in the reaction mixture to form hydrocalumite. Although these reaction conditions are not favourable for katoite formation, as confirmed in Section 4.1.1.

Calcite peaks also remained constant, indicating that more calcite was not formed during this step of the synthesis. Unreacted katoite/calcium hydroxide precursor was detected in all samples. These reaction conditions were not sufficient to allow for complete dissolution of the precursor and precipitation of hydrocalumite. A reaction temperature of 70 ^{o}C is the most favourable at each time interval. The primary hydrocalumite peak intensity increases significantly with increase in reaction time. Quantitative XRD results and SEM micrographs of these samples can be found in Appendix A and Appendix B, respectively for reference.

4.2.2 Sodium carbonate as carbonate source

The results of hydrocalumite formation with sodium carbonate are similar to that of sodium bicarbonate. There is an increase in hydrocalumite peak intensity as time and temperature increase. There is also a significant spike in the intensity of the hydrocalumite peaks at 60 ^{o}C and 70 ^{o}C for 10 h reaction time. These samples have the highest yield of hydrocalumite.

There are no other phases visible on the diffraction patterns of these two samples and the Rietveld refinement show small amounts of unreacted katoite and calcite remaining from the precursor material (see Appendix A). The calcite content is much lower than any of the other carbonate intercalation samples where. It can be concluded that some of the calcite dissolved and precipitated as hydrocalumite.

The calcium hydroxide peak intensity reduces rapidly (Figure 37 and Figure 38) and from 6 h at 40 °C onwards, no calcium hydroxide was detected in any sample with Rietveld refinement (see Appendix A). This indicates that the calcium hydroxide fully dissolved, along with most of the katoite and reacted with the carbonate source to precipitate as the desired hydrocalumite phase.

When comparing these results to that obtained for the sodium bicarbonate samples, it is clear that these samples are much more crystalline. This indicates that reactions at the same time and temperature conditions are more complete for this synthesis route. Allowing for higher dissolution of reagents and precipitation of hydrocalumite. This could be due to the fact that the formation of sodium hydroxide (Equation 7) aids in the dissolution of the aluminium hydroxide (Panias, Asimidis & Paspaliaris, 2001).

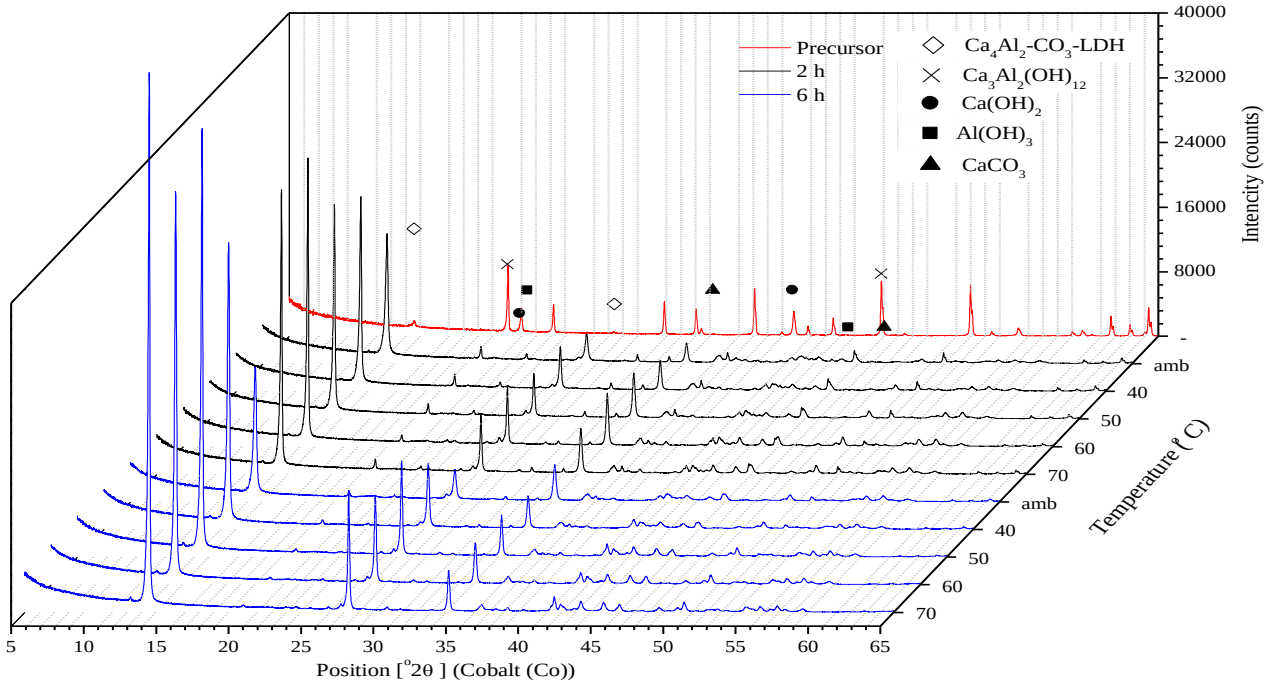

Figure 37: Hydrocalumite synthesis for 2 h and 6 h reaction times.

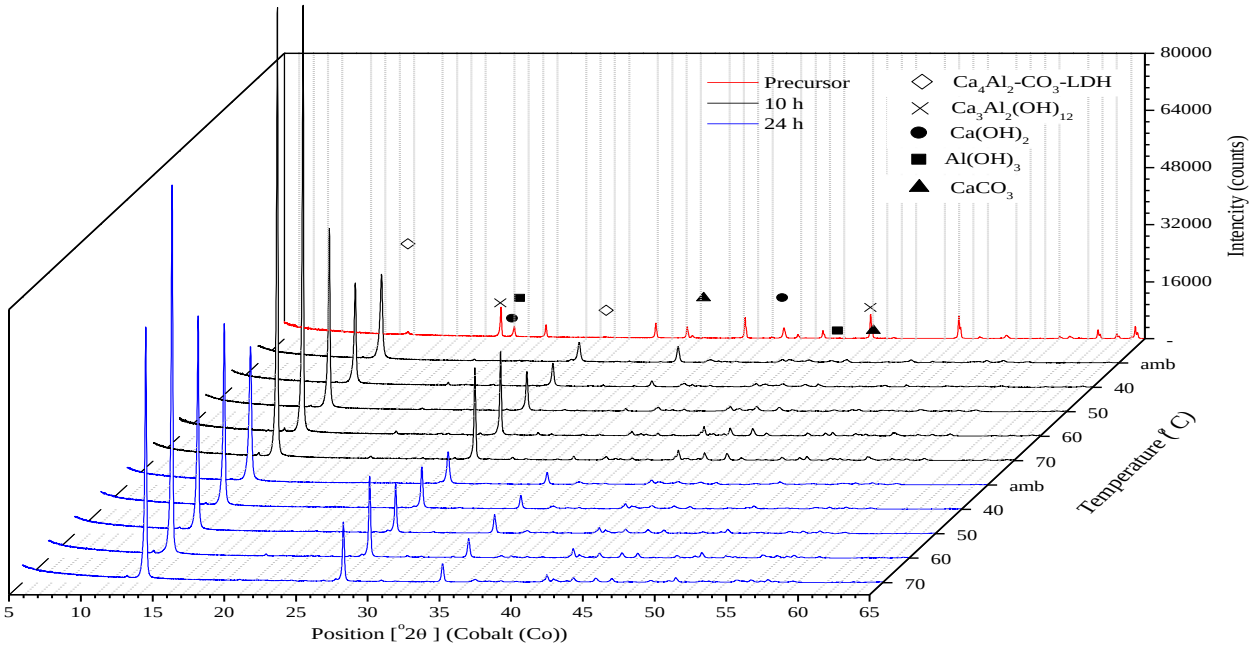

Figure 38: Hydrocalumite synthesis for 10 h and 24 h reaction times.

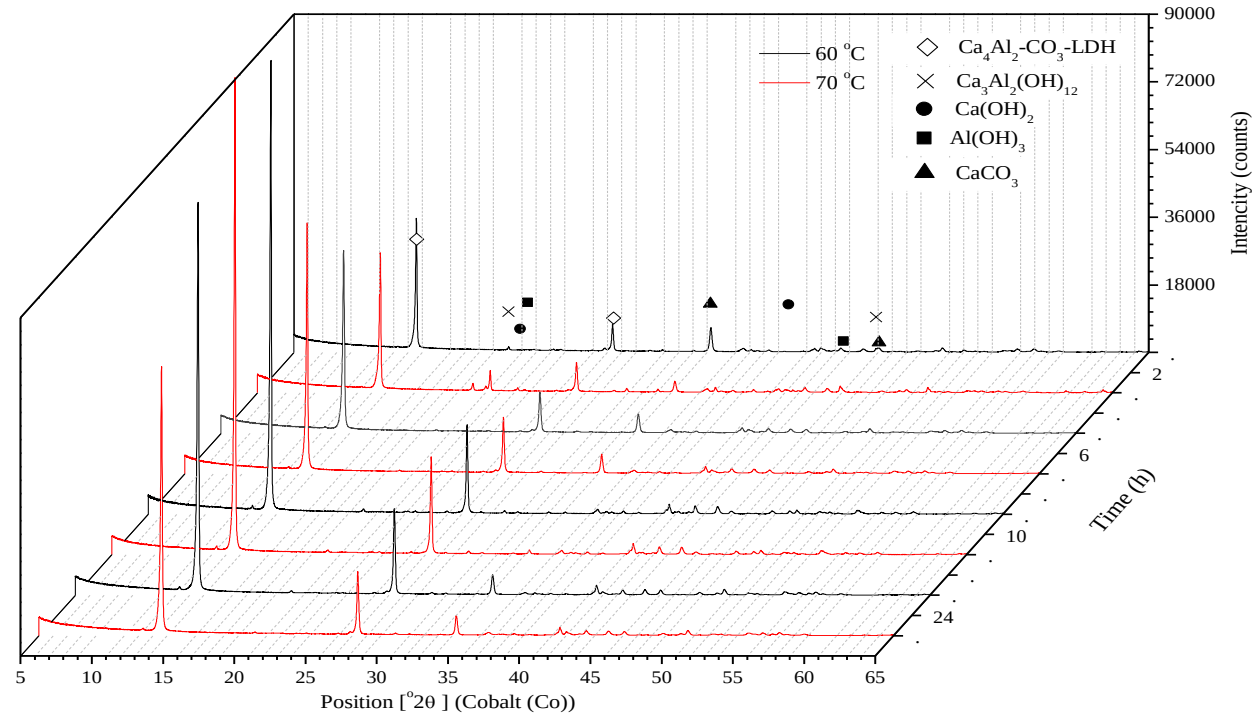

Figure 39: Hydrocalumite synthesis at 60 ºC and 70 ºC.

The XRD results for the 60 ºC and 70 ºC samples are compared in Figure 39. The trend observed above is clearly illustrated. These results show that for time

intervals up to 10 h there is an increase in the intensity of the primary hydrocalumite peak which declines at 24 h. There is a significant increase in this intensity from 6 h to 10 h This shows that there is an optimum around 10 h.

TGA analysis was done on various samples. All showed similar results thus two samples were selected for discussion and are illustrated in Figure 40. TGA results for samples at 60 ^{o}C and 70 ^{o}C show that up to 9 thermal transitions occur similar to those of hydrocalumite produced by Sánches-Cantú *et al* (2013). There are three main decomposition steps for LDH materials. Vieille *et al* (2003) reported that for chloride containing hydrocalumite these steps occur in the ranges of:

- Dehydration 25 ^{o}C $\leq$ T $\leq$ 250 ^{o}C
- Dehydroxylation 250 ^{o}C $\leq$ T $\leq$ 400 ^{o}C
- Anion decomposition 400 ^{o}C $\leq$ T $\leq$ 1200 ^{o}C

Sánches-Cantú *et al* (2013) reported an overlap of these events as discussed in Section 2.2.2. The first three thermal transitions were reported to be due to release of adsorbed surface water and intra-particle pore water between hydroclalumite crystallites. Thermal transitions 4 to 7 are the simultaneous release of calcium bounded water and dehydroxilation. The last transitions are complete dehydroxilation and anion decomposition.

As these samples are not pure hydrocalumite but rather a mixture including katoite, aluminium hydroxide and calcite, the resulting TGA data will deviate from the suggested hydrocalumite only data mentioned above. The 4th transitions also accounts for the decomposition of calcium carbonate and aluminium hydroxide. These decompositions continue up to the 8th transition. Calcite is completely decomposed in the last two transitions as shown in Figure 41.

The TG data of katoite synthesised at 120 ºC and 3 h is compared to the TG data of the intercalation samples at 60 ºC and 70 ºC at 24 h in Figure 40. The three main decomposition ranges of hydrocalumite are indicated by the vertical dashed lines in the TG/DTG results. XRD confirmed the presence of katoite and calcite phases in these samples. Both of these phases each have one major decomposition range. Katoite has its decomposition between 250 ºC and 300 ºC (Figure 40) and for calcite between 650 ºC and 750 ºC (Figure 41). Since these samples are mixtures of these phases the TGA data will be a combination of all phases. Because of this it is extremely difficult to calculate exact information about the hydrocalumite phase.

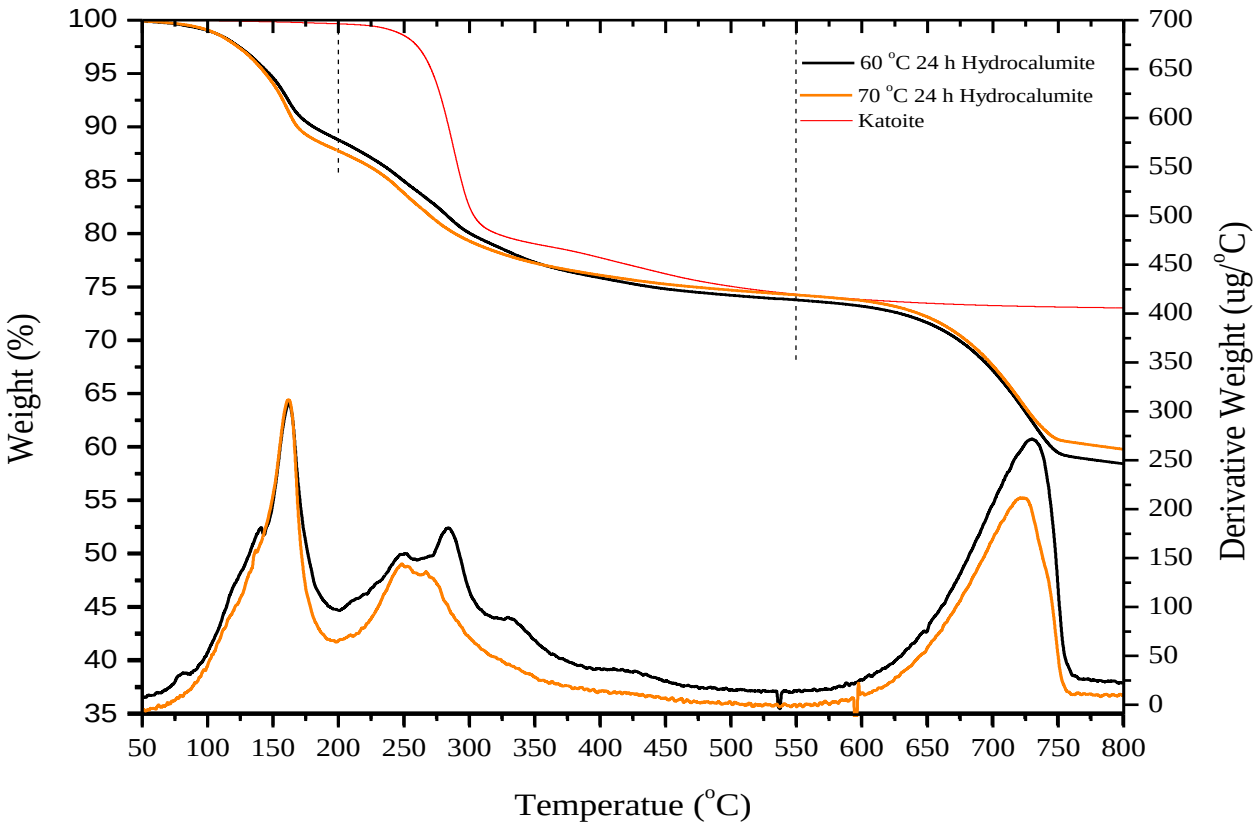

Figure 40: TG and DTG analysis.

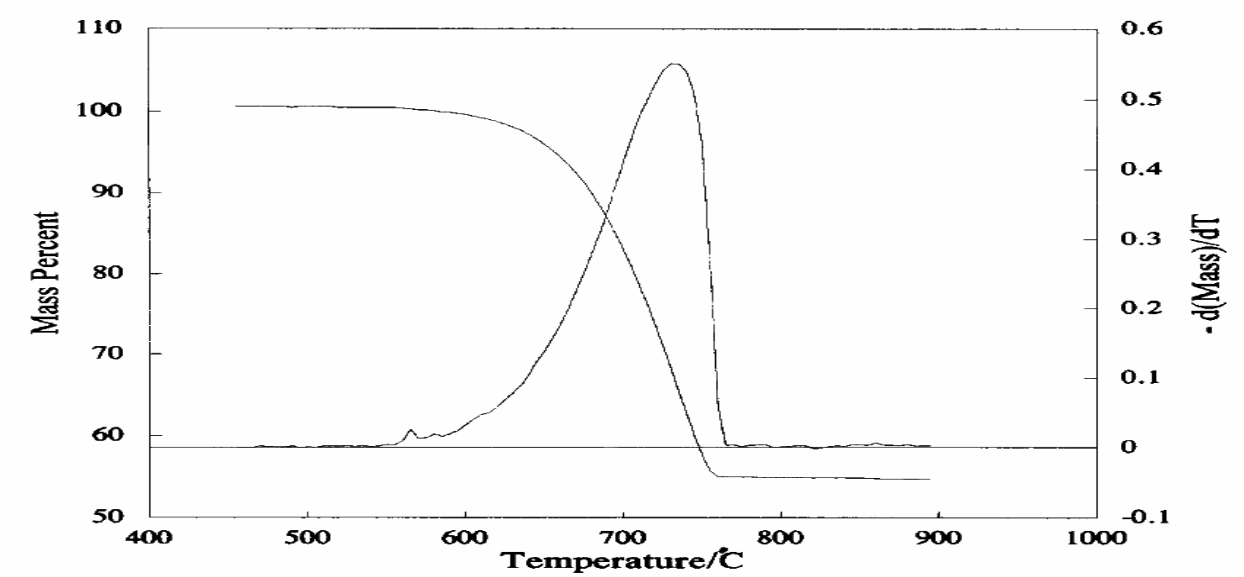

Figure 41: TGA data of $CaCO_3$ (Oniyama & Wahlbeck, 1995).

4.2.3 Air as carbonate source

Quantitative results for air as carbonate source are summarised in Table 10. These experiments were conducted by keeping the slurry solution open to the atmosphere at various controlled temperatures. The formation of LDH does not go above 10 mol%. This is a poor conversion and is not a viable method of intercalation within these synthesis parameters. These conditions are not sufficient for the dissolution of the precursor material.

The conversion of katoite to hydrocalumite is shown in Figure 42. The conversion is extremely low, ranging between 5 % and 15 %. There is an increase in conversion as time and temperature increase. The conversion reaches a slight maximum around 12 h for all temperatures in this range. It should be noted that the amount of calcite is low and thus exposing the reaction slurry should not lead to an increase in calcite formation.

Table 10: Quantitative results of carbonate intercalation from air.

Time (h)	Temperature (°C)	Chemical Species (mol %)				
		Ca_4Al_2-CO_3-LDH	$Ca_3Al_2(OH)_{12}$	$Ca(OH)_2$	$Al(OH)_3$	$CaCO_3$
2	~25	2,38	43,15	45,76	8,72	0,00
	40	2,56	44,15	42,99	10,30	0,00
	60	1,68	46,32	39,33	11,26	1,41
	70	7,39	48,94	31,47	10,22	1,98
6	~25	2,02	44,87	43,22	9,89	0,00
	40	3,26	45,65	41,75	9,35	0,00
	60	6,60	43,22	39,01	11,17	0,00
	70	9,80	55,56	25,69	6,78	2,16
12	~25	6,36	40,59	38,86	14,19	0,00
	40	3,04	46,82	40,42	9,72	0,00
	50	6,19	43,61	40,05	10,15	0,00
	60	5,85	43,28	36,42	11,76	2,69
	70	9,16	53,37	25,11	10,44	1,92
24	~25	4,04	45,78	40,15	8,70	1,33
	40	3,18	45,71	40,08	11,02	0,00
	50	2,82	50,14	35,95	11,09	0,00
	60	5,95	49,14	34,83	7,39	2,69
	70	6,38	64,90	16,88	4,89	6,95

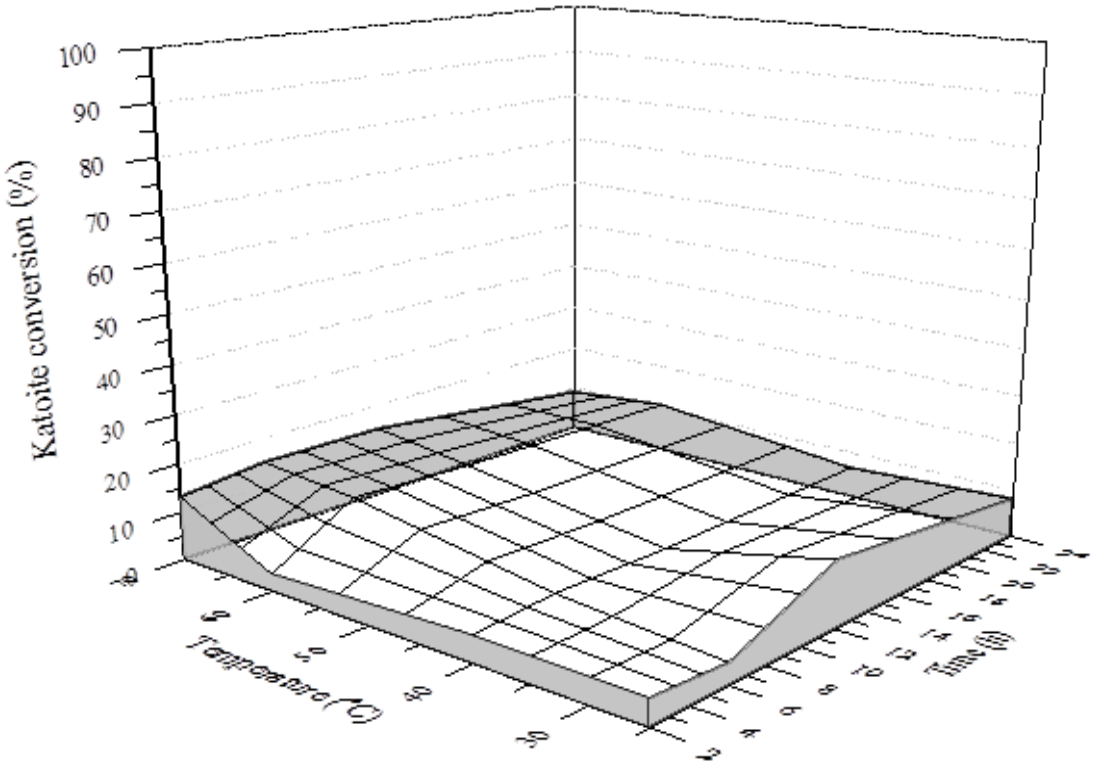

Figure 42: Katoite conversion for air experiments.

4.2.4 CO_2 (g) as carbonate source

XRD results of products formed with CO_2 (g) as carbonate source are summarised in Figure 43 and Table 11. These experiments were conducted at high and low temperature and time intervals with high and low gas flow rates. It is clear that the only samples that show hydrocalumite formation are the two at 2 h reaction time at the lower gas flow rate. The quantitative XRD results in Table 11 show that all of these samples consist mainly of calcite. At these reaction conditions, the katoite is broken down and calcium hydroxide is converted to calcite. The main conclusions made from these results are that lower flow rate andshorter reaction time seem to be the most promising conditions for possible formation of hydrocalumite when using CO_2 (g).

It is believed that this is due to the drop in pH of the reaction solution. The higher flow rate CO_2 (g) results in a higher concentration of carbonic acid formation and

as a result a more rapid reduction of pH. When the pH becomes too acidic the LDH starts to break down and calcite formation becomes more prevalent. It is recommended that this carbonation method be further investigated and the experimental setup changed to allow for more efficient contact between the precursor slurry solution and the gas. This method is the most promising green method since there are no outlet streams that require treatment before re-use.

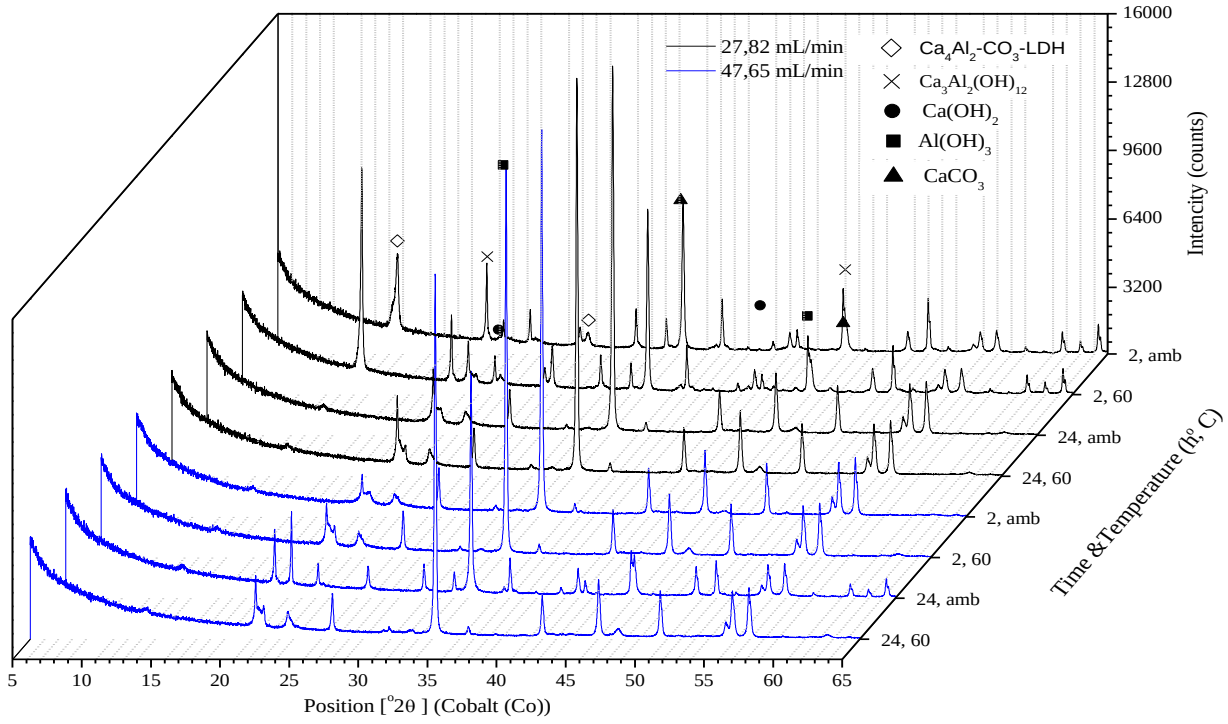

Figure 43: Hydrocalumite synthesis with CO_2 (g) as carbonate source.

Table 11: Quantitative results of carbonate intercalation from CO_2 (g).

Flow rate (mL/min)	Time (h)	Temperature (°C)	Chemical Species (mol %)				
			Ca_4Al_2-CO_3-LDH	$Ca_3Al_2(OH)_{12}$	$Ca(OH)_2$	$Al(OH)_3$	$CaCO_3$
26,82	2	~25	3,76	20,32	-	8,35	67,56
		60	4,65	15,99	-	11,63	67,72
	24	~25	-	-	-	28,57	71,43
		60	-	-	-	26,85	73,15
46,65	2	~25	-	-	-	30,17	69,83
		60	-	-	-	28,07	71,93
	24	~25	-	11,41	-	8,05	80,54
		60	-	-	-	28,31	71,69

4.2.5 Dry ice as carbonate source

Dry ice experiments were conducted by adding increasing masses of dry ice into the katoite/calcium hydroxide precursor mixture (with 1 g being the calculated stoichiometric requirement). In each case, except for the 10 g addition, a small amount of hydrocalumite formed (Figure 44 and Table 12). There are still large amounts of unreacted katoite/calcium hydroxide precursor present in the samples. This could be as a result of the short contact times between the carbonate source and the reaction mixture, since the dry ice was added to an open glass beaker and allowed to sublimes. The sublimation was complete within 10 min.

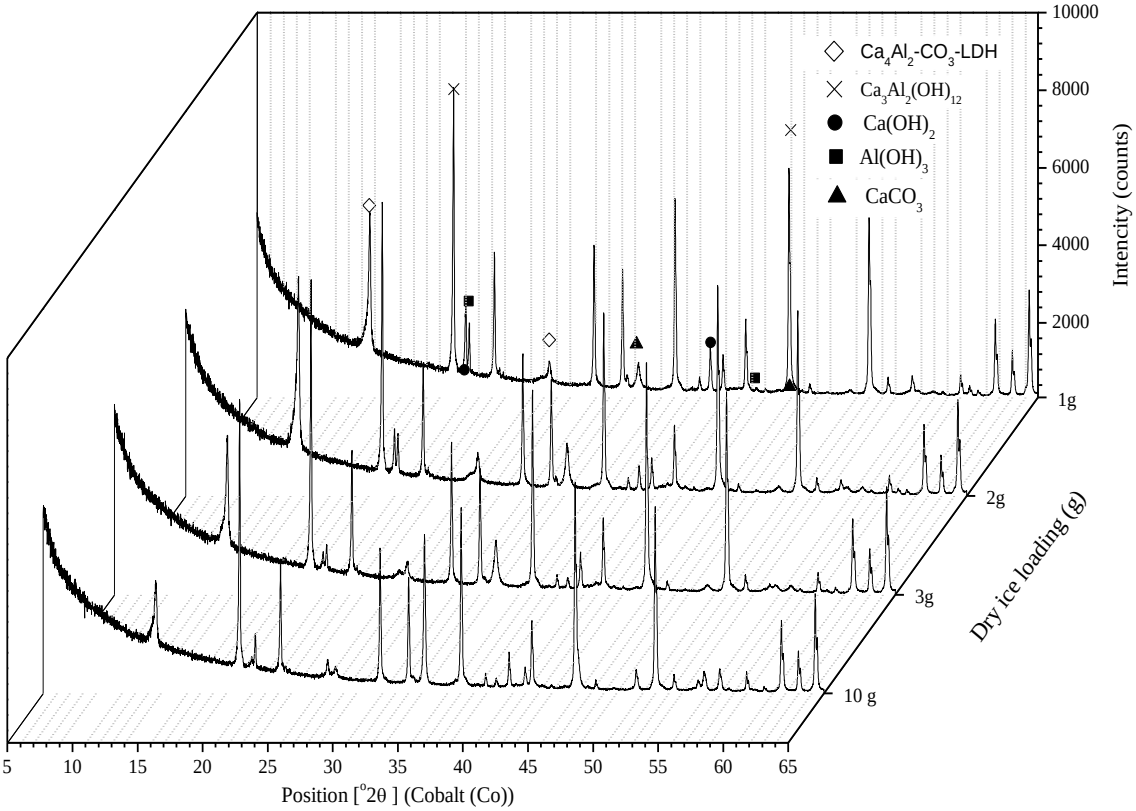

Figure 44: Dry ice intercalation.

Considering the Rietveld refinement results in Table 12, it seems that the calcium hydroxide converts mostly to calcite, and the katoite is not broken down to form calcite. The sample with the most excess carbonate, 10 g dry ice, did not form hydrocalumite. It is recommended to modify the experimental setup to increase contact time and stay within stoichiometric loadings to see if the results will be more favourable. Based on these results this is not a viable method for hydrocalumite synthesis.

Table 12: Quantitative results of carbonate intercalation from dry ice.

Mass (g)	Chemical Species (mol %)				
	Ca_4Al_2-CO_3-LDH	$Ca_3Al_2(OH)_{12}$	$Ca(OH)_2$	$Al(OH)_3$	$CaCO_3$
1	3,79	57,53	18,69	12,30	7,69
2	3,82	56,51	11,79	12,93	14,95
3	4,15	65,37	5,03	9,59	15,87
10	0,00	50,99	3,32	0,00	45,69

4.2.6 Use of calcite as carbonate and calcium source

XRD results for experiments where calcite was added as carbonate source are shown in Figure 45. These results have been adapted from the study conducted by van Graan (2012). It is clear that it is possible to synthesise hydrocalumite with calcite as carbonate source. These experiments were only conducted at short time intervals (up to 1 h) at ambient temperature. It was reported that the highest katoite conversion for these experiments was 30 % in 1 h.

Figure 46 shows results of experiments where calcite was used as both a calcium and carbonate source. Calcite was the only phase detected, which indicates that, for these reaction parameters, it is not a viable method of producing hydrocalumite. Aluminium hydroxide was only present in the 120 ^oC sample at 24 h and is assumed to be mainly in the amorphous phase for all samples.

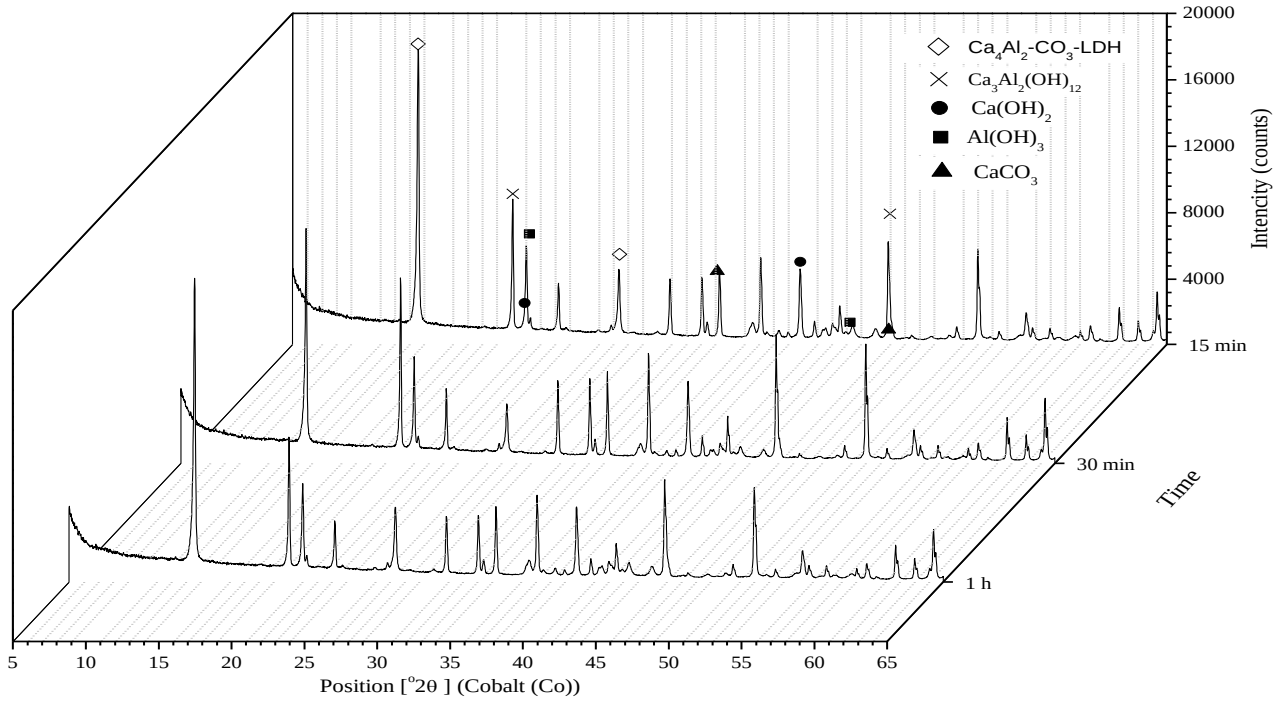

Figure 45: Hydrocalumite synthesis at varying time with calcite as carbonate source (van Graan, 2012).

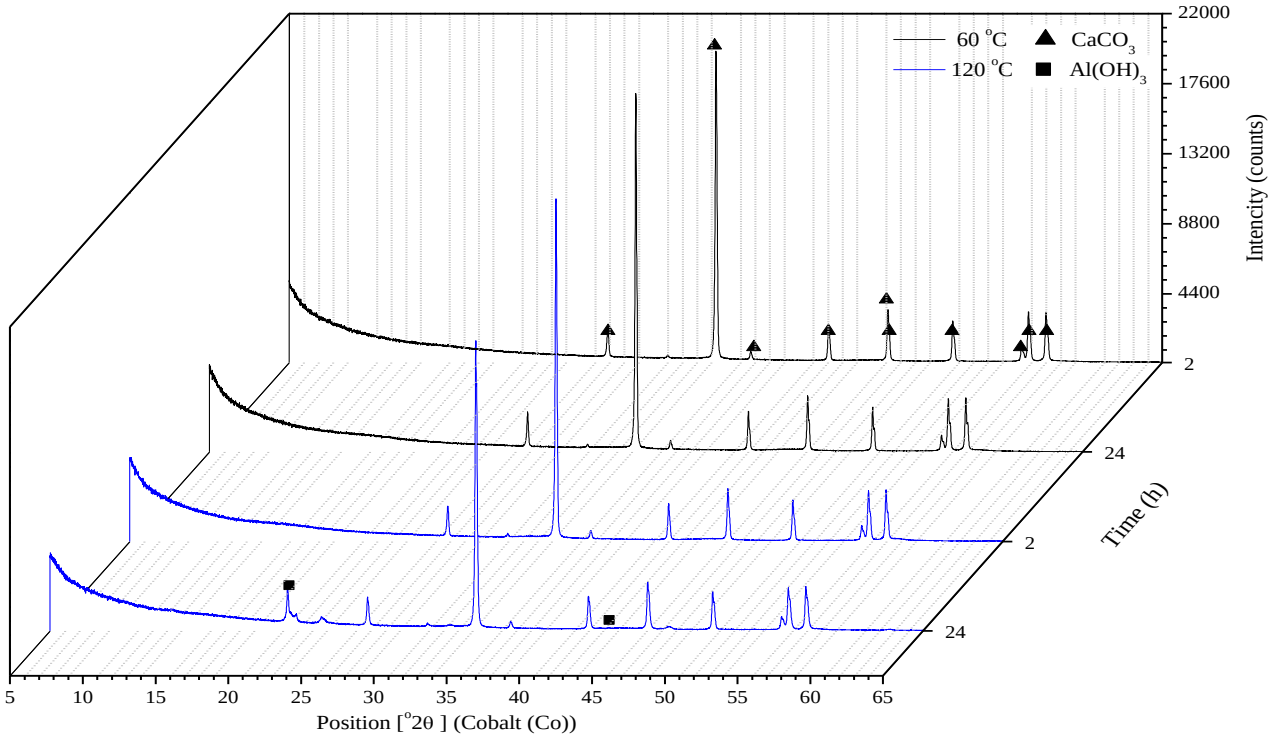

Figure 46: Hydrocalumite synthesis with calcite as calcium and carbonate source.

Considering both these set of results, it is concluded that calcite in a small concentration could serve as a carbonate source. Even with short reaction times at ambient temperatures, hydrocalumite formation is observed. When used in large concentrations, there is no dissolution of calcite to precipitate as hydrocalumite.

4.3 Overall synthesis

Based on the results discussed above it is concluded that for the first step of the synthesis, with calcium oxide and aluminium hydroxide reagents, a reaction temperature of 100 ^{o}C for 30 min is sufficient. This proved to be the lowest reaction time at this temperature at which a high conversion of aluminium hydroxide to katoite was achieved. In the carbonate intercalation step the use of sodium carbonate resulted in the highest yield of hydrocalumite. The results show the best hydrocalumite formation at 10 h reaction time at 60 ^{o}C.

Figure 47 illustrates how this synthesis method can be implemented on an industrial scale. This is based on the same process described by Labuschagne *et al* (2015). Calcium oxide, aluminium hydroxide and water should be added to the reactor and reacted for 30 min at 100 ^{o}C. Thereafter the sodium carbonate should be added to the precursor slurry mixture and reacted at 60 ^{o}C for 10 h. The reaction products then go through filtration and drying steps. The filtrate contains sodium hydroxide formed in the intercalation step which can be regenerated into sodium bicarbonate/sodium carbonate by bubbling CO_2 gas into the solution (IBT, 2003).

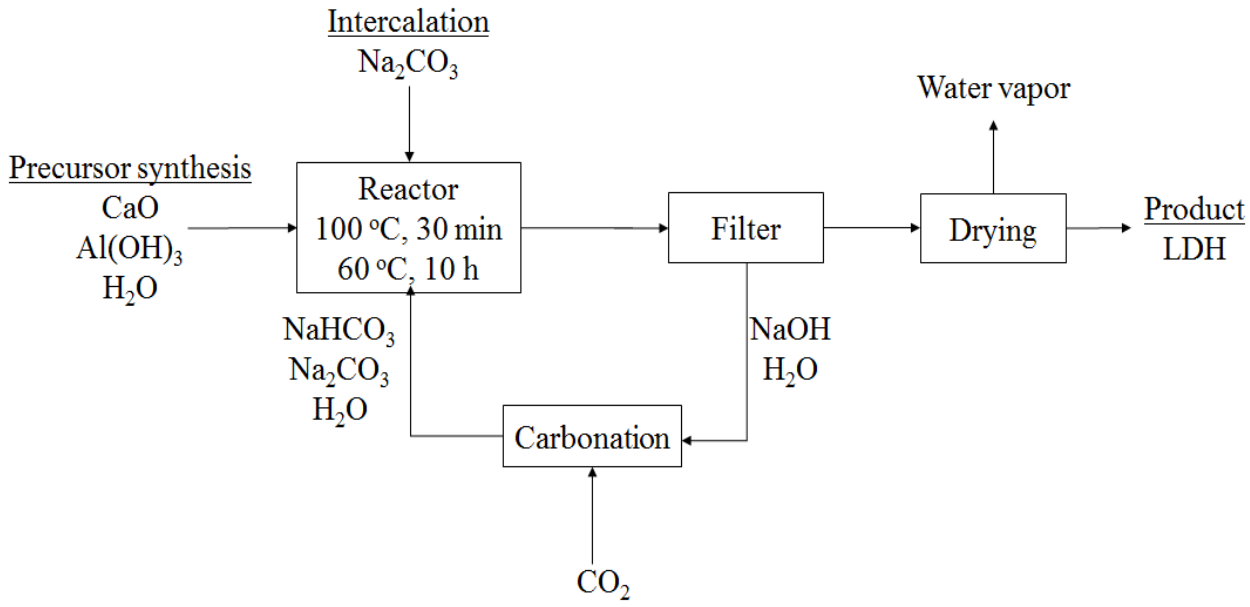

Figure 47: Hydrocalumite production flow sheet.

As discussed with Section 2.3 conventional methods a salt containing effluent is produced. With the use of oxide/hydroxide reagents in this method the effluent stream contains sodium hydroxide instead of salts. The hydroxide can be treated in a lower cost process than the salt effluent. This allows this stream to be recycled back into the reaction system. In doing this sodium carbonate reagent and water demand for the process is reduced. The resulting process is more environmentally friendly.

5 Conclusions and recommendations

5.1 Precursor: katoite synthesis

In the precursor formation step it was found that for the reaction between calcium oxide and aluminium hydroxide the conversion of both the calcium and aluminium source to katoite increases as reaction time and temperature increases. It was confirmed that the dissolution of aluminium hydroxide is the limiting step. A reaction temperature of 60 °C is insufficient to dissolve aluminium hydroxide. Only after 24 h had a small amount of katoite formed and aluminium hydroxide conversion was only ~60 %. An aluminium hydroxide conversion of ~90 % was achieved at 80 °C within 6 h reaction time.

A further increase in temperature reduces the reaction time immensity with ~90 % aluminium hydroxide conversion reached within 30 min at 100 °C and 120 °C. Extending the reaction time beyond 30 min did not have a significant influence on the conversion of aluminium hydroxide as it remains approximately constant at ~90 %. An increase in the crystallinity of the products was observed for longer reaction times at the high reaction temperatures. This was confirmed by an increase in the intensity of the primary and secondary katoite peaks in the diffraction patterns and morphology observed in FE-SEM micrographs. These results also confirm that the effect of time is less significant than temperature.

An increase in calcite formation was observed as time and temperature were increased but always remained below 3 %mol. Thus it does not inhibit the formation of katoite in the first step of the reaction. Calcite formed despite of the fact that the reaction mixtures were not exposed to a carbonate source. This could be due to carbonate uptake from air during the filtering and drying steps or as a result of the intercalation of hydroxide anions. This should be further investigated. On a large scale production facility, reaction temperatures of 100 °C

for ~30 min is suggested in the precursor step. The higher yields obtained by using calcium hydroxide as calcium source will also be important for commercial synthesis. It is recommended that the pH effect of calcium oxide vs calcium hydroxide as calcium source be investigated to determine the effect on katoite formation.

5.2 Carbonate intercalation

Of the various carbonate sources tested sodium carbonate results showed the best yield of hydrocalumite. The results of sodium bicarbonate and sodium carbonate were very similar in that as time and temperature increased the conversion of the precursor material in the presence of the carbonate source to form hydorcalumite increased. There was a significant spike in the hydrocalumite diffraction peak intensity of the sodium carbonate samples at 60 ^{o}C and 70 ^{o}C for 10 h reaction time. These samples showed the highest hydrocalumite yield. There are virtually no other phases visible on the diffraction patterns and Rietveld refinement data of these two samples. Only small amounts of unreacted katoite and calcite remaining from the precursor material were observed. The calcite content was much lower than any of the other samples. It can be concluded that some of the calcite dissolved and precipitated as hydrocalumite.

The reason for this is not clear. It may be due to the sodium hydroxide formed during the reaction of sodium carbonate. It is known that sodium hydroxide helps with dissolving aluminium hydroxide through the formation of sodium aluminate a highly soluble aluminium specie (Panias, Asimidis & Paspaliaris, 2001). The sodium hydroxide enhances the dissolution of the aluminium hydroxide at an acceptable rate and favourable pH, increasing the hydrocalumite yields.

This makes the carbonate intercalation from sodium carbonate and sodium hydrogen carbonate in this two-step synthesis method well suited to large scale production. The sodium hydroxide can be reacted with CO_2 to regenerate the

sodium carbonate (Yoo, Han & Wee, 2013). This will lead to an environmentally friendly synthesis route. Regarding the other carbonate sources the following main conclusions were made:

Air: In the range of temperature and time reaction conditions the hydrocalumite content of all samples stay below 10 %mol. This is not economically viable for large scale synthesis.

CO_2 (g): Small amounts of hydrocalumite (~4 %mol) formed at the lower gas flow rate and lower reaction time of 2 h. The precursor material gets broken down and forms large amounts of calcitewith this carbonate source. Overall, more work must be done to establish the value of this synthesis technique on commercial scale. However, it may be easier to use sodium carbonate as a carbonate source and then regenerate it by reacting CO_2 (g) with the produced sodium hydroxide (Yoo, Han & Wee, 2013).

Dry ice: Small amounts of hydrocalumite formed and large amounts of unreacted precursor material were present in all samples. The low conversion could be a result of the short reaction time. This method does not appear useful for a large scale synthesis of hydrocalumite. The production of CO_2 (s) is also energy intensive making this synthesis route not the best option from a commercial point of view.

5.3 The use of calcite as combined calcium and carbonate source

Hydrocalumite forms when calcite is used as carbonate source within short reaction times at ambient temperature. When calcite is used in a larger concentration as calcium and carbonate source, no dissolution occurs. The reaction dynamics and chemistry behind this is not yet fully understood. The solubility of the calcite at the reaction conditions (along with the low aluminium

hydroxide solubility) may be hindering the reaction. The replacement of some of the calcium oxide / calcium hydroxide as calcium source by calcite, will lead to a lower overall reaction medium pH. This may be hindering the formation of katoite.

More work is needed here to investigate the complex slurry chemistry of this overall reaction. It is recommended to investigate the full effect of reaction time, reaction temperature, reaction slurry pH and slurry solid concentration on the formation of hydrocalumite.

5.4 Overall

Considering the results of the precursor formation and intercalation it is concluded that the best synthesis conditions would be to react calcium oxide and aluminium hydroxide at a temperature of 100 °C for 30 min, where after sodium carbonate should be added to the mixture and reacted for a further 10 h at between 60 °C and 70 °C. These conditions resulted in the .highest conversion of reagents in each step It is recommended that pilot scale testing of this synthesis method be conducted to confirm its usability on a commercial scale.

6 References

Allmann, R (1970), "Doppelschichtstrukturen mit brucitaehnlichen Schichtionen [Me (II) 1^{-x}Me (III) ^{x} (OH) 2] $^{x+}$", *Chimia*, 24(3), 99-108.

Auerbach, S, Carrado, K and Dutta, P (2004), *Handbook of Layered Materials*, Marcel Dekker Inc., New York.

Boclair, JW and Braterman, PS (1999), "Layered double hydroxide stability. 1. Relative stabilities of layered double hydroxides and their simple counterparts", *Chemistry of Materials*, 11(2), 298-302.

Braterman, PS, Xu, ZP and Yarberry, F (2004), "Layered double hydroxides (LDHs)", *Handbook of layered materials*, Marcel Dekker Inc., New York, 373-474.

Carlson, ET and Berman, HA (1960), "Some observations on the calcium aluminate carbonate hydrates", *Journal of Research of the National Bureau of Standards*, 64(4), 333-341.

Cavani, F, Trifirò, F and Vaccari, A (1991), "Hydrotalcite-type anionic clays: Preparation, properties and applications", *Catalysis Today*, 11(2), 173-301.

Connolly, J (2012), "Introduction Quantitative X-Ray Diffraction Methods", prepared for *EPS400-001*, Spring 2012.

Costantino, U, Marmottini, F, Nocchetti, M and Vivani, R (1998), "New synthetic routes to hydrotalcite-like compounds-characterisation and properties of the obtained materials", *European Journal of Inorganic Chemistry*, 1998(10), 1439-1446.

Cullity, B (1956), *Elements of X-Ray Diffraction*: Addison-Wesley Publishing Company, Massachuetts.

Duan, X, Li, D, Lv, Z, Lin, Y and Xu, X (2008), "Clean method for preparing layered double hydroxides", Google Patents.

Fogg, AM, Freij, AJ, Oliveira, A, Rohl, AL, Ogden, MI and Parkinson, GM (2002a), "Morphological control of $Ca_3Al_2(OH)_{12}$", *Journal of Crystal Growth,* 234(1), 255-262.

Fogg, AM, Freij, AJ, Rohl, AL, Ogden, MI and Parkinson, GM (2002b), "Toward a fundamental understanding of molecular recognition: A synthetic and computational study of morphological control of Ca3Al2 (OH) 12", *The Journal of Physical Chemistry B,* 106(23), 5820-5826.

Forano, C, Hibino, T, Leroux, F and Taviot-Guého, C (2006), "Layered Double Hydroxides", in Handbook of Clay Science, Bergaya, F, Theng, BKG and Lagaly, G (Eds.), Elsevier, Amsterdam..

Goh, K-H, Lim, T-T and Dong, Z (2008), "Application of layered double hydroxides for removal of oxyanions: a review", *Water research,* 42(6-7), 1343-1368.

IBT (2003), "Sodium Bicarbonate Chemistry", Integrated Biomedical Technology, Inc.

Kirkpatrick, RJ, Yu, P, Hou, X and Kim, Y (1999), "Interlayer structure, anion dynamics, and phase transitions in mixed-metal layered hydroxides: Variable temperature^3^ 5Cl NMR spectroscopy of hydrotalcite and Ca-aluminate hydrate (hydrocalumite)", *American Mineralogist,* 84,1186-1190.

Kocík, J, Hájek, M and Troppová, I (2015), "The factors influencing stability of Ca–Al mixed oxides as a possible catalyst for biodiesel production", *Fuel Processing Technology*, 134, 297-302.

Kuang, Y, Zhao, L, Zhang, S, Zhang, F, Dong, M and Xu, S (2010), "Morphologies, preparations and applications of layered double hydroxide micro-/nanostructures", *Materials*, 3(12), 5220-5235.

Kuwahara, Y and Yamashita, H (2015), "Synthesis of Ca-based layered double hydroxide from blast furnace slag and its catalytic applications", *ISIJ International*, 55(7), 1531-1537.

Labuschagne, F, Wiid, A, Venter, H and Leuteritz, A (2015), "Green synthesis of hydrotalcite from untreated magnesium oxide and aluminium hydroxide", University of Pretoria, Submitted to Green Chemistry Letters and Reviews.

López-Salinas, E, Serrano, MEL, Jácome, MaC and Secora, IS (1996), "Characterization of synthetic hydrocalumite-type $[Ca_2Al(OH)_6]NO_3 \cdot mH_2O$: Effect of the calcination temperature", *Journal of Porous Materials*, 2(4), 291-297.

Matschei, T, Lothenbach, B and Glasser, FP (2007), "Thermodynamic properties of Portland cement hydrates in the system $CaO–Al2O_3–SiO_2–CaSO_4–CaCO_3–H_2O$", *Cement and Concrete Research*, 37(10), 1379-1410.

Messersmith, PB and Stupp, SI (1992), "Synthesis of nanocomposites: organoceramics", *Journal of materials research*, 7(09), 2599-2611.

Mitchell, S, Biswick, T, Jones, W, Williams, G and O'hare, D (2007), "A synchrotron radiation study of the hydrothermal synthesis of layered double hydroxides from MgO and Al_2O_3 slurries", *Green Chemistry*, 9(4), 373-378.

Miyata, S (1980), "Physio-chemical properties of synthetic hydrotalcites in relation to composition", *Clays and Clay Minerals*, 28(1), 50-56.

Oniyama, E and Wahlbeck, PG (1995), "Application of transpiration theory to TGA data: Calcium carbonate and zinc chloride", *Thermochimica Acta*, 250(1), 41-53.

Panias, D, Asimidis, P and Paspaliaris, I (2001), "Solubility of boehmite in concentrated sodium hydroxide solutions: model development and assessment", *Hydrometallurgy*, 59(1), 15-29.

Pecharsky, VK and Zavalij, PY (2009), *Fundamentals of powder diffraction and structural characterization of materials*, Springer, New York.

Razvan, C, Beck, R, Kuerzinger, A, Puerzer, AW and Rosenthal, M (1993), "Basic calcium aluminum hydroxide dicarboxylates, a process for their production and their use", Google Patents.

Rosenberg, SP, Wilson, DJ and Roworth, DM (2013), "High temperature processs for causticisation of a bayer liquor", Google Patents.

Rousselot, I, Taviot-Guého, C, Leroux, F, Léone, P, Palvadeau, P and Besse, J-P (2002), "Insights on the Structural Chemistry of Hydrocalumite and Hydrotalcite-like Materials: Investigation of the Series $Ca_2M^{3+}(OH)_6Cl\cdot 2H_2O$ (M^{3+}: Al^{3+}, Ga^{3+}, Fe^{3+}, and Sc^{3+}) by X-Ray Powder Diffraction", *Journal of Solid State Chemistry*, 167(1), 137-144.

Roy, R and Osborn, EF (1953), "The system $MgO\text{-}Al_2O_3\text{-}H_2O$ and influence of carbonate and nitrate ions on the phase equilibria", *American Journal of Science*, 251(5), 337-361.

Sánchez-Cantú, M, Pérez-Díaz, LM, Tepale-Ochoa, N, González-Coronel, VJ, Ramos-Cassellis, ME, Machorro-Aguirre, D and Valente, JS (2013), "Green synthesis of hydrocalumite-type compounds and their evaluation in the transesterification of castor bean oil and methanol", *Fuel*, 11, 023-31.

Schmidt, MJ (2015), “Synthesis of mdified hydrocalumite: a novel katoite/portlanite precursor method”, Meng dissertation, University of Pretoria, Pretoria.

Tatematsu, H, Nakamura, T, Koshimizu, H, Morishita, T and Kotaki, H (1995), "Cement-additive for inhibiting concrete-deterioration", Google Patents.

van der Westhuizen, F (2011), "The Green Engineering of Layered Double Hydroxides", Final year research report, University of Pretoria., Pretoria.

van Graan, M (2012), "Layered double hydroxide synthesis for utilisation a catalysts", Final year research report, University of Pretoria, Pretoria.

Vieille, L, Rousselot, I, Leroux, F, Besse, J-P and Taviot-Guého, C (2003), "Hydrocalumite and its polymer derivatives. 1. Reversible thermal behavior of Friedel's salt: A direct observation by means of high-temperature in situ powder X-ray diffraction", *Chemistry of Materials*, 15(23), 4361-4368.

Wen, X, Yang, Z, Yan, J and Xie, X (2015), "Green preparation and characterization of a novel heat stabilizer for poly (vinyl chloride)–hydrocalumites", *RSC Advances*, 5(40), 32020-32026.

Whittington, BI, Fallows, TM and Willing, MJ (1997), "Tricalcium aluminate hexahydrate (TCA) filter aid in the Bayer industry: factors affecting TCA preparation and morphology", *International Journal of Mineral Processing*, 49(1–2), 1-29.

Wiid, A (2013), "Dissolution Precipitation Synthesis of Cu_2Al_4-Layered Double Hydroxide", Final year research report, University of Pretoria, Pretoria.

Wongariyakawee, A, Schäeffel, F, Warner, JH and O'hare, D (2012), "Surfactant directed synthesis of calcium aluminum layered double hydroxides nanoplatelets", *Journal of Materials Chemistry*, 22(16), 7751-7756.

Xu, Z and Lu, G (2005), "Hydrothermal synthesis of layered double hydroxides (LDHs) from mixed MgO and Al_2O_3: LDH formation mechanism", *Chemistry of Materials*, 17(5), 1055-1062.

Yoo, M, Han, S-J and Wee, J-H (2013), "Carbon dioxide capture capacity of sodium hydroxide aqueous solution", *Journal of Environmental Management*, 114, 512-519.

Appendix A: Rietveld refinement

Table 13: Quantitative results of sodium bicarbonate carbonate source.

Time (h)	Temperature (°C)	Chemical Species (mol %)				
		Ca_4Al_2-CO_3-LDH	$Ca_3Al_2(OH)_{12}$	$Ca(OH)_2$	$Al(OH)_3$	$CaCO_3$
2	~25	14,31	14,40	12,78	16,76	41,76
	40	22,07	8,18	13,86	14,67	41,21
	50	23,50	8,26	9,40	12,23	46,61
	60	30,07	3,82	14,96	13,20	37,95
	70	23,53	12,39	10,74	13,96	39,38
6	~25	18,96	8,17	15,64	18,72	38,51
	40	20,26	5,88	15,04	21,09	37,72
	50	25,26	5,38	18,49	13,03	37,83
	60	34,75	5,67	24,10	11,36	24,12
	70	39,31	3,93	10,38	17,24	29,14
10	~25	21,73	7,75	8,01	23,64	38,87
	40	27,81	4,03	16,84	15,14	36,18
	50	30,70	2,77	17,00	20,48	29,05
	60	36,64	2,67	14,36	21,31	25,03
	70	32,02	7,01	8,42	14,02	38,53
24	~25	41,32	3,33	15,42	2,56	37,37
	40	42,11	1,78	10,04	23,02	23,06
	50	50,56	1,23	10,43	18,11	19,67
	60	45,41	2,60	17,54	0,00	34,45
	70	43,39	6,13	20,75	0,00	29,74

Table 14: Quantitative results of sodium carbonate intercalant source.

Time (h)	Temperature (°C)	Chemical Species (mol %)				
		Ca_4Al_2-CO_3-LDH	$Ca_3Al_2(OH)_{12}$	$Ca(OH)_2$	$Al(OH)_3$	$CaCO_3$
2	~25	35,10	13,81	1,22	1,14	48,72
	40	29,05	11,48	0,47	0,00	59,00
	50	20,00	7,49	0,00	0,43	72,08
	60	21,61	4,56	0,00	0,53	73,29
	70	23,77	6,79	0,00	0,00	69,44
6	~25	24,10	5,08	0,14	1,35	69,33
	40	32,66	5,37	0,00	0,00	61,97
	50	34,86	3,43	0,00	0,00	61,71
	60	31,19	2,89	0,00	0,00	65,93
	70	35,56	2,43	0,00	0,00	62,01
10	~25	29,81	3,68	0,00	0,75	65,76
	40	60,16	9,83	0,00	0,00	30,01
	50	81,84	5,41	0,00	0,00	12,75
	60	86,59	8,29	0,00	0,00	5,12
	70	82,87	5,13	0,00	0,00	12,00
24	~25	42,00	0,98	0,00	1,11	55,90
	40	41,54	1,43	0,00	0,13	56,90
	50	36,78	1,23	0,00	0,00	61,99
	60	35,36	4,20	0,00	0,00	60,44
	70	34,64	2,39	0,00	0,00	62,97

Appendix B: FE-SEM micrographs

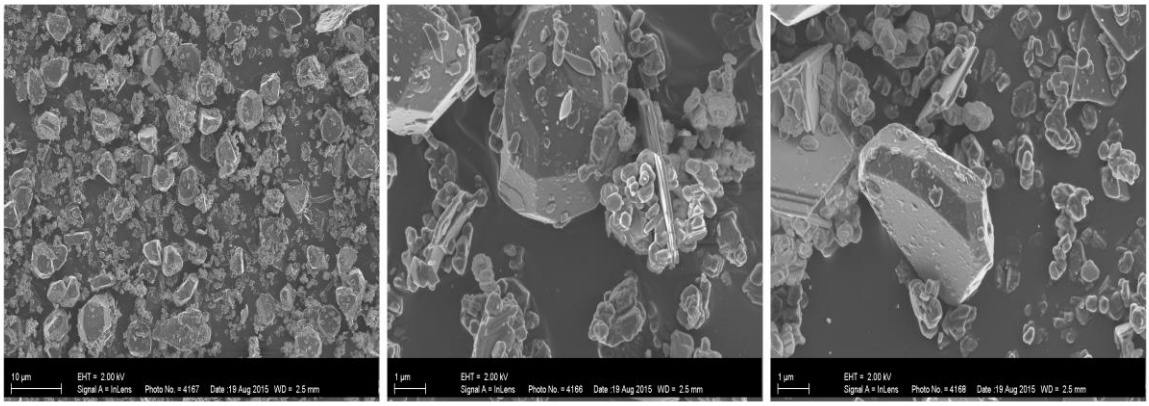

Figure 48: FE-SEM micrographs of katoite formation at 60 ^{o}C for 24 h reaction time.

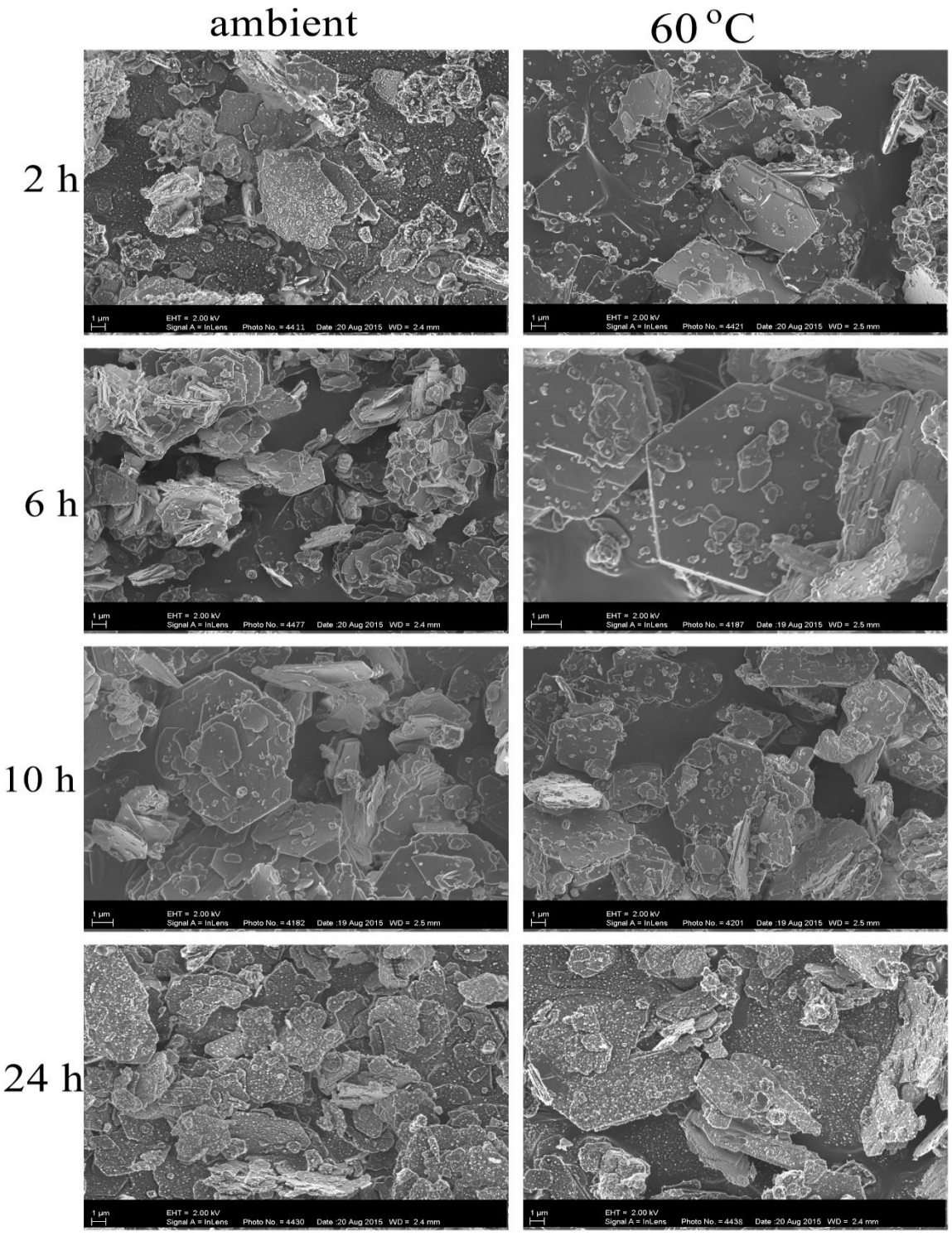

Figure 49: FE-SEM micrographs for intercalation samples with sodium bicarbonate as carbonate source.

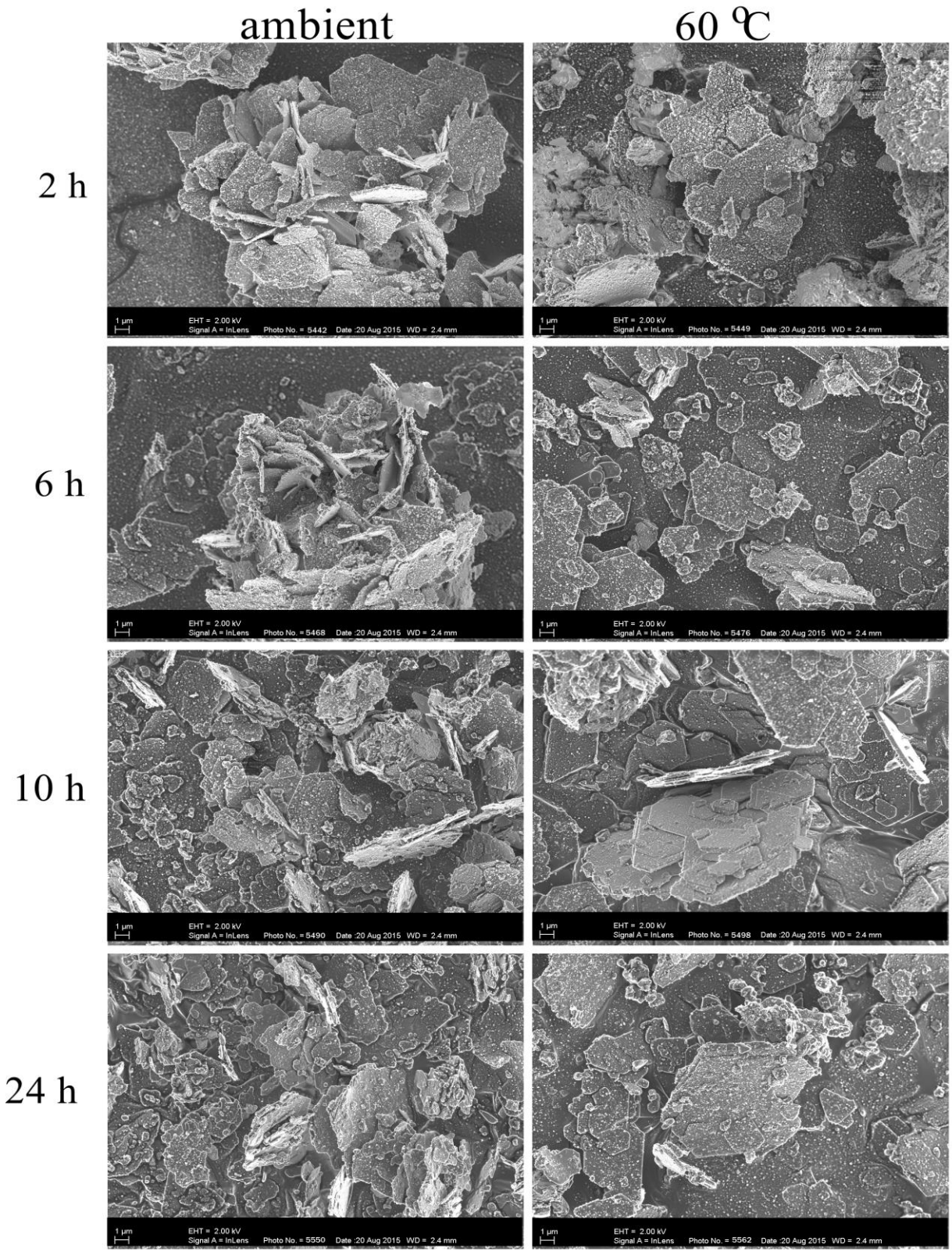

Figure 50: FE-SEM micrographs for intercalation samples with sodium carbonate as carbonate source.